The role of LRP1 in β1-integrin endocytosis

Dissertation

zur Erlangung des Grades

„Doktor der Naturwissenschaften“

am Fachbereich Biologie

der Johannes Gutenberg-Universität Mainz

von

Verena Rabiej

geboren am 18. März 1988 in Bad Soden

Mainz, im Mai 2016

Dekan:

1. Berichterstatter:

2. Berichterstatter:

Tag der mündlichen Prüfung: 07. Juni 2016

Eidesstattliche Erklärung

Hiermit versichere ich an Eides statt, dass ich die vorliegende Promotionsarbeit im Zeitraum von Januar 2013 bis Mai 2016 selbstständig verfasst und nur unter Verwendung der angegebenen Hilfsmittel angefertigt habe.

Mainz, den

_____

Verena Rabiej

Abbreviations

AAxA	multiple alanine cassette
Aβ	Amyloid beta
AD	Alzheimer's disease
ANOVA	Analyzes of variance
ApoE	Apolipoprotein E
AP-2	AP-2-adapter complex
APP	Amyloid precursor protein
BACE1	Beta-site APP cleaving enzyme 1
BSA	Bovine serum albumin
°C	Degree Celsius
Cdc42	Cell division control protein 42 homolog
CHO	Chinese hamster ovary
CNS	Central nervous system
CPZ	Chlorpromazine
Dab2	Disabled homolog 2
DIV	Days *in vitro*
DMSO	Dimethyl-sulfoxide
ECM	Extracellular matrix
E. coli	*Escherichia coli*
EGF	Epidermal growth factor
ER	Endoplasmatic reticulum
ERK	Extracellular-signal regulated kinase
FA	Focal adhesion
FAK	Focal adhesion kinase
g	Gram
GAP	GTPase-activating proteins
GEF	Guanidine nucleotide exchange factors
GFP	Green fluorescent protein
GRB2	Growth factor receptor-bound protein 2
GTP	Guanosine-triphosphate
h	hour
HBSS	Hanks´ balanced salt solution
HRP	Horseradish peroxidase

IgG	Immunoglobin G
IP	Immunoprecipitation
kDa	Kilo Dalton
ki	knock-in
ko	knock-out
LB	Luria-Bertani media
LDL	Low density lipoprotein
LRP	Low density lipoprotein receptor-related protein 1
LTP	Long term potentiation
µ	Micro
m	Milli
M	Molar
MAPK	Mitogen-activated kinase
mDia1	Diaphanous-related formin-1
MEF	Mouse embryonic fibroblasts
MEGF	Multiple EGF-like domain
MEK	Mitogen-activated protein kinase
min	Minute
MLC	Myosin light chain
MMP	Matrix Metalloproteinase
NB	Neurobasal media
nm	Nano meter
NMDA	N-methyl-D-aspartate receptor
NP-40	Nonidet-P40
o.n.	Over night
PAGE	Polyacrylamide gel electrophoresis
PAI-1	Plasminogen activator inhibitor-1
PBS	Phosphate buffered saline
PCR	Polymerase chain reaction
PDGF	Platelet-derived growth factor
PFA	Paraformaldehyde
PSD95	Postsynaptic density protein 95
Pyk2	Protein tyrosine kinase 2
Rac1	Ras-related C3 botulinum toxin substrate 1

RanBP9	Ran-binding protein 9
RAP	Receptor associated protein
rcf	Relative centrifugal force
RCME	Recombinase mediated cassette exchange
RGD	Amino acid sequence of Arginine-Glycine-Asparagine acid
RISC	RNA-induced silencing complex
RIPA	Radioimmunoprecipitation assay buffer
RMS	Rostral migratory stream
ROCK	Rho associated coiled-coil forming kinase
RhoA	Ras homolog gene family member A
rpm	Revolutions per minute
RT	Room temperature
SDS	Sodium dodecyl sulfate
sec	Second
SEM	Standard error of the mean
siRNA	Small interfering ribonucleic acid
Snx-17	Sorting nexin 17
SORLA	Sorting-related receptor containing type-A repeats
SOS1	Son of sevenless 1
SVZ	Subventricular zone
TAE	Tris acetic acid
TBS	Tris-buffered saline
TIMP	Tissue- inhibitors of metalloproteinases
tPA	Tissue-type plasminogen activator
TSP-2	Thrombospondin-2
uPA	Urokinase-type plasminogen activator
VLDL	Very low density lipoprotein receptor
v/v	Volume per volume
WB	Western blot
Wt	Wildtype
w/v	Weight per volume

Table of Contents

1. Introduction

1.1 The low density lipoprotein receptor family

The family of low density lipoprotein receptors (LDLR) is a highly conserved gene family and could be recorded back to very simple organized multicellular nemathelminths. During the progress of evolution, genes sharing similar conserved motifs of the modern LDLR family probably emerged due to exon shuffling. A prominent representative is *Caenorhabditis elegans (C. elegans)*, which is an important model organism for biological research. One of the major functions of LDL receptors is their role in lipid metabolism, they deplete LDL particles from the blood system via endocytosis. Although *C. elegans* owns no circular blood system, the preliminary form of the LDLR is already involved in its lipid metabolism. Furthermore, two members of the LDLR family, LRP1 and LRP1b, are present in this model organism in a similar structure compared to the modern proteins. Signal transduction for instance by LRP1 could already be demonstrated in *C. elegans*, where the preliminary form of LRP1 exported the signal protein EGL-17/FGF and controlled the migration of sex myoblast (Kamikura and Cooper, 2003).

The modern LDLR family comprises 7 members, all sharing several structural characteristics depicted in figure 1: starting from the intracellular side, all members contain a cytoplasmatic tail, harboring a minimum of one ligand binding domain, the NPxY (Asparagine-Proline-x amino acid-Tyrosine) motif. Next, the receptors share a single pass transmembrane domain followed by an epidermal growth factor (EGF) domain and a β-propeller domain. The extracellular domain including cysteine-rich repeats is responsible for extracellular ligand binding. Amongst the LDL family the LDL receptor was the first to be described by Brown and Goldstein (Goldstein and Brown, 1985). The LDLR is expressed ubiquitously in humans, where it plays a major role in lipid metabolism: the LDLR clears the cholesterol, bound to LDL particles from the blood by binding the particle and internalizing it into the cell in a clathrin-dependent manner (Bos et al., 1995; Mokuno et al., 1994). The cholesterol is then transported to the lysosomal compartment for degradation, whereas the LDL receptor is recycled back to the cell surface (Goldstein and Brown, 1976). The importance of the clearance mechanism of cholesterol by the LDL receptor can be highlighted by a genetic disorder, the familial hypercholesterolemia. Patients harboring a homozygous mutation suffer

from extremely high cholesterol levels in the blood and related cardio-vascular diseases like arteriosclerosis. These patients have a high risk for heart attacks already occurring during the first 20 years of their lives.

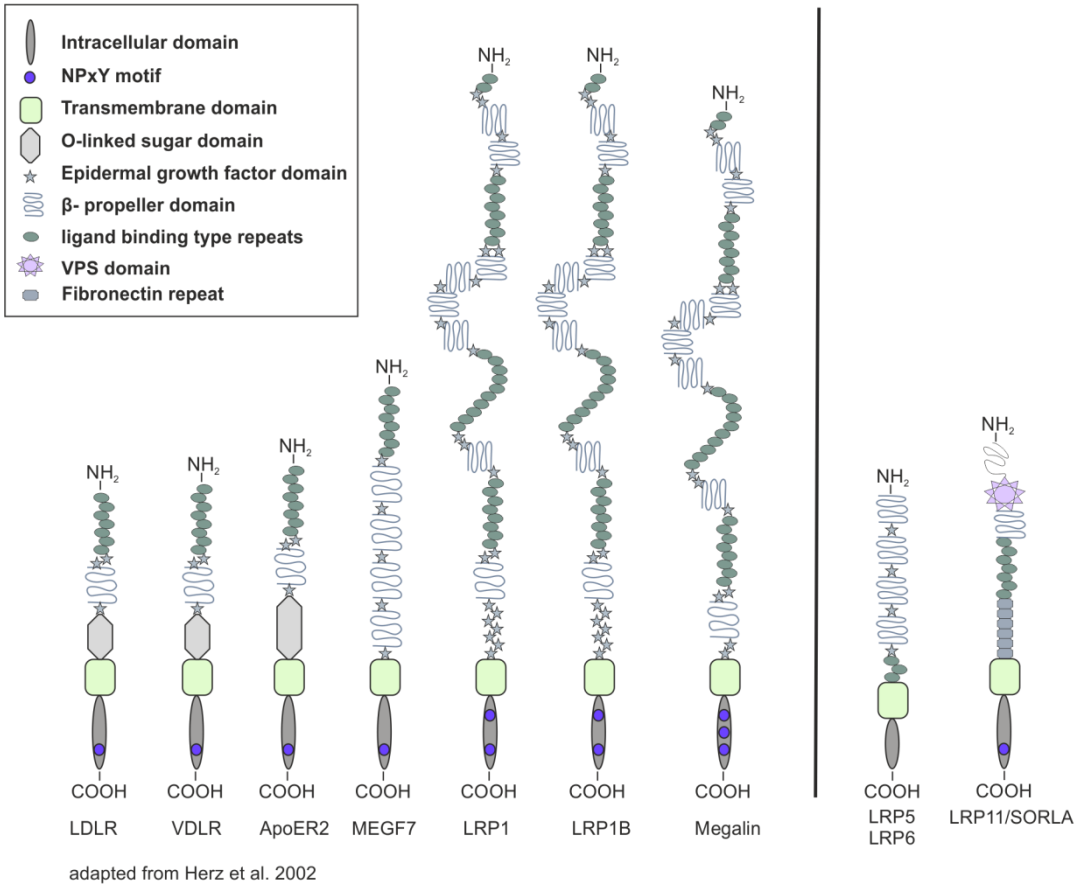

Figure 1: LDL family: The LDL family of mammals comprises of 7 core members and 2 distant family members. Structurally, LDL receptor family members are composed of an intracellular domain harboring a minimum of one NPxY domain, a single pass transmembrane domain, the epidermal growth factor domain, a β-propeller domain and cysteine-rich ligand binding repeats. The structural composition may vary in order and amount of the domains. The distant members LRP5/LRP6 and SORLA are structurally constituted divergent from the core family.

Showing an almost equal structure as the LDL receptor, the very low density lipoprotein receptor (VLDL) also belongs to the LDL gene family. The receptor is able to bind apolipoprotein E (ApoE) containing lipid particles and thus was dedicated to lipid metabolism. However, VLDLR is widely expressed throughout the body, but it is not expressed in hepatocytes, the cell type mainly involved in lipid degradation. VLDLR-deficient mice exhibit normal levels of lipids in the blood and VLDL is metabolized (Frykman et al., 1995). Furthermore, the VLDLR plays a major role in neuronal development by binding its ligand Reelin. The subsequent signaling of Reelin binding

directs proper migration of newly generated neurons and the correct arrangement of neurons into the layers of the neocortex (D'Arcangelo et al., 1999; Hiesberger et al., 1999; Tissir and Goffinet, 2003; Trommsdorff et al., 1999).

The ApoER2 receptor, which is structurally very similar to the LDLR, was discovered in a genome-wide search for homologues of the LDLR (Kim et al., 1996). ApoER2 expression is restricted to the brain and testis. The receptor is able to bind Reelin and therefore, is involved in proper neuronal cell migration in the developing cerebral cortex (Trommsdorff et al., 1999). In addition to its role in neuronal development, ApoER2 also constitutes a major clearance receptor for ApoE, which is mainly produced by astrocytes in the brain (Boyles et al., 1989). Additionally, ApoER2 knock-out mice are sterile; therefore, ApoER2 seems to play a role in sperm viability or production (Andersen et al., 2003).

MEGF7 (the multiple EGF-like domain receptor, also called LRP4) is another core member of the LDL gene family discovered by human brain cDNA screening for genes coding for multiple epidermal growth factor (EGF)-like motifs (Nakayama et al., 1998). The structure of LRP4 deviates from the LDLR; it is comprised of one ligand binding domain, an EGF precursor homology domain, an O-glycosylation domain, a transmembrane domain and a cytoplasmic tail containing an NPxY motif. However, the function of the MEGF7 receptor is still elusive: there is some evidence that the receptor is involved in organogenesis, in neuromuscular junction formation and in bone morphogenesis (Ohazama et al., 2010; Shen et al., 2015).

With a size of 600 kDa, megalin or LRP2 is a relatively big member of the LDLR family. It was first discovered as an autoantigen in an animal model of an autoimmune kidney disease (Kerjaschki and Farquhar, 1982; Saito et al., 1994). Structurally, it is composed of 4 ligand-binding domains, one transmembrane domain and an intracellular domain harboring three NPxY motifs. LRP2 is an endocytic receptor that is mainly expressed in resorptive epithelia such as the proximal renal tubule. It accomplishes the task of an endocytic receptor; its ligands are steroids, lipoproteins and retinoids. Vitamin D and its binding protein also belong to its ligands and is resorbed by the receptor from the urine. A receptor knock-out results in a severe deficiency of vitamin D and correlated bone mineralization defects (Nykjaer et al., 1999). Furthermore, vitamin A and vitamin B12 are resorbed by a similar mechanism via megalin (Christensen et al., 1999; Moestrup et al., 1996). LRP2 is also engaged in brain

development, knock-out animals show cranial midline effects primarily affecting the forebrain (Willnow et al., 1996a).

LRP1 was the second member of the LDLR family to be discovered as a surface protein of hepatocytes (Herz et al., 1988). LRP1 consists of 4 ligand binding domains, which resemble the extracellular LDLR binding-domain. Furthermore, LRP1 harbors two ligand binding intracellular NPxY motifs. The endocytic receptor is expressed ubiquitously and plays a major role in lipid metabolism. Lipoproteins such as apolipoprotein E bind to the chylomicron remnant receptor LRP1 and are subsequently endocytosed and degraded in the lysosomal compartment (Beisiegel et al., 1989). In the process of research LRP1 was identified as a receptor of over 40 ligands such as α2-macroglobulin. LRP1 is not only responsible for endocytosis but is also involved in signal transduction and embryogenesis (Herz et al., 1992; Strickland et al., 1990).

LRP1B, the last member of the LDLR gene family to have been identified, shares a sequence identity of 60% with LRP1. LRP1B represents a potential tumor suppressor, as a homozygous mutation of LRP1B was first identified in non-small lung cancer cells (Liu et al., 2000).

LRP5 and LRP6 constitute distant family members of the LDL gene family, possessing a structural composition that deviates from that of the core members. The two receptors share the same domains as the core family members; the order of the domains, however, is divergent. LRP5 and LRP6 are comprised of EGF precursor homology domains followed by a ligand-binding domain directly bordering on the transmembrane domain. One common feature of the LDL family is missing in the LRP5/6 receptors: the NPxY motif. Both receptors are involved in canonical Wnt signaling and thus influence embryonal tissue development and homeostasis (Pinson et al., 2000; Wehrli et al., 2000).

LR11 also called SORLA (sorting-related receptor containing type-A repeats) is another distant member of the LDLR gene family. SORLA was first described after receptor-associated protein (RAP) purification and in parallel by a genetic screening for novel LDL receptors (Jacobsen et al., 1996; Morwald et al., 1997). The structure of SORLA differentiates from that of the core family; the most outstanding distinction constitutes

the N-terminal vacuolar sorting protein (VPS) domain. As an endocytic receptor for ApoE SORLA is endocytosed in a clathrin-dependent manner and mediates transport between the *trans*-Golgi network and the endosomal compartment (Taira et al., 2001; Yamazaki et al., 1997). SORLA is involved in the pathology of Alzheimer's disease (AD), representing a potential binding receptor for the amyloid beta precursor protein (APP), confining APP in the Golgi apparatus (Andersen et al., 2005; Schmidt et al., 2007), thus reducing APP cleavage. Moreover, SORLA expression levels are severely reduced in neurons of late-onset AD patients (Dodson et al., 2006; Rogaeva et al., 2007).

1.2 The low density lipoprotein receptor-related protein 1 (LRP1)

The *LRP1* gene is located on chromosome 12 and outlines a widely expressed surface receptor, known to bind and/or endocytose about 40 different ligands. LRP1 is involved in extracellular ligand binding and associated endocytosis, intracellular ligand binding and related signal transduction. Aside from LRP1´s contribution to ligand internalization, it plays a crucial role in living organisms, which is emphasized by the fact, that *LRP1* gene knock-out is lethal in early embryonic stage (Herz et al., 1992). After its synthesis LRP1 is released into the endoplasmic reticulum (ER), where a chaperon binds to the immature LRP1. The chaperon, the receptor associated protein (RAP), blocks LRP1 ligand binding sites in order to prevent premature ligand-binding and thus misfolding of the protein (Herz et al., 1991; Strickland et al., 1991; Williams et al., 1992). RAP binds to several members of the LDLR family at a neutral pH and its localization is restricted to the ER (Bu et al., 1995). Following glycosylation, the immature LRP1 receptor is transported to the *trans*-Golgi network, where it is cleaved by furin into the 85 kDa β-chain and the 515 kDa α-chain (Willnow et al., 1996b). Both subunits are associated non-covalently and form the mature LRP1 receptor. The α-chain consists of 4 ligand-binding domains, but it has been shown that the majority of ligands associate with binding domain II and IV (Neels et al., 1999; Willnow et al., 1994) (Fig. 2). Amongst the extracellular ligands are the initially discovered α2-macroglobulin and the tissue plasminogen activator (tPA) (Nassar et al., 2004; Van Leuven et al., 1994). The small β-chain comprises a short extracellular part, a single-pass transmembrane domain and an intracellular tail. Passing the Golgi-apparatus, the β-chain integrates into the plasma membrane and the α-chain is secreted into the extracellular matrix. Subsequently, both LRP1 subunits associate non-covalently to the mature LRP1

receptor. The cell surface receptor is localized to lipid rafts and clathrin-coated pits and is endocytosed in a fast, constitutive manner and recycled back to the plasma membrane (Anderson et al., 1978; Boucher et al., 2002; Goldstein et al., 1979; Harasaki et al., 2005; Kanai et al., 2014; Weaver et al., 1996).

Besides the role of LRP1 in lipid metabolism, the receptor has been demonstrated to be involved in numerous pathological processes and signaling pathways. For instance, LRP1 has a protective role in arteriosclerosis. It is expressed in vascular smooth muscle cells and endothelial cells of the vascular system, where it reduces the activity of the platelet-derived growth factor (PDGF), which is associated with the tyrosine kinases PDGF-receptor- β. Indeed, the PDGF-PDGFR complex activity leads to increased proliferation of smooth muscle cells (Boucher et al., 2003; Loukinova et al., 2002).

The intracellular C-terminal domain of LRP1 is composed of several motifs, being involved in ligand binding, internalization and downstream signaling. This includes two NPxY motifs: the membrane proximal NPxY1 and the distal NPxY2 motif. The distal NPxY2 motif overlaps with the YXXL motif, which represents the dominant endocytosis signal for LRP1. Furthermore, two di-leucine motifs are part of the C-terminus of LRP1, the distal one being involved in endocytosis (Li et al., 2000). Sorting nexin 17 (Snx17) has been shown to be a specific ligand for the proximal NPxY1 motif and to participate in the receptor recycling of LRP1 (Burden et al., 2004; van Kerkhof et al., 2005). It has become apparent, that both NPxY motifs play a crucial role in intracellular ligand-binding of adaptor proteins, including PSD95, Dab-2 and Fe65 (Gotthardt et al., 2000; Klug et al., 2011; Li et al., 2000; Martin et al., 2008). The relevance of the endocytic activity of LRP1 is highlighted by its involvement in AD pathology, since APP has been shown to be internalized in an LRP1-dependent manner via the NPxY-motif binding scaffolding protein Fe65 (Pietrzik et al., 2002; Ulery et al., 2000). In particular, the phosphorylation status of tyrosines inside the NPxY motifs modulates ligand binding and the joint LRP1-ligand endocytosis (Klug et al., 2011; Maier et al., 2013; van Kerkhof et al., 2005) (Fig. 2). The diversity of intracellular ligands and the phosphorylation status of the intracellular part of LRP1 determine LRP1´s endocytic function and downstream signaling. In summary, the major purpose of LRP1 is to bind extracellular ligands, internalize them via endocytosis and potentially transport them to the endosomal/lysosomal compartment for further processing.

Furthermore, LRP1 is involved in the activation of signaling cascades in varying manners, for instance by forming a complex with the PDGFR, which is involved in cell

proliferation signaling. Subsequent to complex formation of LRP1 and PDGFR, the c-terminal NPxY motif of LRP1 is phosphorylated (Loukinova et al., 2002; Newton et al., 2005). Hereafter, the ERK pathway can be activated in an LRP1 dependent manner (Martin et al., 2008; Muratoglu et al., 2010). Additionally, LRP1 influences signaling cascades by modulating the amount of signaling receptors via endocytosis. One example is the urokinase-type plasminogen activator receptor (uPAR) pathway, which is involved in the pathology of cancer (Conese et al., 1995; Weaver et al., 1997).

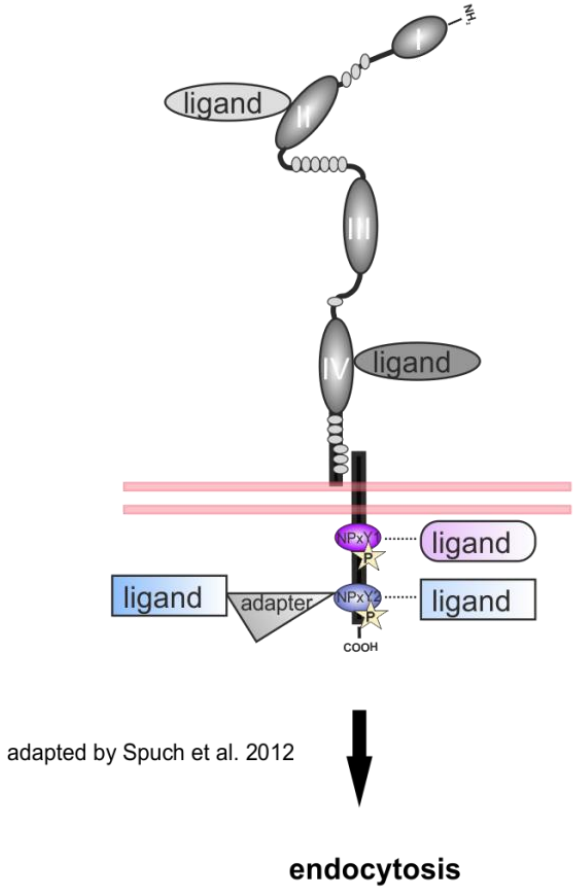

Figure 2: LRP1 signaling: LRP1 is composed of a large α-chain, consisting of 4 ligand binding domains. The α-chain is associated non-covalently with the smaller β-chain, harboring a single-pass transmembrane domain and an intracellular tail containing two NPxY motifs. Extracellular ligands of LRP1 can associate with the receptor mostly at domain II and domain IV. Intracellular ligands bind to the NPxY motifs of the intracellular tail of LRP1 directly or indirectly with an adaptor protein as scaffold. Subsequent to ligand binding, the receptor-ligand complex can be endocytosed in a clathrin-dependent manner, ensued by degradation in the lysosomal compartment or recycling back to the plasma membrane. After ligand binding, the NPxY motifs of LRP1 are phosphorylated and can in turn activate signaling cascades.

An intact structure of the NPxY motif as potential phosphorylation target is obligate for proper endocytosis and intracellular signaling of both receptors (Chao and Kunz, 2009; Maier et al., 2013). Complete LRP1 knock-out is embryonic lethal, as the blastocyst of these animals have been demonstrated to fail in implantation (Herz et al., 1992). The NPxY2 ki model, illustrated in the upper panel of figure 3 outlines a functional knock-out of LRP1.

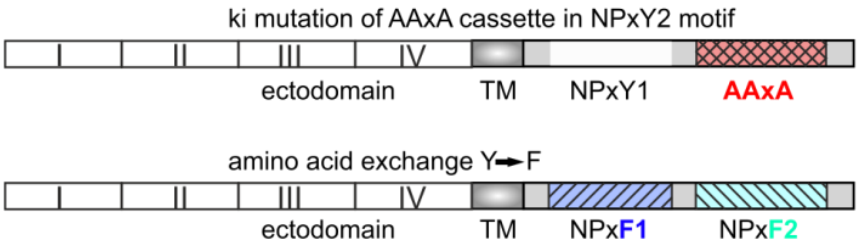

Figure 3: LRP1 variants: The used variants of LRP1 in this study are schematically illustrated. The upper panel depicts the NPxY2 ki model, harboring a substitution of a multiple alanine cassette (AAxA) into the NPxY2 motif of LRP1. The lower panel shows a LRP1 variant with single amino acid exchanges from tyrosine to phenylalanine in the NPxY motifs.

The generated LRP1 NPxY2 ki animals harboring an insertion mutation of the NPxY2 motif of LRP1 by a multiple alanine cassette (AAxA) are vital and fertile. Consequently, this model allows investigations in LRP1's role in ligand endocytosis and further linked downstream signaling pathways (Roebroek et al., 2006). The endocytosis rate of LRP1 in cells expressing the NPxY2 ki mutation is severely declined, as the NPxY2 motif overlaps with the major internalization motif (YATL). Furthermore, the tyrosine of the NPxY motif depicting an important phosphorylation site, is eliminated, further reducing LRP1 endocytosis (Klug et al., 2011; Li et al., 2000; Reekmans et al., 2010). However, the substitution of an alanine cassette into the NPxY1 motif or in both NPxY motifs of LRP1 resulted in embryonic lethality, providing a strong indication for the role of the NPxY motifs in embryonic development (Roebroek et al., 2006). The lower panel of figure 3 shows a sketch of a generated LRP1 construct, harboring single amino acid exchanges from tyrosine (Y) to phenylalanine (F) either in the NPxY1 or NPxY2 motif.

1.3 LRP1 in the neuronal system

LRP1 is highly expressed in cells of the central nervous system such as neurons. In order to investigate the role of LRP1 in the neuronal system, LRP1 was conditionally

knocked-out in neurons. Mice harboring this knock-out were vital; however, severe behavior phenotypes such as hyperactivity, tremor and dystonia were observed with these animals (May et al., 2004). Besides these phenotypes, the examination of mice harboring a conditional forebrain knock-out of LRP1 in neurons revealed a tremendous deficit in learning (Liu et al., 2010). The loss of LRP1 in neurons resulted in the reduction of the post synaptic density protein 95 (PSD95) and synaptophysin, both proteins are present in synapses, and are commonly used as synaptic marker proteins (Liu et al., 2010). Therefore, LRP1 might be involved in synapse formation as such or in synaptic density. Moreover, LRP1 was detected to associate with a subunit of a glutamate receptor, the N-methyl-D-aspartate receptor (NMDA-receptor), which hinted at the participation of LRP1 in neuronal signal transduction (May et al., 2004). LRP1 NPxY2 ki mice show behavioral abnormalities as they were demonstrated to be hyperactive (Maier et al., 2013). For cortical neurons of the LRP1 NPxY2 ki mice a decline in the uptake of a NMDA receptor subunit could be demonstrated in previous studies, which might provoke the hyperactivity to a certain extend (Maier et al., 2013).
One major hallmark of LRP1 in the neuronal system is its role as a cell surface endocytosis receptor. LRP1 is capable of internalizing numerous surface proteins such as APP, and can influence their processing through secretases. Depending on the site of processing, different cleavage products arise from APP, therefore, endocytosis might regulate the outbreak and the progression of AD (Asai et al., 2003; Koo and Squazzo, 1994; Pietrzik et al., 2004). LRP1 downstream signaling subsequent to ligand binding was shown to be involved in neurite outgrowth in previous studies. Here, ligand binding induced neurite outgrowth by the activation of the Ras/Raf/MEK/ERK pathway in vitro along with adult dorsal root ganglions and *in vivo* upon spinal cord injury (Qiu et al., 2004; Yoon et al., 2013).

1.4 The extracellular matrix

The extracellular matrix represents a physical anchor for cells inside a complex tissue and interconnects the whole organism. Cells frequently secrete proteins of the ECM themselves, whereby they determine the composition of their surrounding ECM. The composition of the ECM is influences numerous cellular processes such as cell differentiation and survival (Theocharis et al., 2016). Its structure varies depending on the body region; typical components are glycoproteins such as fibronectin and vitronectin, collagens, and proteoglycans such as heparan, elastin et cetera (Sidenius et

al., 2002). Cell motility depends on the composition of the ECM and its degradation by proteases.

1.5 Matrix metalloproteases

Matrix metalloproteases (MMPs), first described in 1962 as ECM degrading enzymes, belong to the family of zinc metalloproteases and are dedicated to the subdivision of the M10A matrixin proteases (Gross and Lapiere, 1962; Nagase et al., 1992). In a physiological system, MMPs are present in the extracellular milieu, at the plasma membrane and inside the cell. Their dominant function is to degrade proteins of the ECM by proteolytic cleavage. Among other effects, this results in the release of ECM bound growth factors, which affects amongst others cell proliferation (Fowlkes et al., 1994). MMPs can also process other substrates such as proteins located at the plasma membrane and therefore influence cellular behavior (Han et al., 2015). Structurally, MMPs are composed of a pro-peptide, a catalytic metalloproteinase domain with a $zinc^{2+}$ ion in its catalytic center, a hemopexin domain and a linker peptide. The majorities of MMPs are secreted into the extracellular space as inactive pro-forms; where, an unpaired cysteine of a highly conserved sequence of the pro-domain bridges the catalytic center and prevents ligand binding. During the cysteine switch, the cysteine binding is removed either by proteolytic cleavage or by chemicals, which results in MMP activation (Van Wart and Birkedal-Hansen, 1990). There are also membrane-bound MMPs, such as the membrane-type 1 MMP (MT1-MMP), and some proteinases are already in their active confirmation when they are secreted into the extracellular (Osenkowski et al., 2004). Here, the pro-domain has been removed intracellularly via furin cleavage (Pei and Weiss, 1995). Due to their proteolytic substrate and localization, MMPs are subdivided into five major categories: collagenases, gelatinases, stromelysins, matrilysins and type-I transmembrane MMPs. Through the interaction of MMPs with their endogenous inhibitors, the tissue- inhibitors of metalloproteinases (TIMP), MMP activation is regulated. The balanced regulation of MMP activation and expression is crucial to obtain health; if a dysbalance occurs, diseases such as cancer or atherosclerosis emerge (Newby, 2005; Stearns and Stearns, 1996). Both receptors, LRP1 and β1-integrin, participate in the regulation of MMP expression and activity, which is elucidated below.

1.6 The involvement of LRP1 in cell migration in health and disease

The role of LRP1 in cell migration has been mainly examined in the context of cancer. However, its role in cancer is still elusive, since published data are contradictory. There are several early studies reporting a reduction of LRP1 levels in carcinogenic cells (Jensen et al., 1989; Van Leuven et al., 1979), which was affirmed by recent studies investigating the LRP1 expression of hepatocellular carcinoma and colorectal carcinoma (Huang et al., 2012; Obermeyer et al., 2007). However, converse results were described for LRP1 levels in malignant astrocytomas and endometrial carcinomas (Baum et al., 1998; Catasus et al., 2011; Yamamoto et al., 1997). The transformation of healthy cells to malignant cells and the correlated alterations in homeostasis and invasiveness is a complex process, most likely involving LRP1 to a certain extend.

In a physiological environment, cells are part of a 3D system by connecting themselves to proteins of the ECM. For cell movement, the cytoskeleton is reorganized and the ECM is degraded by proteinases. Besides the influence of cell surface receptor distribution on motility, the distribution of surface receptors determines cell proliferation by receptor-mediated outside-in signaling of growth factors. LRP1 is known to trigger the proliferation of smooth muscle cells by the PDGFR pathway. The dysregulation of the PDGFR pathway represents a major hallmark in the pathology of arteriosclerosis (Boucher et al., 2003; Boucher et al., 2002; Loukinova et al., 2002). However, a direct impact of LRP1 on proliferation of malignant cells is yet unknown.

Healthy cells and transformed cells can only migrate, and in the case of metastasis invade further organs or tissues by degrading their surrounding ECM. MMPs and serine proteases are capable of degrading the ECM and thus facilitate cell movement (Kerkela and Saarialho-Kere, 2003; Okada et al., 1997). Strikingly, an immense increase in MMPs has been observed in several types of cancer. The role of LRP1 in cell migration was demonstrated by inactivating the surface receptor via siRNA, which resulted in severe reduction of cell migration rates in Schwann cells (Mantuano et al., 2010). Interaction between LRP1 and several metalloproteases was demonstrated, in particular with the gelatinases MMP2 and MMP9, which are often referred to in the context of cancer pathology (Komatsu et al., 2004; Song et al., 2009). LRP1 can either regulate MMP expression on mRNA levels, or via altered receptor-ligand binding endocytosis, thereby impairing cell migration and cell invasion (Emonard et al., 2005; Song et al., 2009). LRP1 is able to bind complexes of MMP2 and thrombospondin-2 (TSP-2), of MMP9 and tissue inhibitor of metalloproteinases 1 (TIMP-1), as well as proMMP-2-

TIMP-2 and mediates their endocytosis (Yamamoto et al., 2015). The inhibitors TIMP-1, TIMP-2 and TIMP-3 are also cleared by LRP1 from the ECM by endocytosis via LRP1, thus preventing MMP endocytosis (Yamamoto et al., 2015). The plasma protein α2-macroglobulin can regulate MMP levels in the extracellular space by entrapping metalloproteinases, probably ensued by LRP1 endocytosis (Moestrup et al., 1993; Nagase, 1997). In addition, binding of the serine protease tissue-type plasminogen activator (tPA) to LRP1 induces MMP9 gene expression and enhances tyrosine phosphorylation of the intracellular part of LRP1. Subsequently, the mitogen activated kinase pathway (MAPK) is activated by the intracellular domain of LRP1 in renal interstitial fibroblasts (Hu et al., 2006; Wang et al., 2003).

A further mechanism regulating motility in healthy and malignant cells involving LRP1 is the urokinase-type plasminogen activator receptor (uPA-uPAR) pathway. Indeed, increased levels of the uPA receptor were present in various types of tumors (Alpizar-Alpizar et al., 2010; Nielsen et al., 2007). LRP1 is capable of internalizing the complex of uPA-uPAR and the plasminogen activator inhibitor-1 (PAI-1/2) resulting in lysosomal degradation of the complex or recycling to the plasma membrane. The components of the complex have a pro-migratory character by driving ECM degradation. If the zymogen pro-uPA binds to the uPA-receptor, uPA is converted into its active form. uPA in turn can activate the zymogen plasminogen, whereby the active serine protease plasmin degrades proteins of the ECM and releases membrane-bound MMPs (Fisher et al., 2001). In a positive feedback manner, plasmin can activate pro-uPA and thus promote cell migration. Once LRP1 levels are altered in tumor cells, the uPA-uPAR pathway gets into dysbalance in favor of cell migration (Fisher et al., 2001; Sato et al., 2016).

1.7 The integrin receptor family

Besides the role of LRP1 in degradation of the ECM and the regulation of correlated downstream signaling after ligand binding in cancer, LRP1 partially regulates the composition of the plasma membrane. Therefore, extracellular ligands are bound and subsequently endocytosed in a clathrin-dependent manner. Furthermore, an impact of LRP1 on the surface representation and maturation of β1-integrin was demonstrated previously (Salicioni et al., 2004).

Integrins are surface transmembrane proteins consisting of a large extracellular domain, a single pass transmembrane domain and a small intracellular part harboring a

membrane-proximal NPxY motif and a membrane distal NxxY motif. Monomeric integrins assemble to non-covalently bound heterodimeric receptors composed of 18 α- and 8 β-subunits resulting in 24 distinct receptors. One prominent representative is β1-integrin, which can associate with 12 different α-subunits (DeSimone et al., 1987).

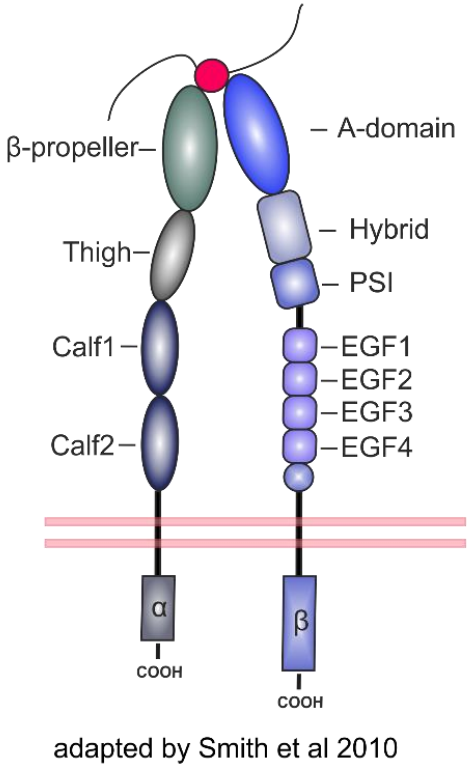

Figure 4: Structure of the α5β1-intergin receptor: The β-subuntit is composed of a short intracellular domain ensued by a single transmembrane domain and the membrane proximal β-tail. Subsequently, the β-subunit comprises of the hybrid domain, containing epidermal-growth factor repeats (EGF). The plexin/semaphorin/integrin (PSI)-domain is followed by the ligand binding A-domain. The α-subunit is structurally composed of an intracellular domain, a single-pass transmembrane domain, two calf domains, a thigh domain and a ligand binding β-propeller head domain.

In the course of evolution, integrins emerged during the development of the metazoan, whereby integrin representatives are already present in invertebrates like *C. elegans* and *drosophila melanogaster*. Moreover, homologues of the α- and β-subunits could already be detected in prokaryotes (Johnson et al., 2009). Integrins are ubiquitously expressed and play a pivotal role in development; therefore, the complete knock-out of for instance β1-integrin prohibits gastrulation and is lethal during the peri-implantation period (Brakebusch et al., 1997; Fassler and Meyer, 1995; Stephens et al., 1995). First described in 1986, integrins are major ECM-binding receptors and can be categorized into four major groups (Tamkun et al., 1986): the laminin-binding receptors, the collagen-binding receptors, the RGD-sequence-binding receptors (amino acid sequence

of Arginine-Glycine-Asparagine acid) and the leukocyte specific receptors (Hynes, 2002). After translation, integrin subunits associate with their binding partner in the ER, are translationally modified by passing through the Golgi apparatus and finally reach the cell surface as a heterodimeric receptor. Integrins are the major extracellular matrix protein binding receptor, thus connecting cells physically to their environment via the integrin ligand binding head. This allows cells to react on changes of the ECM in a dynamic manner. However, integrins have turned out to not only play a role in cell adhesive processes, but to be also involved in numerous signaling cascades. When reaching the cell surface, the heterodimeric receptor is in a bent, inactive conformation (Xiong et al., 2001; Xiong et al., 2002). After activation, integrin receptors can mediate signaling in a bidirectional manner across the plasma membrane.

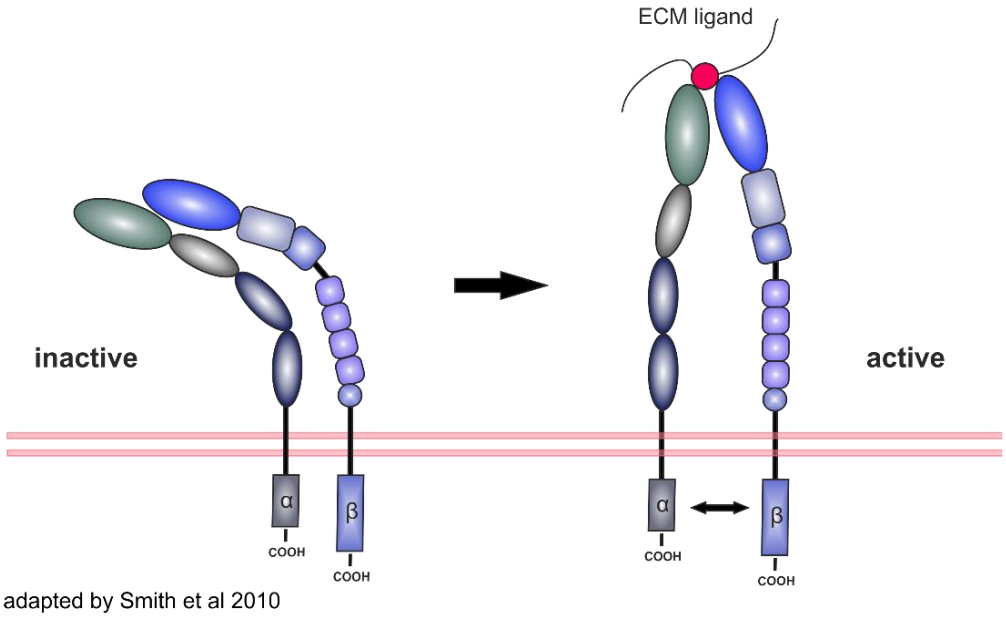

Figure 5: Activation of integrin receptors: The integrin receptor, reaching the cell surface is in its bent, inactive state. Subsequent to ligand binding or via inside-out signaling, the integrin receptor shifts into its active, extended conformation, whereby the intracellular domains of the integrin receptor separate from each other.

One possibility is the inside-out directed activation of integrins mediated by the intracellular binding of the cytoskeletal protein talin head domain to the membrane-proximal NPxY motif of adherent cells (Calderwood et al., 2002; Kim et al., 2012). In addition, the cytoskeletal linker protein kindlin binds to the membrane-distal NxxY motif of β-integrin for its activation (Ma et al., 2008; Moser et al., 2008). Then, the extracellular part of the integrin receptor switches into an extended conformation with a free ligand-binding head showing high ligand binding affinity. Furthermore, due to the switch, the intracellular domains of the α- and β-integrins separate from each other

(Xiao et al., 2004; Zhu et al., 2007). The inside-out signaling seems to play a major role in non-adherent cells such as platelets; in adherent cells however, the outside-in signaling pathway seems to be more relevant (Moser et al., 2008; Nieswandt et al., 2007). In addition to the fully activated conformation, an intermediate state of structure and ligand affinity has been described (Adair et al., 2005; Chigaev et al., 2003).

By means of outside-in signaling the availability of ECM ligands induces the activation of integrins. After association with an ECM molecule at the extracellular domain, the active conformation of the integrin receptor is stabilized. As a positive feedback, further integrin receptors are recruited to the site of integrin-ECM binding. Subsequently, due to the extracellular ligand binding and receptor clustering, an intracellular signaling cascade is activated, resulting in the formation of an intracellular adhesive complex. Subsequent to cell adhesion, the components of the adhesion complex activate signaling cascades, which are involved in cell adhesion, migration, proliferation, differentiation and survival (Legate et al., 2009; Rainero and Norman, 2015; Wang et al., 2011a).

1.8 Integrins in the neuronal system

Integrins are expressed in neuronal cells, where they constitute key players in neuronal development and homeostasis. The subventricular zone (SVZ) and the dentate gyrus are the only sites of the brain, where new neurons are generated during the entire lifespan. Neuronal progenitors of the SVZ migrate to the center of olfactory perception, the *bulbus olfactorius*, which has been shown to be dependent on integrin presence (Belvindrah et al., 2007; Emsley and Hagg, 2003). After reaching their destination, neurons start to sprout and form protrusions becoming dendrites and one axon. At the distal, moving edge of the outgrowing axon there is the axonal growth cone. Equal to other cell types, neurons connect themselves to their environment by integrin-ECM contacts. Especially at the dynamic growth cone focal adhesion like structures, so called focal point contacts, assemble (Gomez et al., 1996; Robles and Gomez, 2006; Warren et al., 2012). Subsequent to integrin-ligand binding, the intracellular adhesome assembles similar to other cell types. Amongst others FAK, vinculin and paxillin are recruited to sites of contact to the ECM (Renaudin et al., 1999). After neuronal sprouting, cells start to form a network by connecting themselves to other neurons via synapses. All these processes require a crosstalk of the interior and exterior of neurons and result in a rearrangement of the cytoskeleton (Belvindrah et al., 2007; Ribeiro et al., 2013; Tan et al., 2011; Warren et al., 2012). Especially the process of synapse formation and the

capacity of modulating the connections in morphology and location by plasticity are dependent on a dynamic actin cytoskeleton, which also forms the site of synaptic contacts. In mature axons of neurons, integrins are not prominently present, but after injury β1-integrin is expressed and drives axonal regeneration by focal adhesion signaling (Bi et al., 2001; Carlstrom et al., 2011; Tan et al., 2011). Integrins hence seem to play a pivotal role in processes of the neuronal system by regulating the remodeling of the actin cytoskeleton and thus affect cell migration, neuronal sprouting and synapse plasticity (Huang et al., 2006).

1.9 The course of cell adhesion and migration

Cells connect themselves to the ECM with heterodimeric cell surface receptors, composed of α-integrins and β-integrins. After ECM ligand binding, intracellular proteins are recruited to sites of adhesion (Hotchin and Hall, 1995). Without own enzymatic activity, integrins transduce signals across the plasma membrane and regulate the cytoskeletal organization by assembling focal adhesions. All proteins connecting the integrin receptor directly or indirectly with the cytoskeleton, comprise the adhesome with about 150 interaction partners (Zaidel-Bar et al., 2007). The composition of the adhesome may vary between the different integrin receptors and cell types. Formation of the adhesome after β-integrin activation commonly starts with the initial binding of talin to the cytoplasmic tail of the β-subunit, linking the integrin receptor directly to actin filaments (Campbell and Ginsberg, 2004b). Subsequently, vinculin associates with talin and can also link the complex to actin (Marchisio et al., 1988). Further molecules are recruited to sites of activated integrins such as paxillin and the non-receptor tyrosine kinase, the focal adhesion kinase (FAK) (Burridge et al., 1992; Guan et al., 1991; Schaller et al., 1992; Turner and Miller, 1994). Integrins initially connect cells to their surrounding and generate a seeding point for the assembly of the adhesome.

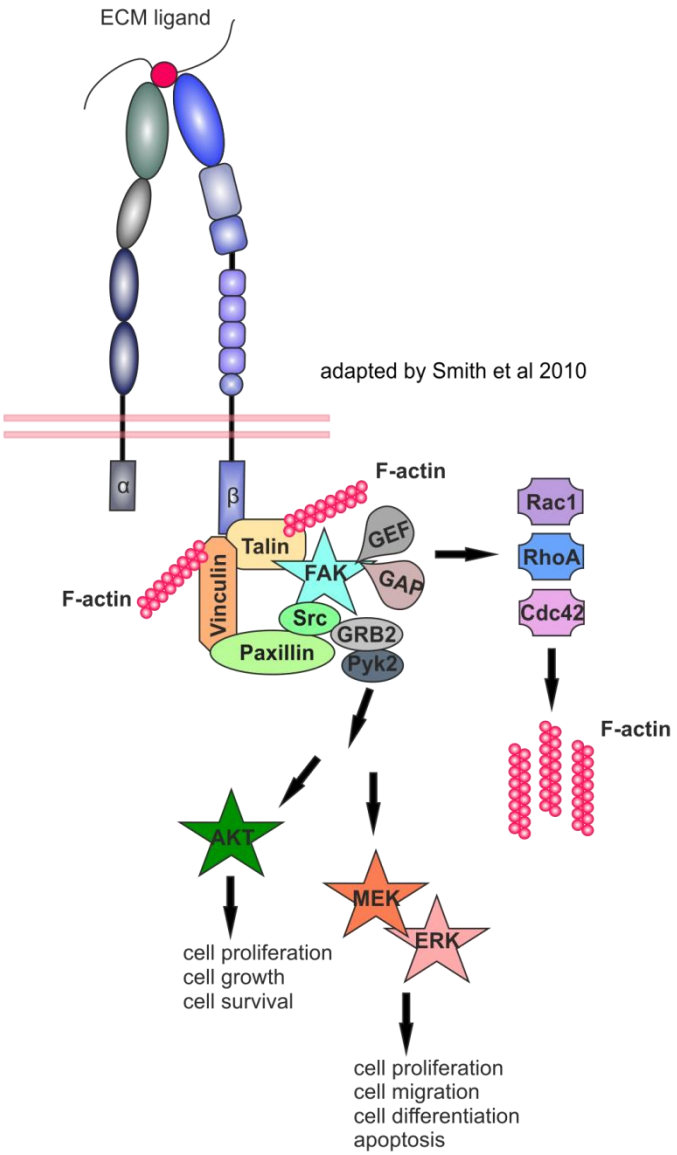

Figure 6: The adhesome: The adhesome is composed of the initial ligand talin, directly associated with the intracellular tail of the β-subunit of the integrin receptor. Talin directly connects the adhesome to the actin cytoskeleton. Subsequent to talin binding, numerous components of the adhesome are recruited to the site of integrin-ECM-binding. Vinculin binds to talin and bridges the adhesome to the cytoskeleton. The non-receptor tyrosine kinase focal adhesion kinase (FAK) is recruited to the complex and downstream of its autophosphorylation at tyrosine 397 further components associate. GTPase activating proteins (GAPs) and guanidine nucleotide exchange factors (GEFs) initiate the activation of the GTPases RhoA, Rac1 and CDC42, which regulate the actin cytoskeleton organization. Src-kinases are recruited to the phosphorylated FAK, which results in the binding of the growth factor receptor-bound protein 2 (GRB2) and the protein tyrosine kinase 2 (Pyk2). This emerging complex can activate the AKT pathway, regulating cell proliferation, growth and survival, or the mitogen-activated protein kinase (MAPK) pathway by phosphorylating the extracellular signal-regulated kinas (ERK). The ERK signaling cascade affects cell proliferation, migration, differentiation and cell apoptosis.

Subsequent to adhesion, cells start to spread on their chosen surface in a 2D model. In the first phase of spreading, cells protrude radially from the point of adhesion in a passive manner to explore the substrate (Dubin-Thaler et al., 2004). Focal contacts

mature to nascent focal complexes and subsequent downstream signaling of the recruitment of components initiates one major event: the autophosphorylation of FAK at tyrosine 397. This induces other proteins such as guanidine nucleotide exchange factors (GEFs) and GTPase activating proteins (GAPs) to engage to the adhesome. In the next step, the GTPases Rho, Rac1 and CDC42, are activated. This results in a reorganization of the actin cytoskeleton by actively protruding the plasma membrane. For this purpose, cells polarize actin filaments and protrude the membrane at the leading edge of the movement. Fingerlike filopodia and flat hand like lamellipodia emerge subsequently to actin reorganization and display structures of cellular protrusion (Fig. 7). Moreover, stress fibers, which are composed of contractile actomyosin filaments, are formed in a GTPase driven manner (Tojkander et al., 2012). Stress fibers, depicted as stars in figure 7 are mostly connected to FAs. Henceforth, the second phase of cell spreading is a force dependent mechanism, which can be generated by the ECM or by cells themselves via contraction of the myosin containing fibers. Subsequent to cell adhesion, the components of the adhesion complex activate signaling cascades, which are involved in cell adhesion, migration, proliferation, differentiation and survival (Legate et al., 2009; Rainero and Norman, 2015; Wang et al., 2011a).

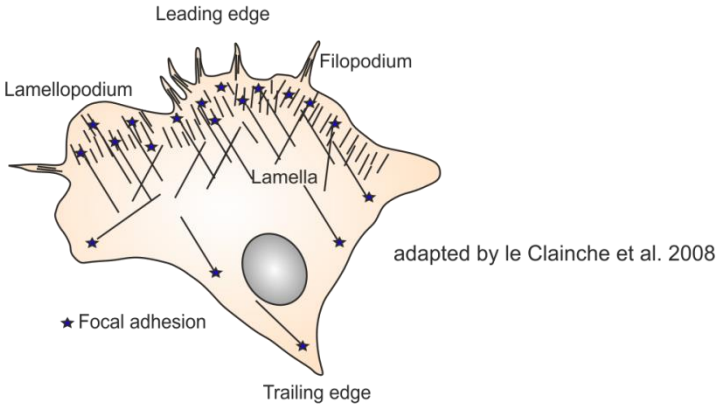

Figure 7 Spreading of a cell: After adhering to a substratum, cells start to protrude their membrane driven by actin cytoskeleton (actin fibers shown as black lines) re-organization. Lamellopodial and filopodial structures emerge. Stress fibers which are composed of contractile actomyosin fibers, form driven by Rho signaling and are commonly connected to focal adhesions (FAs) (blue stars). Focal contacts or nascent adhesions are mainly present at the leading edge of a moving cell; however, FAs are present throughout the whole cell.

Moreover, downstream of FAK autophosphorylation, SH2-domain containing adaptor proteins such as the growth factor receptor-bound protein 2 (GRB2) and the tyrosine kinase Src are recruited to FAs (Cheng et al., 2014; den Hertog et al., 1994; Xing et al.,

1994). Further downstream targets are the mitogen-activated protein kinase (MEK); which in turn can either induce ERK1/2 activation via phosphorylation or the activation of the Akt pathway (Acosta et al., 2003; King et al., 1997; Sanders and Basson, 2000).
Cell migration of adherent cells is mostly directed by external factors such as growth factors, chemokines, mechanical force or the composition of the ECM (Friedland et al., 2009; Kolega, 1986; Royce and Baum, 1991; Senior et al., 1983; Staquet et al., 1995). Cells polarize and protrude their plasma membrane by polymerizing actin filaments at the leading edge of movement in the direction of the external signals. This protrusion is composed of flat, broad lamellipodia and finger-like filopodia. At the edge of these structures, cells assemble focal contacts, further maturing into nascent adhesions that connect the cytoskeleton to the ECM. Cytoskeleton reorganization and traction caused by actomyosin fiber contraction pulls the cell body in the direction of the protrusion. Cell migration requires an equilibrium of focal adhesion formation, maturation at the leading edge and disassembly at the trailing edge (Webb et al., 2002). In the 1990`s, integrin trafficking from the plasma membrane by endocytosis and recycling back to the surface was demonstrated by the group of Bretscher (Bretscher, 1989). Mostly, integrins are recycled back to the plasma membrane involving two distinct recycling pathways, or as demonstrated for the ligand bound α5β1-integrin receptor, integrins can undergo lysosomal degradation (di Blasio et al., 2010; Lobert et al., 2010; Woods et al., 2004). The pathway of endocytosis for integrin receptors depends on the type and tissue of the receptor: Possible endocytosis variants known for integrins are: macropinocytosis, clathrin-mediated endocytosis and clathrin-independent endocytosis either via caveolae or via clathrin-independent carriers (Bridgewater et al., 2012; Pellinen et al., 2006; Shi and Sottile, 2008). Integrin receptors can be internalized in an inactive and active state, even if they are bound to an extracellular ligand. The process of internalization is crucial for FA disassembly. Turn-over was reported to be dependent on myosin contraction, dynamin and clathrin presence, both proteins were located close to FAs (Chao and Kunz, 2009; Ezratty et al., 2005). Further components were shown to be involved in a functional disassembly of FA such as FAK, Src-kinases, paxillin, ERK, p130Cas and the myosin light chain (MLC) kinase (Webb et al., 2004).

1.10 The Ras/Raf/MEK/ERK signaling pathway

Surface receptors such as β1-integrin and LRP1 are linked to the Ras/Raf/MEK pathway by indirectly activating the extracellular-signal regulated kinase (ERK1/2). The serine/threonine kinase ERK can be recruited to adhesomes by integrin clustering and subsequent downstream signaling or through growth factor binding (Asati et al., 2016; Fincham et al., 2000; Hauck et al., 2000; Kim et al., 1997; Roberts and Der, 2007). The indirect signaling function of integrin triggers binding of Src-kinases to sites of integrin clustering, which is facilitated by the non-receptor tyrosine FAK phosphorylation. Following, the GRB2 is recruited to the adhesome (Smith and Marshall, 2010). This adaptor protein mediates the association of the guanine nucleotide exchange factors son of sevenless 1 (SOS1) signaling molecule to the complex. Hereafter, the membrane associated guanine nucleotide binding protein Ras enriches to the region of FAs and is switched to its ON state while being bound to guanosine-triphosphate (GTP). Subsequently, the serine-threonine kinase Raf1 is activated via phosphorylation. Following, Raf-1 triggers activation of the mitogen effector kinase (MEK) which in turn activates the serine/threonine kinase mitogen activated protein kinase (MAPK) ERK1/2 by phosphorylation. ERK is a key regulator of cell proliferation and survival since its activated form pERK1/2 translocates into the nucleus, where it induces changes in gene expression by phosphorylation and regulates transcription factors (Cruzalegui et al., 1999; De Cesare et al., 1998). Misregulation of this pathway is commonly observed in numerous cancer types.

LRP1 is also linked to the activation of ERK1/2 via phosphorylation, for instance demonstrated for tPA stimulation of primary cortical neurons (Martin et al., 2008). Binding of tPA or α2-macroglobulin to LRP1 results in the activation of Src-familiy kinases, which subsequently phosphorylate their downstream targets and consequently ERK1/2 (Shi et al., 2009). Neurons generated from the NPxY2 ki mouse model harboring the functional knock-out of LRP1 revealed decreased levels of phosphorylated ERK1/2 (Maier, 2013). LRP1 is linked to carcinogenic pathogenesis by influencing cell migration and thus invasiveness in a controversial manner. A former study has identified LRP1 as a major docking site for focal adhesion components and regulating focal adhesion disassembly via ERK signaling in human follicular thyroid carcinoma FTC133 cells (Langlois et al., 2010).

1.11 The link between LRP1 and β1-integrin

The uPA receptor as LRP1 ligand is involved in cell adhesiveness and motility by directly binding to vitronectin, a protein of the ECM (Wei et al., 1994). A triple complex of uPA-uPAR and vitronectin can be formed. Besides the direct interaction with the ECM, the uPA receptor affects cell adhesion by interacting with several integrin receptors such as β1, β2, β3 and β5 as described for several malignant cell lines (Reinartz et al., 1995; Wei et al., 1996; Xue et al., 1997). Integrins are heterodimeric cell surface receptors connecting cells to the ECM (Hynes, 2002). An integrin receptor described to physically interact with uPAR is the αvβ5 vitronectin integrin receptor, whereby interaction of the two surface receptors promoted cell migration of breast cancer cells (Carriero et al., 1999). The vitronectin-binding integrin receptor αvβ3 was also shown to physically interact with uPAR by activating downstream integrin signaling and thus enhancing cell migration (Schiller et al., 2009; Wei et al., 2008). An interaction between the fibronectin receptor α5β1 and uPAR was reported to enhance the binding of the integrin receptor to fibronectin (Wei et al., 2005). After β1-integrin-uPAR association, the MAPK pathway is activated by phosphorylation of the extracellular signal-regulated kinase 1/2 (ERK) (Aguirre-Ghiso et al., 2001; Liu et al., 2002). A further indication of the participation of LRP1 in the migrating process is the detection of augmented amounts of LRP1 at the leading edge of invasive breast cancer cells (Chazaud et al., 2002). Integrins have been shown to be upregulated in various tumor types, such as in ovarian cancer cells, and are involved in many steps of tumor development and invasiveness (Eke et al., 2012; Zhang and Zou, 2015). Especially the regulation of cell migration and thus the metastatic potential of a tumor have revealed integrins as a major target for cancer therapy and as a possible biomarker. Integrins have a strong impact on the regulation of the activity state and amount of MMPs in the ECM. MMPs can associate with integrin receptors to complex clusters at sites of adhesion and facilitate cell migration by dissolving points of contact between the cell and the ECM. This was observed in keratinocytes (Yamamoto et al., 2015). Furthermore, blocking of β1-integrin in human breast cancer cells resulted in a decrease of active MMP2 (Borrirukwanit et al., 2014; Missan et al., 2015). Interestingly, LRP1 has been shown to influence MMP activity by either internalizing the proteases or their activity-controlling-inhibitor TIMPs. MMP expression can also be affected by LRP1 signaling (Emonard et al., 2005; Song et al., 2009).

There are some studies linking LRP1 and β1-integrin to each other. After LRP1 silencing in Schwann cells, alterations in the actin-cytoskeleton and decreased cell migration rates were observed (Mantuano et al., 2010). These processes are closely linked to integrin activity, raising the hypothesis of an interaction between LRP1 and β1-integrin. The presence of LRP1 was shown to regulate surface levels of β1-integrin, a further indication for a crosslink between the two receptors (Salicioni et al., 2004). However, it is still elusive, if and where both receptors interact, and the influence of the potential interaction on related processes is also unknown.

2. Purpose of the study

Due to the endocytic function of LRP1 and its variety of extracellular and intracellular ligands, LRP1 is involved in the regulation of the composition of the plasma membrane and the regulation of protein levels in the extracellular milieu. Furthermore, the presence of LRP1 has been shown to influence the maturation of another dominant surface receptor, the integrin receptor (Salicioni et al., 2004). Both receptors mediate cellular communication with the exterior and are involved in downstream signaling pathways. As a consequence, both receptors affect the signaling complexes, modulating the cytoskeletal organization and therefore cell morphology and motility (Cao et al., 2006; Dedieu et al., 2008; Hergott et al., 1993; Zhang and Zou, 2015). A specific knock-out of LRP1 in Schwann cells led to altered cytoskeletal organization and a change in migration behavior, underlining a correlation between LRP1 and β1-integrin (Mantuano et al., 2010). Additionally, the phosphorylation state of the intracellular part of LRP1 has been shown to affect the surface recruitment of β1-integrin (Czekay et al., 2003; Hu et al., 2007). One major regulatory motif concerning receptor-mediated endocytosis of LRP1 is the intracellular membrane-distal NPxY2 motif. Its crucial role in the clathrin-mediated receptor endocytosis was investigated in previous studies by generating a mouse model harboring an insertion of a multiple alanine cassette into the NPxY2 motif, changing it to an AAxA motif (Roebroek et al., 2006). As a result, the endocytosis rates of LRP1 itself and of its ligands were dramatically reduced (Maier et al., 2013; Pflanzner et al., 2011; Reekmans et al., 2010).

The main aim of this study was to investigate the interplay between LRP1 and β1-integrin in receptor endocytosis and to analyze related biochemical and behavioral cellular changes. The results of the crosslink between LRP1 and β1-integrin and the possible impact on cell behavior such as migration then can be projected to the pathogenesis of cancer. Cell motility determines the invasive potential of tumors and hereby the prognosis of patients. Through the use of mouse embryonic fibroblasts generated from the LRP1 NPxY2 ki model, the consequences of the extremely reduced endocytosis of LRP1 and the loss of the tyrosine phosphorylation site on the β1-integrin receptor were examined via various biochemical methods such as biotinylation of surface proteins, internalization studies and co-immunoprecipitations. Furthermore, the downstream effects on cell morphology, adhesion and migration were surveyed by imaging methods such as immunocytochemistry and assays studying the adhesion and

migration capacity of cells. In order to get further insight into processes being linked to the coupled endocytosis of the two receptors, downstream signaling events were analyzed via SDS-PAGE and further methods. Additionally, the interplay of both receptors in a neuronal setting was examined. LRP1 and β1-integrin are both expressed in neurons and have been described to be involved in dendritic outgrowth (Goh et al., 2008; Warren et al., 2012; Wolf et al., 1992; Yoon et al., 2013). The role of the potentially LRP1-mediated endocytosis of β1-integrin was therefore analyzed in primary cortical neurons, generated from LRP1 NPxY2 ki mice. Cell migration in the brain was assayed by analyzing cell migration along the rostral migratory stream. For this purpose, proliferating cells were marked *in vivo* by BrdU injection and examined by immunohistological staining. The migration behavior to the *Bulbus olfactorius* was examined, since LRP1 and β1-integrin are involved in cell migration regulation. Finally, the spine morphology of neurons generated from the NPxY2 ki animals was analyzed by imaging methods.

3. Material

3.1 Chemicals

Acetic acid	Roth, Karlsruhe
30% Acrylamide 37.5:1 Bis-Acrylamide	National Diagnostics, USA
40% Acrylamide 29:1, Bis-Acrylamide	National Diagnostics, USA
Agar	Roth, Karlsruhe
Agarose-A-Beads	Thermo Fisher, USA
α-MEM	Lonza, Basel, Switzerland
2-Amino-2-methyl-1.3-propanediol (Ammediol)	Sigma-Aldrich, Taufkirchen
Ammoniumpersulfate (APS)	Sigma-Aldrich, Taufkirchen
B27-supplement	Thermo Fischer, USA
β-Mercaptoethanol	Roth, Karlsruhe
Bromphenolblue	Roth, Karlsruhe
Bovine Serum Albumin (BSA)	Sigma-Aldrich, Taufkirchen
Calciumchloride (CaCl2)	Merck, Darmstadt
Chlorpromazine (CPZ)	Sigma-Aldrich, Taufkirchen
Coomassie Brilliant Blue	Merck, Darmstadt
Coppersulfate (CuSO4)	Sigma-Aldrich, Taufkirchen
Collagen I (rat tail)	Thermo Fisher, USA
Crystal violet	Sigma-Aldrich, Taufkirchen
Desoxynucleotide-tri-phosphate	New England Biolabs, Frankfurt
Dimethylsulfoxide (DMSO)	Sigma-Aldrich, Taufkirchen
DMEM	Invitrogen, Karlsruhe
DRAQ5TM	Biostatus Limited, UK
Dry-milk (fat-free)	Roth, Karlsruhe
Ethanol	Roth, Karlsruhe
Ethidiumbromide	Sigma-Aldrich, Taufkirchen
Ethylendiaminetetraacetic acid (EDTA)	Roth, Karlsruhe
Fetal Calf Serum (FCS)	Invitrogen, Karlsruhe
Fibronectin	Sigma-Aldrich, Taufkirchen
Gelatine	VWR Chemicals, Darmstadt

GlutaMax	Thermo Fisher, USA
Glycerine	Roth, Karlsruhe
Glycin	Merck, Darmstadt
Goat Serum	Invitrogen, Karlsruhe
Histofix	Roth, Karlsruhe
HEPES	Sigma-Aldrich, Taufkirchen
Hydrochloric acid (HCl)	Roth, Karlsruhe
Immobilion™ Western HRP Substrate Reagents	Millipore, USA
Iodoacetamide (IAA)	Sigma-Aldrich, Taufkirchen
Isofluoran	Forene® Abbot, Wiesbaden
Isopropanol	Roth, Karlsruhe
Magnesium-chloride (MgCl2)	Roth, Karlsruhe
Methanol	Roth, Karlsruhe
Neurobasal Media	Thermo Fisher, USA
NeutrAvidin-Agarose beads	Thermo Fisher, USA
Nitrocellulose membrane	Hartenstein, Würzburg
Nonidet-P40	Roche, Mannheim
Paraformaldehyde	Sigma-Aldrich, Taufkirchen
Pefa-bloc	Sigma-Aldrich, Taufkirchen
MMP2 and MMP9 specific peptide	Enzo Lifescience, Lörrach
Polyethylenimine (PEI)	Polysciences, Eppelheim
Poly-L-Ornithine	Sigma-Aldrich, Taufkirchen
Ponceau S	Sigma-Aldrich, Taufkirchen
Potassium chloride (KCl)	Sigma-Aldrich, Taufkirchen
Potassium di-hydrogen phosphate (KH2PO4)	Roth, Karlsruhe
Protease inhibitor cocktail tablets, EDTA-free	Roche, Mannheim
Prolong®Gold antifade reagent	Invitrogen, Darmstadt
Roti-Load (4 x Protein loading buffer)	Roth, Karlsruhe
Seakem LE Agarose	Cambrex, USA
Sodium azide (NaN3)	Merck, Darmstadt
Sodium chloride (NaCl)	Roth, Karlsruhe
Sodium di-hydrogen phosphate (NaH2PO4)	Merck, Darmstadt
Sodium dodecyl sulfate (SDS)	BioRad, Munich
Sodium hydroxide (NaOH)	Merck, Darmstadt

Sodium 2-mercaptoethanesulfonate (MesNa)	Sigma-Aldrich, Taufkirchen
Sodium pyruvate	Invitrogen, Karlsruhe
Sucrose	Sigma-Aldrich, Taufkirchen
Sulfo-NHS-LC-LC-Biotin	Pierce, Rockford, USA
TEMED (N,N,N+,N+-Tetramethylendiamine)	BioRad, Munich
Tris-Hydrochloride (HCl)	Roth, Karlsruhe
Tris-Base	Roth, Karlsruhe
Triton X-100	Sigma-Aldrich, Taufkirchen
Trypsin/EDTA	Invitrogen, Karlsruhe
Tween-20	Roth, Karlsruhe
Yeast Extract	Roth, Karlsruhe
Zinc chloride (ZnC_2)	Roth, Karlsruhe

3.2 Antibiotics

Ampicillin	Sigma-Aldrich, Taufkirchen
Kanamycin	Sigma-Aldrich, Taufkirchen
Penicillin/Streptomycin (Pen/Strep)	Invitrogen, Karlsruhe

3.3 Software

Adobe Photoshop CS5

CorelDraw X7

EndNote X5

GraphPad Prism4

ImageJ

Microsoft Office 2010

MultiGauge Vers.3

SECentral 7.0/ Clonemanager

SnapGene Viewer 2.8.2

ZEN 2008 (Zeiss)

3.4 Laboratory equipment

Agarose gel electrophoresis system	Biometra, Göttingen
Agarose gel documentation imager	INTAS, Göttingen
BioPhotometer plus UV/vis	Eppendorf, Hamburg

Centrifuge Eppendorf 5415D	Eppendorf, Hamburg
Centrifuge Hettich	Universal 32 Hettich, Tuttlingen
Centrifuge Hereus Fresco Kendro	Langenselbold
CO2 incubators	New Brunswick, USA
Cryo Freezing Container	Nunc, Wiesbaden
Flat bed shaker	Infors Bolmingen, Switzerland
Freezer -20 C	Liebherr, Bieberach
Freezer -80°C	Heraeus, Hanau
Fridge +4°C	Liebherr, Bieberach
Confocal laser scanning microscope LSM 700	Zeiss, Germany
Glassware	Schott, Mainz
Heating block	Grant, Berlin
Incubator for bacteria	Binder, Tuttlingen
Laminar flow	Nunc, Wiesbaden
LAS 3000 FujiFilm	Fuji, Japan
Light-optical microscope	Zeiss, Oberkochen
Mini Protean III, Western Blotting System	BioRad, Munich
Microplate Reader Anthos 2000	Anthos, Microsystem, Krefeld
Magnetic stirrer	Heidolph, Kehlheim
Microwave	Sharp, Hamburg
Multipette, HandyStep	Brand, Wertheim
Pasteur pipettes	Roth, Karlsruhe
pH-Meter	inoLab, Weinheim
Pipettes 0.1 µl – 1000 µl	Eppendorf, Hamburg
Spectrophotometer	Eppendorf, Hamburg
T3 Thermocycler	Biometra, Göttingen
Vortex-Genie 2TM	Bender & Hobein AG, Zurich
Waterbath GFL1086	GFL, Burgwedel

4. Methods

4.1 Animals

The mouse model which was used for the study was a C57Bl6 NPxY2 ki mouse harboring an insertion of a multiple alanine cassette (AAxA) into the membrane distal NPxY2 motif of LRP1. The mutation inside the *Lrp1* gene was generated by a recombinase mediated cassette exchange (RCME) technique. Therefore, the amino acid sequence of the membrane distal intracellular NPxY2 motif of LRP1 was mutated from NPVYATL to the AAVAATL sequence. But as the NPxY2 motif overlaps with the major endocytosis motif of LRP1, the YXXL (YATL) motif, the exchange of the tyrosine of the NPxY2 motif with an alanine prevents tyrosine phosphorylation and thus reduces LRP1 endocytosis (Reekmans et al., 2010; Roebroek et al., 2006). Furthermore, ligand binding and LRP1 mediated ligand endocytosis were reported to be altered due to the fact, that the tyrosine of the NPxY2 motif as substantial phosphorylation site had been replaced by an alanine (Klug et al., 2011; Maier et al., 2013).

4.2 Ethical statement

Experiments involving animals were performed under abidance of the German Animal Welfare Act, and were authorized by the animal care committee of the Johannes Gutenberg University of Mainz and the national investigation office in Koblenz (file number 23 177-07/G 11-1-012). Mice were housed, anesthetized and sacrificed according to the state law of Rhineland-Palatinate and the European and German guidelines for the care and use of laboratory animals. All applicable international, national, and institutional guidelines for the care and use of animals were followed. Experiments performed with animals were conducted at the University Medical Centre of the Johannes Gutenberg -University, Institute of Pathobiochemistry.

4.3 Cell culture methods

4.3.1 Cell culture

All works were performed under sterile conditions beneath a laminar flow hood and in certified S1 or S2 laboratories. Culture media was stored at 4°C; before usage it was

prewarmed to 37°C. Materials used for cell culture were either sterilized by autoclaving or certified for cell culture usage by the manufacturer. Cell morphology and growth rates were checked daily by transmitted light microscopy.

4.3.2 Cultivation of adherent eukaryotic cells

Mouse embryonic fibroblast (MEF) cells either generated from LRP1 wild-type (wt) animals or LRP1 NPxY2 ki animals harboring an insertion of a multiple alanine cassette into the NPxY2 motif of LRP1 were cultured in Dulbecco's Modified Eagle Medium (DMEM) supplemented with 10% fetal bovine serum, 1 mM sodium pyruvate, 100 units/ml penicillin and 100 µg/ml streptomycin. Adherent cells can grow until they reach a confluency of approximately 90-100%, then they have to be passaged to fresh culture dishes (10cm, Greiner). Therefore, cells were washed once with PBS followed by Trypsin-EDTA treatment for 2-5 minutes to detach cells. Then, cells were resuspended and singularized in fresh media. Afterwards, cells were transferred into a new culture dish containing 10 ml fresh media in an appropriate amount and divided equally across the culture dish by gentle shaking. Cells were cultivated at constant 37°C and 5% CO_2.

The procedure for the cultivation of Chinese hamster ovary cells (CHO) expressing LRP1 wt (CHO K1) and LRP1-deficient CHO 13-5-1 cells was performed equally as described above. Cells were cultivated in Alpha Minimum Essential Medium (α-MEM) supplemented with 10% fetal bovine serum, 1 mM sodium pyruvate, 100 units/ml penicillin and 100 µg/ml streptomycin.

4.3.3 Preparation and cultivation of primary cortical neurons

Embryos of C57BL6 LRP1 *NPxY2 ki* and correlating wild-type C57BL6 animals were dissected during pregnancy at embryonic day 15 or 16. The mother animal was anesthetized with isoflurane and killed by cervical fracture. The abdomen was opened to dissect the uterus, which was transferred directly into a sterile dish containing cold PBS. Subsequently, cervical dislocation of the embryos was performed under sterile conditions. The brains were dissected and the meninges were peeled off to isolate the cortices of the embryos which were subsequently transferred into cold HBSS media. After trypsination (0.5% Trypsin, 0.02% EDTA) of the brain tissue for 20 min at room temperature, the singularized cells were pelleted for 2 minutes at 1200 rpm. The pellet then was resuspended in NB media. In order to eliminate tissue parts from the solution,

the isolated tissue was filtered through a double layer of nylon mesh. After filtering, the cell suspension was centrifuged for 5 min at 1200 rpm, and the emerging pellet was dissociated by numerous pipetting steps. Cell numbers were determined by counting in the Neubauer counting chamber and seeded in respective numbers.

For cultivation, culture dishes were coated with poly-L-ornithine (100µg/ml) diluted in PBS for 30 minutes, washed twice with PBS and stored dry over night at 4°C. Primary cortical neurons were cultured in Neurobasal media supplemented with 2% B27, 100 units/ml penicillin and 100 µg/ml streptomycin. Glutamate (Glutamax) was added freshly on the day of preparation in a dilution of 1:100 (Maier et al., 2013). For western blot analyses, cells were seeded in a density of 6.5x 10^5 into 6cm dishes and cultured at 37°C in a humidified 5% CO2 incubator for 14-16 days. For GFP transfection, neurons were seeded in a density of 1.25 x 10^5 on 24-Well plates and cultured for 15-16 days before transfection. For immunocytochemistry, neurons were seeded into 6-well plates in a density of 2.5 x 10^5 and cultured for 4-5 days.

Neurobasal media
2% (v/v) B27 supplement
100 u/ml penicillin
100µg/ml streptomycin
1x Glutamax

PBS
137mM NaCl
2,7mM KCl
10mM NaHPO4
1.8mM KH2PO4

HBSS
$CaCl_2$
$MgCl_2$
phenol red

Trypsin-EDTA in PBS
0.05% trypsin
0.02% EDTA

4.3.4 Cryopreservation of cells

For longtime storage, immortalized cells were cryopreserved and stored at -80°C or in liquid nitrogen. Accordingly, cells were grown until they reached a density of approximately 70%, detached from the culture dishes as described before, and after pelleting, cells were diluted in media containing 10% dimethyl sulfoxide (DMSO). DMSO protects the cells from crystallization during freezing. Cell suspension was transferred into cryovials and directly stored on ice. For shorter time spans cells were frozen at -80°C; for long-term storage cells were embedded in liquid nitrogen.

4.3.5 Revitalization of frozen cells

Cells were revitalized by shortly thawing the cell suspension at 37°C and immediately transferring it into culture media free of DMSO. This step is very important for the viability of the cells, since DMSO is cell toxic from a concentration of 2%. After the suspension is transferred, it is centrifuged and resuspended in fresh media to remove the remaining DMSO completely.

4.3.6 Transient transfection

For transient transfection of CHO 13-5-1 cells the transfection reagent polyethylenimine (PEI), a polymer that condenses DNA into positively charged particles, was used in this study. Exposure of the particles containing the target DNA to cells, results in the binding of the particles to the negatively charged residues of the cell surface. Via endocytosis the plasmid-DNA containing PEI particles are internalized into the cell, where an ionic influx of negatively charged ions into the particle leads to its burst. Once inside the cytoplasm, the plasmid DNA can diffuse into the nucleus and be transcribed and translated by the cell.

CHO 13-5-1 were grown until a confluency of 60% in 6cm culture dishes. Double transfection of the following constructs was performed with 1µg DNA of each plasmid-DNA: human β1-integrin transcript variant 1A cDNA containing a C-terminal myc/flag-tag in the pCMV6 vector and various LRP1 constructs such as LRP1 domain I, domain III, domain IV and LRP1 domain IV ΔNPxY2 mini-receptors containing a C-terminal myc-tag in the plBCX vector and myc-tagged LRP1 domain IV tailless in pcDNA3.1 vector, lacking the intracellular part of LRP1. Hereto, plasmid DNA was pre-incubated with 60µl serum free culture media; in parallel, 8µl of PEI were diluted into 60µl of serum-free culture media and incubated for 10 min at RT. Next, the solutions were mixed and incubated for further 15 min at RT, and finally applied to the cells dropwise. After 4h of incubation time at 37°C, the media was exchanged with fresh culturing media. 24h post-transfection cells were lysed and co-immunoprecipitation experiments were performed by precipitating LRP1. Co-IP and corresponding lysates were analyzed by SDS-PAGE and western blotting following antibody detection of the amount of co-immunoprecipitated β1-integrin via flag-tag.

4.3.7 Transient transfection of primary cortical neurons

Primary cortical neurons were transiently transfected with pEGFP in DIV15 by the calcium phosphate method first described by Graham and Eb (Graham and van der Eb, 1973). With this method, precipitated, negatively charged calcium phosphate-DNA particles are endocytosed into the cells. The incorporated plasmid DNA can diffuse into the nucleus, where it can be transcribed.

For the transfection of primary cortical neurons in a 24-well plate a transfection mix was prepared containing 1µg DNA per well, 10µl H_20 and 1.25µl $CaCl_2$ (2,5M). After 5 min incubation at RT the DNA mix is added dropwise to 10µl 2xHBS buffer under air bubble formation and vortexing. During a 20 min incubation time at room temperature the culture media was removed from the neurons and replaced by 400µl freshly prepared and prewarmed Neurobasal media containing 2% B27.Tthe removed culture media was stored in the incubator during the time of the transfection. Next, 22.5µl transfection mix was added dropwise to every well and cells were incubated for 3.5 h at 37°C in the incubator. In order to remove the calcium phosphate precipitates, neurons were washed twice with 500µl prewarmed 2x HBS, therefore, 500µl of the incubation media was removed from each well and replaced by 500µl HBS. In the second washing step the whole amount of liquid was removed and it was assured, that cells didn´t fall dry during this step. 500µl of the conditioned media was added to each well, cells were harvested after 1-2 days. Hereafter, cells were washed once with PBS and fixed for 30 min with 4% PFA containing 4% sucrose. Cells seeded on coverslips were mounted with ProLong Gold antifade reagent. Images were acquired at the LSM710 confocal laser scanning microscope using ZEN 2008 software (Carl Zeiss).

2x HBS
274 mM NaCl
10 mM KCl
1.4 mM Na2HPO4
15 mM D-Glucose
42 mM HEPES pH 7.1
H_2O_d
adjust pH exactly on 7.07

4.3.8 SiRNA transfection

Small interfering RNA's are synthetic double-stranded RNA molecules with an average length of 20-25bp. Entering the cell, siRNAs can directly bind to the RNA-induced silencing complex (RISC) and bind to the complementary mRNA of the siRNA. The

Argonaut proteins within the RISC complex can inhibit the translation of the mRNA or act as endonucleases and degrade the target mRNA of the siRNA.

In order to use the mechanism of RNA interference to knock-down β1-integrin expression, MEF wt and MEF LRP1 NPxY2 ki cells were transiently transfected with siRNA by using lipofectamine 2000 (Thermo Fischer). The used siRNA itgb1-4 obtained the sequence CCAGCTAATCATCGATGCCTA and itgb1-5 harbored the sequence CAGGAGAACCACAGAAGTTTA, both siRNA´s were specifically directed against β1-integrin. For this purpose, equal cell amounts were seeded on 6-well plates and cultured for 24h. Next, a pre-mix of Opti-MEM (Thermo Fischer) with lipofectamine and Opti-MEM with siRNA was prepared and incubated for 5 min. The mixture of the pre-mixes was incubated for further a 25 min at RT. Meanwhile, media of the cells was replaced by 1ml Opti-MEM following a dropwise addition of the transfection mix. After 3h the medium was replaced by fresh culture media and cells were cultivated for a further 24h. Inhibition of β1-integrin expression was examined by analyzes of protein levels by performing a Tris-glycine gel electrophoresis (8%) followed by western blotting.

4.4 Biochemical methods

4.4.1 Cell lysis of cultured cells

MEF and CHO cells were grown until confluency. For harvesting, cells were placed on ice and washed once with cold PBS. Thereafter, cells were scraped off in PBS and pelleted for 4 min at 7000 rpm. The cell pellet was resuspended in an appropriate amount of lysis buffer depending on the size of the pellet by frequently pipetting. During this step cell membranes dissociate and all proteins of cytoplasmatic and membrane bound origin are dissolved. Dependent on the cell type different lysis buffers were used: MEF and CHO cells were lysed in NP40 containing complete protease inhibitor cocktail (1x). Neurons were lysed in RIPA buffer supplemented with complete protease inhibitor cocktail for 20 min on ice. For phosphorylation analyzes phosphatase inhibitor was added to the lysis buffer. Thereafter, cell lysates were centrifuged for 20 minutes at 14.000 rpm at 4°C in order to eliminate cell debris. Protein concentrations were determined by bicinchinolin acid (BCA) method (Pierce).

RIPA lysis buffer
50mM Tris-HCl, pH 8
150mM NaCl
0.1% (w/v) SDS
1% (v/v) Nonidet P-40
0.5% (w/v) Sodium deoxycholate
1mM Sodium-orthovanadate

NP40 lysis buffer
500mM Tris, pH 7.4
150mM NaCl
1% (v/v) Nonidet P-40
0.02% (v/v) sodium azide

4.4.2 Bicinchinoline acid assay (BCA)

In order to be able to analyze equal amounts of proteins the concentration of lysates had to be determined. The bicinchinolin acid protein assay specifies the protein quantification by a color change measured via absorption (Smith et al., 1985). Peptide bonds trigger the reduction of copper in the BCA-assay solution, whereupon reduced ions bind to two molecules of bicinchinolin acid. The generated complex represents a chelator, whose color is violet. The color intensity directly correlates with the protein amounts in the analyzed samples. The BCA assay was performed according to the manufacturer's protocol (Pierce). For the exact protein concentration determination a standard curve using 1 mg/ml BSA was prepared.

Standard (µg/ml)	BSA 1 mg/ml (µl)	H_2O (µl)
0	0	50
100	5	45
200	10	40
300	15	35
400	20	30
500	25	25

Cell lysate samples were diluted 1:10 in H_2O. The reaction mix was prepared from the BCA Reagent A and B in a ratio of 50:1 and 1ml was added to each sample and the standard. After a 30 min incubation time at 60°C first the standard and following the samples were loaded as duplicates on a 96-well plate for the absorption measurement at 560 nm.

4.4.3 Sodium dodecyl sulfate (SDS) - polyacrylamide gel electrophoresis

The SDS-PAGE system enables the separation of protein lysates due to their size. Therefore, samples were prepared by adding SDS and β-mercaptoethanol containing loading buffer and heated up to 95°C for 5 min in order to regain the primary structure of proteins. The added negatively charged SDS covers the intrinsic charge of proteins, therefore they can be separated by size. Another determining factor for protein

separation is the size of the acrylamide grid being defined by the polyacrylamide concentration. Tris glycine SDS gels with 6-12% polyacrylamide were used to separate protein extracts for this study.

Resolving gel (pH: 8.8)
1.5 M Tris
0.4% (w/v) SDS

Stacker gel (pH: 6.2)
0.6 M Tris-HCl
0.4% (w/v) SDS

Running buffer (pH: 8.3)
192 mM glycine
25 mM Tris-Base
0.1% SDS

SDS sample buffer (1x)
62.5 mM Tris-HCl
10% glycine
2% SDS
0.2% bromophenol blue
0.6% β-mercaptoethanol

4.4.4 Western Blotting

After separation, proteins were transferred on a nitrocellulose membrane by a wet-electroblotting system (BioRad) following the method developed by George R. Stark in 1979 (Renart et al., 1979). Therefore, a vertical electric field was applied for 90-120 min with a constant electric force of 70V. After western blotting, the membrane was stained by a 0.5% Ponceau-solution to validate the success of the transfer. Following, unspecific binding sites of the primary antibody were blocked by incubating the membrane with 5% non- fat milk in tris-buffered saline containing 0.1% Tween-20 for 60 min. Hereinafter, the membrane was incubated with the primary antibody overnight at 4°C by gentle shaking. After washing the membrane with TBST three times for 10 min in order to eliminate unbound primary antibody, secondary horse-radish peroxidase (HRP) conjugated antibody generated against the species of the primary antibody was applied on the membrane. Blots were incubated for further 60 min with secondary antibody diluted in 5% non-fat milk in TBST at RT. For detection of the antibody labelled target proteins chemiluminescence reagents (dilution 1:1) were applied to the western blot and imaged by using LAS 3000mini (Fujifilm).

Blocking buffer
5% non-fat milk powder
TBST

Ponceau-S-solution
0.5% Ponceau-S (w/v)
1% acetic acid
H_2O

Transfer buffer (pH: 8.8)
25 mM Tris-Base
192 mM glycine
20% methanol

TBST (pH: 7.4)
25 mM Tris-Base
137 mM NaCl
270 µM KCl
0.1% Tween-20

4.4.5 Surface biotinylation

Surface protein amounts of β1-integrin and LRP1 were analyzed by marking them with biotin following a biotin dependent pulldown. With this method, biotinylated surface proteins were isolated from the total cell lysate and could be analyzed. Therefore, cells were grown until confluency. The surface biotinylation was performed on ice to prevent surface protein internalization or degradation. In order to wash away all proteins of the media, cells were washed three times with PBS and subsequently they were incubated with a 0.25 mg/ml Sulfo-NHS-biotin-PBS solution for 20 min at 4°C, this step was repeated once. Here, biotin can bind to all surface proteins. Afterwards cells were washed four times with a 50 mM ammonium chloride (NH_4Cl) containing PBS solution to quench the unbound biotin from the surface. Labelled cells were lysed as described above and equal amounts of cell lysates were used for the pull-down of biotin labelled proteins by Neutravidin Agarose resins (20µl). Therefore, samples and beads were diluted in NP40 lysis buffer containing complete protease inhibitor and placed on a spinning wheal at 4°C overnight. On the next day, the beads were washed three times with cold NP40 buffer to eliminate unbound proteins. For recovering bound surface proteins the biotin-neutravidin bond was destroyed by adding 2x SDS loading buffer and boiling the samples for 5 min at 95°C. Following the recovered proteins were analyzed by 6-10% SDS-PAGE and western blotting.

4.4.6 Biotin-based internalization assay

In order to analyze β1-integrin internalization possibly mediated by LRP1, a biotin based internalization assay was performed. Thereto, MEF wt cells and MEF LRP1 NPxY2 ki cells were grown until a confluency of 90% and serum starved for 60 min at 37°C. For blocking clathrin mediated internalization, cells were pre-treated with

chlorpromazine (10 µM) during the last 20 min of serum starvation or a corresponding solvent concentration (DMSO). All steps, besides the internalization step were performed with cold solutions and at 4°C. Surface proteins were marked by cleavable biotin, the Sulfo-NHS-SS-Biotin at 4°C (0.25 µg/ml) for 30 min. An inserted disulfide bond between biotin and the NHS molecule allows the cleaving of biotin under reducing conditions by using the dissociation reagent sodium 2-mercaptoethanesulfonate (MesNa). After labelling, cells were washed three times with PBS. Different conditions were chosen for the experiment: Time point zero represents labeled cells, which were kept on 4°C during the whole experiment in order to prevent internalization of surface proteins. Furthermore, the second control was to dissociate the surface bound biotin by the treatment of surface labelled cells with 20 mM MesNa in 50 mM Tris (pH: 8.6) and 100 mM NaCl on a shaker at 4°C. For the examination of the internalization, culture media was added to surface biotinylated cells and incubated for 9 min at 37°C. After the 9 min time period of internalization the remaining surface biotin was removed by MesNa treatment. MesNa was quenched by the addition of 20 mM iodoacetamide (IAA) for 10 min at 4°C. Following, cells were lysed in NP40 containing complete protease inhibitor complex as described before. Equal amounts of proteins were used for the biotin-neutravidin agarose bead pulldown as described above. Surface proteins and cell lysates were analyzed on 8% Tris-glycine SDS-PAGE followed by western blotting. This experiment was performed by Thorsten Pflanzner.

MesNa buffer
20 mM MesNa
50 mM Tris pH:8.6
100 mM NaCl
H_2O_d

IAA buffer
20 mM iodacetamide
PBS

4.4.7 Co-immunoprecipitation

Prior to co-immunoprecipitation CHO 13-5-1 cells were transiently double transfected via the PEI method with human β1-integrin transcript variant 1A cDNA and various LRP1 constructs: LRP1 domain I, LRP1 domain III and LRP1 domain IV mini-constructs, LRP1 domain IV ΔNPxY2 and LRP1 domain IV tailless. 24h post-transfection, cells were lysed in NP40 containing protease inhibitor as previously described. Furthermore, CHO 13-5-1 cells stably expressing the LRP1 domain IV mini receptor harboring either no mutation, or an amino acid exchange from tyrosine to phenylalanine inside the NPxY1 or the NPxY2 motif were transiently transfected with human β1-integrin transcript variant 1A cDNA. Equal amounts of cell lysates were

mixed with the rabbit polyclonal anti-LRP1 (1704, 1:300) antibody and 30µl of Protein-A-agarose beads (Invitrogen) diluted in NP40 containing protease inhibitor cocktail. Samples were rotated overnight on a spinning wheel at 4°C. Next, the co-immunoprecipitation mix was washed three times with NP40 to eliminate unbound proteins from the samples. Proteins were recovered by boiling the samples with 2x SDS sample buffer for 5 min at 95°C and were separated on 8% tris-glycine gels. Co-immunoprecipitated β1-integrin was detected by the primary monoclonal anti-flag antibody and visualized by a secondary HRP-conjugated antibody.

4.4.8 Gelatine zymography

The matrix metalloproteases 2 and 9 (MMP) play a major role in cell motility by degrading the proteins of the ECM. Accordingly, the activity of MMP2 and MMP9 were determined by gelatine zymography. MMP2 and MMP9 are gelatinases which proteolytically process gelatine. After coomassie blue staining one can analyze the MMP activity by the size of the lytic plaques.

Therefore, MEF wt and MEF LRP1 NPxY2 ki cells were seeded in 6cm dishes; 24h after seeding media was replaced by serum free media and reduced in order to concentrate MMPs in the supernatant. Cells were grown until confluency for further 24h, then the supernatant was collected, centrifuged 4 min at 4000 rcf to at 4°C get rid of cell debris, Subsequently, the supernatant was further concentrated from 7.5ml to 0.5ml by the usage of centricons, being permeable for proteins smaller than 15kDa in a centrifugation step (30 min, 4000 rcf). Then, Pefa block (0.5 mM), which inhibits the activity of serine proteases, was added to the supernatant. Samples were prepared by adding SDS containing 2x sample buffer. For the zymography a SDS-polyacrylamide gel containing 0.1% gelatine with a width of 0,75mm was prepared. Samples were separated by electrophoresis; next, the gel was washed once with H_2O_d. In order to eliminate the reducing SDS, gels were washed three times for 20 min in Triton-X-100 containing renaturation buffer. Proteolytic activity of the MMPs was examined over night at 37°C in renaturation buffer for a time span of 14-16h. Gels were stained by the coomassie blue method for 30 min and after 1h destaining, images were acquired by the LAS 3000mini (Fujifilm) for ½ second. Lytic plaques were analyzed densitometrically by ImageJ.

reagent	12%	10%	stacker 3.8%
Tris-glycine buffer (pH: 8.8)	2.0ml	2.0ml	1.0ml
dH_2O	2.788ml	3.318ml	2.494
acrylamide (30%)	3.2ml	2.67ml	0.506ml
TEMED	6µl	6µl	3µl
APS (100%)	6µl	6µl	3µl
gelatine	8mg/ml	8mg/ml	8mg/ml

2x sample buffer (pH: 8.3)
84 mM ammediol
0.02% NaN_3 (w/v)
2% SDS
0.1% (w/v) bromphenol blue
H_2O_d

Renaturation buffer pH: 7.5
50 mM Tris
0.2 M NaCl
5 mM $CaCl_2$
5 mM $ZnCl_2$
0.02% NaN_3
2.5% Triton-X-100 (v/v)
H_2O_d

Coomassie blue staining
50% (v/v) EtOH
20% (v/v) acetic acid
0.1% (w/v) Coomassie blue
H_2O_d

Destaining solution
30% EtOH (v/v)
1% (v/v) acetic acid
H_2O_d

4.4.9 *In vitro* MMP2/9 enzyme activity assay

The activity of MMP2 and MMP9 in MEF wt and MEF LRP1 NPxY2 ki cells was examined by using a fluorescently marked peptide including a quenching molecule, which is cleaved off by proteinase activity. The enzymatic activity can be analyzed by measuring the fluorescence intensity detectable after the cleavage of the MMPs, thus the fluorescence intensity directly correlates with the activity of the MMPs.

For the activity assay 1.5x 10^4 cells were seeded in black 96well plates with a clear bottom. After cultivation for 24h cells were washed once with PBS and further incubated with serum free media lacking phenol red for additional 24h. The MMP2 and MMP9 specific peptide (2,4-Dinitrophenol-Pro-Leu-Gly-Met-Trp-Ser-Arg-OH, Enzo Lifescience) was added to triplets in a final concentration of 50 µM (solved in DMSO). Following fluorescence was measured at an excitation of 280nm and emission of 360nm in a multi fluorescence plate reader under constant temperature conditions of 37°C every 15 seconds for 1h. As negative control 20 mM EDTA was used, which inhibits

MMP activity. Furthermore, in a preliminary experiment the effect of the solvent was evaluated.

For analyzes of MMP2 and MMP9 cleavage activity, the auto fluorescence of cells was subtracted from the mean of the triplets, and values were set on the same starting point. The regression line was generated by GraphPad Prism 4 software (GraphPad, La Jolla, CA, USA). For graphical display only values until 40 min were shown, afterwards the fluorescence declined due to the instability of the fluorophore.

4.4.10 Immunocytochemistry

Prior, coverslips were prepared by coating them with either fibronectin or collagen I over night at 4°C. Coated coverslips were washed twice with PBS following seeding of equal amount of MEF wt and MEF NPxY2 ki cells under serum free conditions for 2, 3 or 4h. For the examination of the number of FAs, unattached cells were washed away by PBS and fixed with 4% PFA for 30 min at RT. After a subsequent washing step with PBS, cells were permeabilized for 30 min with Triton-X-100. Following, unspecific antibody binding sites were blocked by incubating the cells for 90 min with blocking buffer followed by primary antibody incubation for 60 min at 37°C. Next, unbound antibody was removed by PBS washing steps followed by secondary antibody incubation which lasted for 90 min at RT. Following, all samples were incubated with DRAQ5 for 10 min in order to stain the nucleus. The staining procedure was identical for staining of neurons. Coverslips were pre-coated with poly-ornithine (100 µg/ml) and cells were cultured for 4.5 days. Neurons were fixed with a PBS-based solution containing 4% PFA and 4% sucrose. For surface staining, cells were directly incubated with blocking-buffer without permeabilization. Coverslips were mounted with ProLong Gold antifade reagent and images were acquired with the LSM710 confocal laser scanning microscope using the ZEN 2008 software (Carl Zeiss).

Permeabilization buffer
0.1% (v/v) Triton-X-100
PBS

Blocking buffer
10% goat serum
1% (w/v) BSA
PBS

4.4.11 Nissl staining

For the Nissl staining, mouse brains of three mice of each genotype (C57Bl6 LRP1 *NPxY2 ki* and C57Bl6) were dissected and immediately fixed in 4% PFA- PBS solution

at 4°C overnight. Following, brains were incubated in a 30% sucrose solution to protect the tissue from crystal formation during freezing. Brains were frozen at -20°C and embedded in a cryoprotection solution and were cut as frozen sagittal sections (12µm). After drying the sections overnight, they were stained with a 0.5% cresyl violet solution (Sigma-Aldrich) following washing with H_2O_{dest} and dehydration. The sections were fixed by Roti Histol (Karl Roth) and coverslips were mounted with the Roti Histokit II (Karl Roth). Images were acquired with a transmitted light microscope (used objectives: 15x, upper panel and 45x, middle panel) and a LSM710 confocal laser scanning microscope (lower panel) using ZEN 2008 software (Carl Zeiss).

4.4.12 BrdU assay

5-Bromo-2'-deoxyuridine is a synthetic analogue of thymidine. During the proliferation, in particular during the S-phase, BrdU can be inserted into the newly synthesized DNA. *In vivo* BrdU injection into an organism allows amongst others to purchase proliferating cells in their migratory behavior.

In order to survey cell migration of neuronal progenitor cells along the rostral migratory stream, C57Bl6 LRP1 *NPxY2 ki* mice (LRP1 NPxY2 ki) and corresponding C57Bl6 control mice were intraperitoneally injected with 40µl per 20 g mouse weight of a stock solution of 100 mg/ml BrdU in 0.9% NaCl. 24h post-injection animals were anesthetized with Medetomidine (1 mg/ml, injected amount: 125µl) and Ketanest (110 mg/ml, injected amount: 200µl) until the animals showed no reflexes anymore. Following, animals were perfused with 4% PFA in PBS (Histofix). Brains were dissected by cutting off the nose of the animal and opening the cranium as far as possible in direction of the nose to be able to dissect the brain with intact olfactory bulbs. Dissected brains were postfixed o.n. in 4% PFA (4°C) and incubated in 30% sucrose solution. 30µm sagittal cryosections were cut and subsequently washed three times with Triton-X-100 containing TBS. Next, the tissue was incubated for 1h with 1N hydrochloric acid (HCl) (60°C) at 37°C. After three washing steps with PBS the sections were incubated in blocking buffer for 1h, thereafter sections were incubated with the primary BrdU antibody (1:500) o.n. at 4°C. After removing unbound primary antibody by washing with PBS sections were incubated with Alexa 488 marked secondary antibody and counterstaining of nucleus was performed with DRAQ5 (1:1000 in PBS). Sections were mounted with ProLong Gold antifade and analyzed by the LSM710 confocal laser scanning microscope (Carl Zeiss).

4.5 Cell biological methods

4.5.1 Cell spreading

For analyzing cell spreading and thus the cytoskeleton organization of cells seeded on different ECM proteins, the actin cytoskeleton was stained by phalloidin fluorescently marked by Alexa488. Prior to cell seeding coverslips were coated in 6-well plates with either collagen I (10 µg/cm^2) diluted in 20 mM acetic acid or fibronectin (10 µg/ml) in PBS over night at 4°C. Plates were washed twice with PBS followed by cell seeding in equal amounts under serum free conditions for 2 or 4h at 37°C. Next, seeded cells were washed twice with PBS and fixed for 10 min with 4% PFA in PBS. After fixation the slides were washed three times with PBS and permeabilized by PBS containing 0.4% Triton-X-100 for 5 min. For blocking unspecific binding sites of phalloidin cells were incubated with blocking buffer for further 30 min. Actin was stained by using 5 units of Alexa-488 labelled phalloidin diluted in 200µl blocking buffer by incubating the samples for 20 min. Subsequently, after three washing steps with PBS the nucleus is stained for 10 min by DRAQ5 (1:1000 in PBS) and coverslips were mounted with ProLong Gold antifade reagent. Images were acquired with the LSM710 confocal laser scanning microscope using ZEN 2008 software (Carl Zeiss). Cell size was measured by converting the LSM generated images into a monochrome illustration followed by increasing the threshold. Cells were visualized white on a black background hence the cell area could be selected as region of interest and measured by using ImageJ.

Permeabilization buffer
0.4% (v/v) Triton-X-100
PBS

Blocking buffer
0.4% (v/v) Triton-X-100
2% (w/v) BSA
PBS

4.5.2 Cell adhesion assay

In order to investigate in the cell adhesion behavior of MEF wt and MEF LRP1 NPxY2 ki cells, 96-well plates were coated with either fibronectin (10 µg/ml in PBS) or collagen I (100 µg/ml in 20 mM acetic acid) overnight at 4°C. Subsequently, plates were washed twice with PBS and blocked for 60 min at 37°C. Following, the plates were washed twice and 1x 10^5 cells were seeded in each well under serum free conditions (37°C). Cell adhesion was analyzed after two distinct time point, after 30

min and 60 min. Therefore, plates were washed twice with PBS to rinse the non-attached cells away. Adhered cells were fixed for 20 min with 4% PFA in PBS. Following, after washing away the PFA cells were stained by a crystal violet solution for 10 min. After extensive washing with H_2O plates were dried upside down, whereupon cells were solubilized by incubating them with 1% SDS solution for 20 min. The absorption of the diluted crystal violet, whose intensity directly correlated with the amount of adhered cells, was measured at 595nm in a multiplate reader.

Blocking buffer
2% (w/v) BSA
PBS

Crystal violet solution
2 mg/ml crystal violet
2% (v/v) ethanol

Blocking buffer
2% (w/v) BSA
PBS

4.5.3 Cell migration assay

Cell migration of MEF wt and MEF NPxY2 ki cells was determined using a Boyden chamber assay. These 48-well microchemotaxis plates contain polycarbonate filters with a pore size of 8µm and were coated on the upper side, where the cells are seeded with either fibronectin (10 µg/ml in PBS) or collagen I (1.5 mg/ml in 20 mM acidic acid). The lower part of the filter, the arrival side, was coated with gelatine (100 µg/ml). The wells on the arrival side were filled with cell culture media and the cell lines of interest were suspended and seeded in a density of $1x\ 10^4$ per well, on the upper side of the filter. After an incubation time of 6.5h at 37°C and 5% CO_2 cells remaining on the side of seeding were removed by scraping them off. Migrated cells, which reached the lower side of the Boyden chamber, were fixed by methanol and stained with hemacolor®.

For investigating the role of β1-integrin in cell migration cells were treated with an antibody specifically blocking the active form of β1-integrin. Cells were pre-incubated with the specific monoclonal hamster anti mouse antibody (clone Ha2/5, 25 µg/ml) for 30 min before they were seeded into the Boyden chamber.

The digital microphotographs were turned into monochrome images in Photoshop and computer based counting of migrated cells were carried out using ImageJ. This experiment was performed by Kristina Götze.

4.5.4 Statistical analyzes and densitometric analyzes

Western blots were quantified by densitometry using ImageJ 1.44 and MultiGauge 3.0. Protein intensity level measurements were normalized to tubulin or actin, besides the levels of surface proteins. Focal adhesions were counted in ImageJ by marking sites of focal adhesion complexes. The mean of counted numbers was analyzed by *t*-test comparing the two cell lines (MEF wt vs. MEF NPxY2 ki). $p < 0.05$ was considered as statistically significant. All graphs and statistical analyses were prepared by using the GraphPad Prism 4 software (GraphPad, La Jolla, CA, USA). Data were analyzed by one-way analysis of variance (ANOVA) coupled to Newman-Keuls or Tukey posttest for multiple comparison, or *t*-test. $p < 0.05$ was considered as statistically significant.

4.5.5 Statistical analyzes of spines

Spines of primary cortical neurons, transiently transfected with pEGFP in DIV15 were analyzed by using the free software NeuronStudio. Therefore, z-stack overlay projection images acquired at the LSM710 (Zeiss) were uploaded. After choosing a dendrite of second degree for analyzes, spines were automatically purchased by the software and categorized in three types: thin, mushroom and stubby. The used NeuronStudio program measured the length of the neck, and the diameter of the head and the neck. If a spine had a head to neck diameter ratio value greater than 1.100 the spine could be a thin or a mushroom spine. For being identified as mushroom a minimum of a head diameter of 0.35µm had to be fulfilled. Spines that do not meet the neck ratio and have a length to head diameter greater than 2.500 are classified as thin, otherwise as a stubby spine. The automatic detection and categorization of the spines was manually checked. Statistical analyzes of two distinct neuronal preparations per genotype and a minimum of five dendrites per preparation were performed via *t*-test using GraphPad Prism 4 software (GraphPad, La Jolla, CA, USA) by comparing C57BL6 spine amounts of one kind with the amounts of this spine type of C57BL6 LRP1 NPxY2 ki neurons. $p < 0.05$ was considered as statistically significant.

4.5.6 Antibodies

antigen	species	dilution	Supplier/ reference
anti-β1-integrin KKGCPPDDIENPRGC	polyclonal/ rabbit	WB: 2µg/ml	GenScript
anti-LRP1 β-chain 1704	Polyclonal/ rabbit	WB: 1:10.000 IP: 1:300	Pietrzik, 2002
anti-LRP1 α-chain B411E2	Monoclonal/ mouse	WB: 1:10.000	Storck, 2016
Anti-FAK	Polyclonal/ rabbit	WB: 1:1000	Cell Signalling
Anti-pFAK Y397	Polyclonal/ rabbit	WB: 1:1000	Cell Signalling
anti-flag M2	Monoclonal/ mouse	WB: 1:2000	Sigma-Aldrich
anti-myc 9E10	Monoclonal/ mouse	WB: 1:500	Hybridoma cell line
anti-vinculin	Monoclonal/ mouse	ICC: 1:500	
anti-α-tubulin clone DM1A	Monoclonal/ mouse	WB: 1:5000	Sigma-Aldrich
anti-actin	Polyclonal/ rabbit	WB: 1:1000	Sigma-Aldrich
anti-BrdU	monoclonal/ mouse	IHC: 1:500	Sigma Aldrich
anti-active β1-integrin clone Ha2/5	monoclonal/ hamster	Blocking: 25 µg/ml	BD Pharmingen
pERK 1/2	Monoclonal/mouse	WB: 1:500	Cell Signalling
ERK 1/2	Polyclonal/ rabbit	WB: 1:500	Cell Signalling

antigen	conjugate	dilution	Supplier/ reference
donkey anti mouse IgG	HRP	WB: 1:5000	Sigma-Aldrich
Goat anti rabbit IgG	HRP	WB: 1:10.000	Jackson Immunoresearch
goat anti mouse IgG	Alexa-Fluor 488	ICC: 1: 1000	Invitrogen
Goat anti rabbit IgG	Alexa-Fluor 546	ICC: 1: 1000	Invitrogen

4.6 Molecular biology

4.6.1 Cloning of LRP1 stub constructs

LRP1 stub domain IV is composed of the last 3762 nucleotides of LRP1 (kindly provided by Anton J. M. Roebroek) that have been subcloned into a plBCX backbone with the 5´BamH1 and 3´Xba1 restriction sites and were fused to a myc tag at the 5´end. The LRP1 stub minireceptor constructs are composed of the c-terminus, the transmembrane domain and a short part of the ectodomain of LRP1. The LRP1 stub domain IV construct harboring a substitution inside the NPxY2 motif from TTC ACC

AAC CCC GTG TAT GCC ACA CTC to ACC *GCC GCA* GTG *GCT GCC* ACG CTC, whereby the NPxY2 motif was changed from NPVYATL to AAVAATL was kindly provided by Anton Roebroek and was subcloned into the plBCX backbone by using the same primers as described above. LRP1 domain I and III each linked to a short stub construct composing of a small part of the extracellular domain (207 nucleotides), the transmembrane domain (75 nucleotides) and the intracellular part of LRP1 composing of 303 nucleotides. The domain and the stub were fused into the pcDNA3.1 vector. The restriction sites for the LRP1 stub part were 5' BamHI and 3' XbaI, the restriction sites for the LRP1 domain I and III were BamHI at the 5' and at the 3' end, additionally a myc tag was added to the 5' end with the 5' KpnI and 3'BamHI restriction sites. The next step was to subclone the LRP1 domain I and LRP1 domain III into the plBCX vector with the 5' XhoI an 3' NotI restriction sites. Furthermore, the LRP1 domain IV tailless construct was generated by introducing a preliminary stop codon after the transmembrane domain of LRP1. By the means of single amino acid exchange of the tyrosine of both NPxY motifs to a phenylalanine the method of site-directed primer mutagenesis was used with the following primers for the NPxY1 motif: forward 5´-CCCTACCTTCAAGATGTATG-3´ and the reverse 5´-CATACATCTTGAAGGTAGGG-3´; for the NpxY2 motif the forward primer 5´-CCAACCCAGTGTTTGCCACG-3´and the reverse primer 5´-CGTGGCAAACACTGGGTTGG-3 ´were used. Cloning experiments were performed by Thorsten Pflanzner and Sebastian Jäger.

Primer name	**Sequence 5' → 3'**	**Restriction enzyme**
LRP1-dom IV fwd plBCX	GAGCTCGGATCCGATTGCAGCATCGACCCC	BamHI
LRP1-dom IV rev plBCX	GGGCCCTCTAGACTATGCCAAGGGATCTCC	XbaI
Myc-tag fwd	AAGCTTGGTACCATGCTGACCCCGCCGTTGCT	KpnI
Myc-tag rev	CGGCGGCTATCGACGCCCCTGAACAAAAACTTATTTCTGAAGAAGATCTGGGATCCACTAGT	BamHI
LRP1-domain I fwd	GAGCTCGGATCCAAGACTTGCAGCCCCAAGCA	BamHI
LRP1-domain I rev	ACTAGTGGATCCGGCCTTGCAGGAGCGGTTAT	BamHI
LRP1 stub fwd	GAGCTCGGATCCTCTGAGTACCAGGTCCTGTA	BamHI
LRP1 stub rev	GGGCCCTCTAGACTATGCCAAGGGGTCCCCTA	XbaI
Myc-tag fwd	AAGCTTGGTACCATGCTGACCCCGCCGTTGCT	KpnI

Primer name	Sequence 5' → 3'	Res-triction enzyme
Myc-tag rev	CGGCGGCTATCGACGCCCCTGAACAAAAACTTATTTCTGAAGAAGATCTGGGATCCACTAGT	BamHI
LRP1-domain III fwd	GAGCTCGGATCCTGTGAACTCTCTCCATGCCG	BamHI
LRP1-domain III rev	ACTAGTGGATCCAGCCTTGCAGCTGTGGGGGT	BamHI
LRP1 stub fwd	GAGCTCGGATCCTCTGAGTACCAGGTCCTGTA	BamHI
LRP1 stub rev	GGGCCCTCTAGACTATGCCAAGGGGTCCCCTA	XbaI
LRP1 dom. I-stub-myc plBCX fwd	CTCGAGATGCTGACCCCGCCGTTGCT	XhoI
LRP1 dom. I-stub-myc plBCX rev	GCGGCCGCCTATGCCAAGGGGTCCCCTA	NotI
LRP1 dom. III-stub-myc plBCX fwd	CTCGAGATGCTGACCCCGCCGTTGCT	XhoI
LRP1 dom. III-stub-myc plBCX rev	GCGGCCGCAGCCTTGCAGCTGTGGGGGT	NotI
LRP1 dom IV NPxF1 plBCX (amino acid exchange Y-F) fwd	CCCTACCTTCAAGATGTATG	
LRP1 dom IV NPxF1 plBCX (amino acid exchange Y-F) rev	CATACATCTTGAAGGTAGGG	
LRP1 dom IV NPxF2 plBCX (amino acid exchange Y-F) fwd	CCAACCCAGTGTTTGCCACG	
LRP1 dom IV NPxF2 plBCX (amino acid exchange Y-F) rev	CGTGGCAAACACTGGGTTGG	

4.6.2 Transformation of competent *E. coli* bacteria

DH5α chemo-competent cells are bacteria, being able to take up free DNA from their surrounding media after chemical treatment. For transformation, an aliquot was thawed and 5-200ng plasmid DNA was added and incubated for 20 min on ice. Following, cells were heat shocked by placing them into a 42°C water bath for 1 min. After 2 min regeneration, 500µl LB-media (Luria-Bertani-media) was added and the bacteria were allowed to grow for 1h at 37°C under slight shaking. Grown cells were pelleted and resuspended in fresh LB-media. Depending on the applied plasmid, cells are plated onto bacterial agar plates containing either the selective antibiotic Kanamycin (50 µg/ml) or Ampicillin (100 µg/ml) and incubated overnight at 37°C.

LB media pH: 7.0
0.5% (w/v) NaCl
1% (w/v) Bacto-Tryptone
0.5% (w/v) yeast extract
20 mM Tris/HCl pH 7.5
for agar plates add 15g Bacto agar on 1L media

4.6.3 DNA-plasmid preparation

4.6.3.1 Mini preparation

For mini plasmid preparations single colony clones were picked from the agar plates and incubated in 2-5ml LB- media including the corresponding antibiotic concentration for 4-8h under constant shaking. After the incubation time the DNA was isolated by using the high pure plasmid isolation kit (Roche) being based on the alkaline lysis method. Therefore, DNA is immobilized by binding to the fiber glass fleece of the provided kit.

This part of the molecular experiments was performed by Thorsten Pflanzner and Sebastian Jäger.

4.6.3.2 Midi preparation

In order to generate bigger amounts of DNA-plasmids picked single clones were precultured in 5ml of LB-media containing the appropriate amount of antibiotic for 8h under constant shaking at 37° C. 500µl of the pre-culture were transferred into a flask containing 150-300ml LB media including antibiotics and were allowed to grow

overnight. The midi plasmid preparation was performed by using the kit endotoxin-free Plasmid DNA purification (Macherey-Nagel).

4.6.4 DNA concentration measurement by absorption

The DNA concentration was determined by measuring its absorption. Therefore, DNA was diluted 1:100 in H_2O and the absorption at 260nm was measured at a spectral photometer. The purity of the DNA was measured by detecting the absorption at 280nm (maximum for proteins), the ratio of 260nm/280nm should be between 1.8 and 2.

4.6.5 Restriction digestion of plasmid DNA

Plasmids contain various recognition sites for bacterial restriction enzymes, which are palindromic DNA motifs. In order to linearize the circular plasmids and to be able to insert a construct of interest, plasmids are digested by certain restriction enzymes creating sticky ends with single stranded base overlaps. DNA fragments digested by the same restriction enzyme can be ligated.

Thereto, 1µg DNA was restricted by either one or two enzymes and incubated for 2h at 37°C. The digested DNA fragments were visualized by separating the fragments on an agarose gel electrophoresis.

For cloning, the restriction mix was directly cleaned up by using High Pure PCR Clean Up (Roche) kit to eliminate the restriction enzymes.

solutions	**amounts**
DNA	1µg DNA or 10µl of cleaned up DNA
Buffer mostly CutSmart	5µl
Enzyme (NEB)	1µl
$H_2O_{nuklease\ free}$	Fill up to 50µl

4.6.6 Agarose gel-electrophoresis

DNA fragments are separated by size in an agarose gel system. Depending on the agarose concentration fragments of different size separate, smaller fragments run further than larger DNA fragments.

Agarose gels were prepared by diluting agarose into TAE buffer and heating the solution until no streaks are visible anymore. Ethidium bromide, intercalating into the DNA, was added in a concentration of 5 µg/ml. The electrophoresis was run at 100V for 30-60 min. Samples were mixed with 10x OrangeG loading buffer. Gel analyzes was

performed under the INTAS imager device by using UV light to visualize the ethidium bromide.

OrangeG 10x
39% (v/v) glycerole
0.5% (w/v) SDS
10 mM EDTA
0.025g Bromphenol blue
0.025g xylene cyanol
Fill up to 10ml with H_2O

TAE buffer
40 mM Tris-acetate
1 mM EDTA pH 8

4.6.7 DNA extraction from agarose gel

For preparative intention DNA fragments were isolated from the agarose gel by using UV light (254nm). DNA was extracted out of the gel (NucleoSpin Gel and PCR Clean Up kit, Macherey-Nagel) for further processing. This part of the cloning was performed by Thorsten Pflanzner and Sebastian Jäger.

4.6.8 Ligation

Restricted DNA fragments with compatible ends can be ligated by the enzyme T4 ligase. The ligase, originating from bacteriophages is able to ligate double stranded DNA and RNA by closing nicks in the phosphodiester backbone of the DNA. For cloning, vector and insert were restricted by the same enzymes and for ligation they were applied in a ratio of 1:3 (vector: insert). Ligation was performed overnight at room temperature in a total volume of 30µl. This part of the cloning was performed by Thorsten Pflanzner and Sebastian Jäger.

solutions	**amounts**
DNA	Vector: insert 1:3, ca. 50ng
T4 ligase buffer	3µl
T4 ligase	1µl
$H_2O_{nuklease\ free}$	Fill up to 30µl

4.6.9 PCR

Polymerase chain reaction is a method to amplify specific DNA sequences. Therefore, DNA double strands are singularized by heat denaturation, followed by binding of short oligonucleotides to the template DNA and elongation via DNA-polymerase (Mullis and Faloona, 1987). Dependent on the sequence of interest, all these steps can vary such as in temperature and time spans. For cloning experiments the Phusion^{TM} high fidelity polymerase was used. Below an exemplified protocol of a PCR program is depicted:

PCR protocol	**time**	**temperature**	**cycles**
initial denaturation	30 sec	98°C	1
denaturation	5-10 sec	98°C	25-35 cycles
annealing	30 sec	55-60°C	
extension	30 sec/1kb	72°C	
final extension	10 min		1
hold	for ever	4°C	-

5. Results

The presented results were published in parts in the Journal of Experimental Cell research, January 1st, 2016 (Rabiej et al., 2016).

LRP1 and β1-integrin are both cell surface receptors interacting with extracellular and intracellular ligands and thus influencing cellular behavior in ranges such as cell migration. In former studies an LRP1 mediated dependence of β1-integrin maturation and cell surface expression β1-integrin has been demonstrated (Salicioni et al., 2004). LRP1 as a major endocytic receptor is responsible for binding extracellular ligands and clearing them from the extracellular milieu by endocytosis in a clathrin dependent manner (Taylor and Hooper, 2007). β1-integrin internalization is crucial for maintaining cellular dynamics, as it links the intracellular signaling of the cytoskeleton with the ECM. Dynamics in integrin receptor internalization are necessary for the capacity of cells to react on interior or exterior changes. There are different endocytosis routes known for β1-integrin, however, one common pathway shared with LRP1 is the clathrin mediated endocytosis (Ezratty et al., 2009). Moreover, a cellular knock-out of LRP1 evokes phenotypes like reduced cellular motility, a process closely related to the activity and signaling of integrin receptors (Mantuano et al., 2010). The purpose of this work was to narrow down the site of interaction between LRP1 and β1-integrin and analyzing the correlated cellular behavior. To examine the consequences of the possible crosslink and potentially coupled endocytosis between LRP1 and β1-integrin a cellular model with severely reduced LRP1 internalization rates was used, which might influence β1-integrin.

5.1 LRP1 alters β1-integrin surface levels

Here, it was investigated, whether LRP1 not only influences β1-integrin maturation as previously described but is also engaged in the endocytosis of the major ECM binding surface receptor. The first indication for the involvement of LRP1 in β1-integrin internalization would be altered surface levels of β1-integrin in LRP1 functionally knock-out MEF NPxY2 ki cells. These knock-in cells were generated from the previously described animal model (Reekmans et al., 2010). For unravelling the possible interaction of both receptors, surface levels of LRP1 and β1-integrin were

examined marking surface proteins with biotin and analyzing surface protein levels by western blotting.

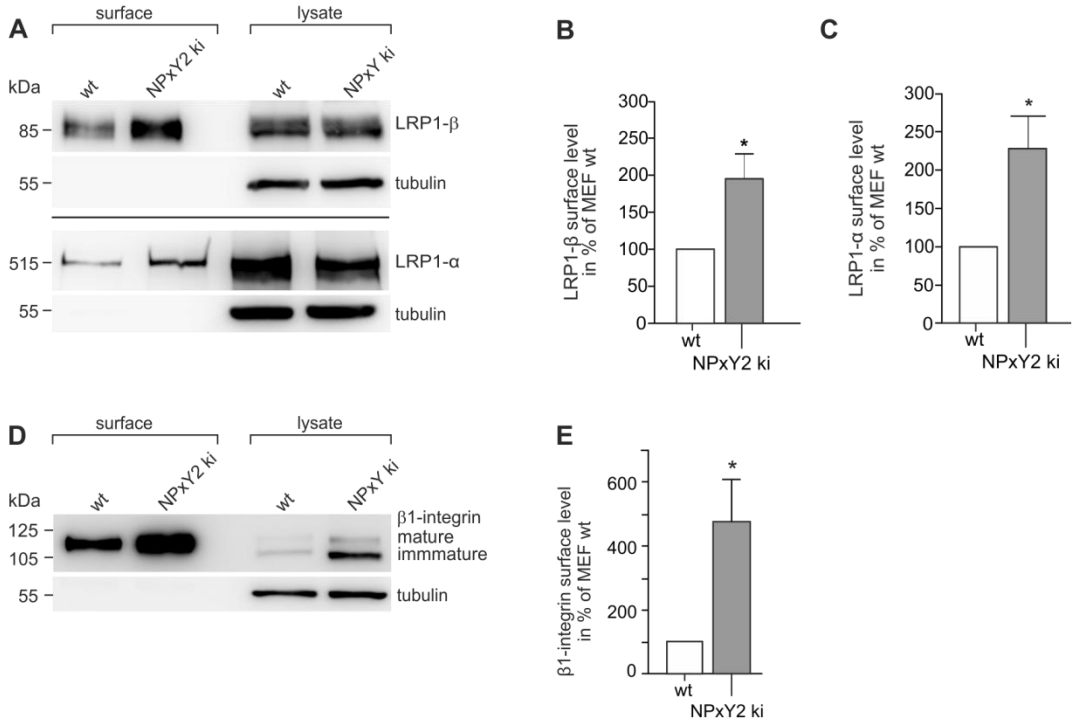

Figure 8: Surface accumulation of LRP1 and β1-integrin in the LRP1 NPxY2 ki MEF cells: A) Surface biotinylation of MEF LRP1 NPxY2 ki MEF cells and MEF wt cells was performed after cells reached confluency. Equal amounts of proteins were used for the precipitation of the biotin-labelled proteins (NeutrAvidin beads). The pulldown and 20µg of corresponding cell lysates were analyzed by SDS-PAGE and western blotting. The LRP1 β-chain was detected with the polyclonal rabbit anti LRP1 1704 antibody, the α-chain was probed with the monoclonal mouse anti LRP1 B411E2 (Storck et al., 2016) followed by α-tubulin detection as loading control. Moreover, the lack of the tubulin signal in the surface biotinylated samples revealed that cells were viable during biotinylation. The surface levels of LRP1 α- and β-chain were elevated in the NPxY2 ki MEF cells. **B, C)** Results are shown in percent (%) of wt protein surface levels, which were set as 100%. Densitometric results represent mean + s.e.m. of a minimum of three independent experiments. $p < 0.05$ (*t*-test) was considered statistically significant *. **D)** Surface protein levels of β1-integrin were examined by surface biotinylation in the same manner as described for A, ensued by SDS-PAGE and western blotting analyzes. β1-integrin was detected by using the rabbit polyclonal pAb7- β1-integrin antibody followed by tubulin detection. Remarkably, β1-integrin surface amounts were elevated in MEF LRP1 NPxY2 ki cells compared to MEF wt cells. **E)** Results of surface β1-integrin biotinylation are expressed in percent (%) of wt protein surface levels, which were set as 100%. Densitometric results represent mean + s.e.m. of a minimum of three independent experiments. $p < 0.05$ (*t*-test) was considered statistically significant *.

The first step was to validate surface accumulation of endogenous LRP1 in the NPxY2 ki cell culture model compared to MEF cells expressing LRP1 wildtype (wt). The results of the surface biotinylation revealed a surface accumulation of LRP1 β-chain as well as the LRP1 α-chain (Fig. 8 A-C). Total protein levels were not influenced by the NPxY2 ki mutation, as LRP1 levels of whole cell lysates were comparable between MEF wt and MEF NpxY2 ki cells. Densitometric analyzes elucidated a two-fold enhancement of surface LRP1 β-chain and LRP1 α-chain levels in the LRP1 NPxY ki

MEF cells versus MEF wt cells (Fig. 8 B,C). Examination of surface β1-integrin levels via biotinylation experiments depicted a five-fold increase in surface β1-integrin in the MEF NPxY2 ki cells compared to MEF wt cells (Fig. 8 D,E). In the lysate, one band at approximately 105kDa was detected constituting the immature form of β1-integrin, also named p105. The upper band ran on a height of 125kDa and represents the glycosylated, mature β1-integrin, p125. Noticeably, the immature, unglycosylated p105 β1-integrin level is markedly elevated in the NPxY2 ki model. The functional knock out of LRP1 in the NPxY2 ki model also resulted in an impairment of β1-integrin maturation. Remarkably, surface accumulation of LRP1 caused increased surface amounts of β1-integrin.

5.2 Narrowing down the potential interaction sight of LRP1 and β1-integrin

As demonstrated in figure 8, there seems to be a correlation between LRP1 surface accumulation due to reduced internalization and surface accumulation of β1-integrin. As it has been proposed that LRP1 intracellular phosphorylation induces β1-integrin recruitment, the intracellular domain of LRP1 was the most likely part of interaction between the two receptors (Czekay et al., 2003; Hu et al., 2007). In order to unravel the possible interaction sight between the two surface receptors, co-immunoprecipitation experiments were performed. LRP1 deficient CHO 13-5-1 cells were transiently double transfected with different LRP1 constructs and human flag-tagged β1-integrin. The pulldown was performed with the anti LRP1 1704 antibody. Precipitated β1-integrin was subsequently analyzed by using an anti-flag antibody.

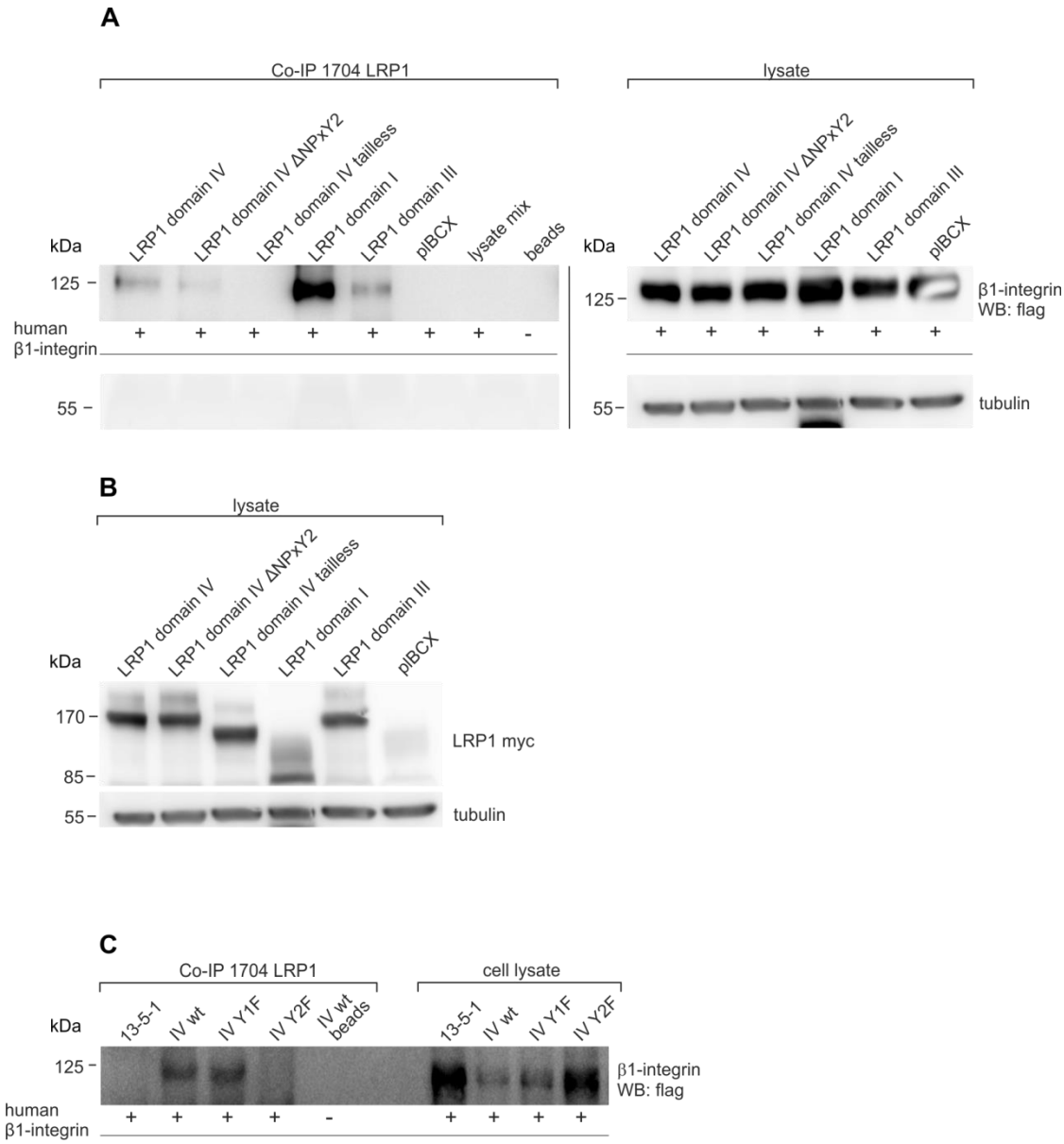

Figure 9: LRP1 and β1-integrin possibly interact via the C-terminus of LRP1: A) Co-immunoprecipitation experiments of CHO 13-5-1 cells expressing LRP1 mini-receptor constructs of the domain I, III and IV, the domain IV lacking the intracellular tail, the domain IV ΔNPxY2 and β1-integrin revealed interaction of LRP1 and β1-integrin. The LRP1 constructs were myc-tagged, the β1-integrin-construct was flag-tagged. After SDS-PAGE and western blotting, the amounts of fag-tagged β1-integrin, precipitated with the LRP1 antibody 1704 were probed with the M2-anti flag-tag antibody and subsequently with the α-tubulin antibody as loading control. If the intracellular domain of LRP1 is missing, no co-immunoprecipitation of LRP1 and β1-integrin was possible. 20µg of the same lysates were analyzed as expression control for β1-integrin (right blot) **B)** To ensure proper expression of the LRP1 constructs, 20µg of the same samples were examined for their LRP1expression. The western blot was incubated with the mouse anti myc-tag antibody 9E10 followed by α-tubulin antibody incubation. All samples expressed LRP1, deviations in size between the LRP1 constructs resulted from different sizes of the LRP1 domains. **C)** Co-immunoprecipitation of LRP1 deficient CHO 13-5-1 cells stably expressing different myc-tagged mouse LRP1 domain IV mini-receptor (mLRP1 IV) constructs, harboring an amino acid exchange (Y to F) either in the NPxY1 or in NPxY2 motif, were transiently transfected with flag-tagged β1-integrin. The western blot was incubated with the anti flag M2 antibody to detect β1-integrin, which could be precipitated with the LRP1 antibody 1704. Only in LRP1 NPxF1 and LRP1 wt expressing cells β1-integrin and LRP1 could be co-immunoprecipitated.

Interestingly, β1-integrin could be detected in the co-expression with LRP1 domain I, III and IV. However, β1-integrin was absent in the LRP1 tailless sample, here the complete intracellular domain of LRP1 was missing. β1-integrin could be co-immunoprecipitated in very low amounts in cells co-expressing β1-integrin and an LRP1-domain IV construct harboring in insertion mutation of the NPxY2 motif with a multiple alanine cassette (Fig. 9 A) as described in figure 3. As a control, lysates of CHO 13-5-1 cells expressing either only the β1-integrin construct or only the LRP1 domain IV construct post-lysing mixed. Co-immunoprecipitation of LRP1 and β1-integrin in this sample failed, therefore, the observed interaction of LRP1 and β1-integrin did not happen after lysing the cells, but is already existing in living cells (Fig 9 A). The absence of tubulin in the immunoprecipitation experiments revealed the proper experimental procedure, since only LRP1 and interacting proteins were pulled by the beads. The expression control of LRP1 and β1-integrin revealed the presence of the two receptors in the examined cells. Differences in size concerning the LRP1 domain constructs observed in figure 9 B are caused by distinct lengths of the domain constructs.

In order to investigate in detail the possible interaction site of LRP1 and β1-integrin, LRP1 domain IV mini-constructs with single amino acid exchange from tyrosine to phenylalanine inside the NPxY motifs were generated. Co-immunoprecipitation experiments were performed with LRP1 deficient CHO 13-5-1 cells stably expressing the LRP1mini-receptor constructs harboring single amino acid exchanges in the NPxY motifs and the LRP1 deficient 13-5-1 cells as controls. All cell lines were transiently transfected with flag-tagged human β1-integrin. This experiment was performed by Thorsten Pflanzner (Fig. 9 C). Here, β1-integrin could be co-immunoprecipitated with LRP1 in cells expressing the LRP1 domain IV wt construct and the LRP1 domain IV NPxF1 construct (described in Fig. 3). However, in the absence of LRP1 and in samples of cells expressing the LRP1 domain IV NPxF2 construct, LRP1 and β1-integrin could not be co-immunoprecipitated (Fig. 9 C).

These results indicate a potential interaction of LRP1 and β1-integrin implying the intracellular tail of LRP1. However, whether the two receptors interact directly or indirectly via scaffolding protein could not be determined with this experimental setup.

5.3 LRP1 mediates β1-integrin internalization

Due to the interaction of LRP1 and β1-integrin in co-immunoprecipitation experiments one cannot draw conclusions on the physiological relevance of the interaction. LRP1 knock-out has been proclaimed to be participating in cell motility in the context of cancer pathology (Dedieu et al., 2008). Cells can only move, if their adhesion contact to the ECM at the sight of movement is dissipated by integrin endocytosis.

To verify if the interaction of both proteins is also coupled with correlated endocytosis, the internalization of endogenous β1-integrin was examined by a biotin based internalization assay. Surface proteins of MEF wt cells and MEF LRP1 NPxY2 ki cells were labeled with the cleavable Sulfo-NHS-SS-Biotin variant and allowed to internalize the labelled proteins for 9 min (the timespan for LRP1 endocytosis). As a control, one batch of cells was left on ice in order to inhibit the internalization of surface proteins. MEF wt cells were pre-treated with chlorpromazine (CPZ), prohibiting clathrin mediated endocytosis of surface proteins or were treated with the MesNa buffer to cleave off surface bound biotin (Isbert et al., 2012). This experiment was performed by Thorsten Pflanzner. Moreover, the impact of β1-integrin in LRP1 maturation was examined by siRNA knock-down of β1-integrin in the MEF wt cells.

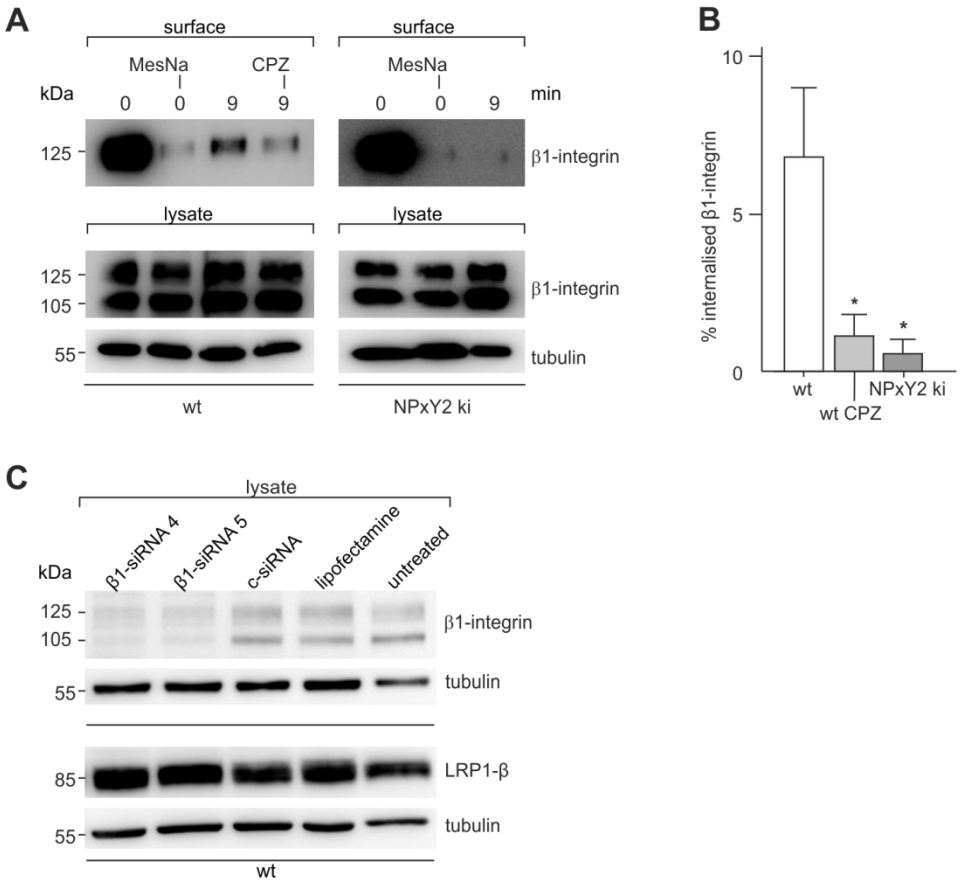

Figure 10: LRP1 has an impact on β1-integrin internalization: A) β1-integrin internalization in the MEF LRP1 NPxY2 ki cells and respective wt controls was surveyed by a biotin-based internalization assay for a time period of 9 min. As negative control, MEF wt cells were pretreated with 10µM CPZ to inhibit clathrin mediated endocytosis. MesNa treated cells, which were kept on ice, were used as further control. The upper panel depicts the surface pulldown; the lower panel shows the corresponding lysates. Immunoblotting with the anti β1-integrin antibody pAb7 revealed a severely declined internalization rate of β1-integrin in the MEF LRP1 NPxY2 ki cells compared to MEF wt cells. Blocking clathrin-mediated endocytosis in MEF wt cells resulted in a notable reduction in β1-integrin internalization. **B)** Densitometric analyzes represent mean + s.e.m. of at least three independent experiments. After one-way analyzes of variance $p < 0.05$ was considered to be significant *.The decrease in β1-integrin internalization of MEF LRP1 NPxY2 ki cells and CPZ treated MEF wt cells was ascertained as significant. **C)** siRNA knockdown of β1-integrin with two distinct siRNA variants was performed in MEF wt cells. As negative controls, wt cells were transiently transfected with unspecific siRNA or treated with the transfection reagent only. Analyzes of samples by SDS-PAGE and subsequent by western blotting depicted a severe reduction in in β1-integrin expression in the β1-integrin-siRNA expressing cells after probing the blot with the anti β1-integrin pAb7 antibody. Detection of LRP1 with the 1704 antibody revealed a slight increase in LRP1 β-chain expression in the β1-integrin-silenced MEF wt cells.

β1-integrin was endocytosed after a time-span of 9 min in the MEF wt cells, whereby surface levels of biotin-linked β1-integrin was decreased. Strikingly, MEF wt cells treated with CPZ and thus showing hardly any clathrin mediated endocytosis exhibited a severely declined endocytosis of β1-integrin compared to untreated wt cells. In comparison, MEF NPxY2 ki cells displayed an even lower endocytosis rate in β1-integrin than wt cells treated with CPZ (Fig 10 A,B). Densitometric analyzes revealed

the immense decline in β1-integrin endocytosis in the functional LRP1 knock-out MEF cells (Fig. 10 B). MEF NPxY2 ki cells have previously been shown to endocytose LRP1 in very low amounts (Maier et al., 2013; Reekmans et al., 2010). It therefore seems that LRP1 is at least involved in β1-integrin internalization. Furthermore, the results indicate that β1-integrin internalization in MEF cells is clathrin dependent to certain extent. The next objective was to find out whether β1-integrin can affect LRP1 maturation or if the system works merely the other way around. Therefore, MEF wt cells were transfected with two distinct types of siRNA directed against β1-integrin. As controls, cells were transfected with unspecific siRNA or with the transfection reagent only. β1-integrin knock-down reduced protein levels tremendously with both siRNA variants 4 and 5 (Fig 10 C upper panel). Focusing on LRP1, a slight increase in LRP1 protein levels could be observed in the β1-integrin knock-down samples in relation to controls (Fig. 10 C lower panel). Due to this result one could hypothesize that LRP1 impacts β1-integrin maturation, however, LRP1 maturation is not impaired by β1-integrin knockdown since the detected β-chain is the shorter part of the mature LRP1 receptor. Furthermore, the function of LRP1 as major endocytic receptor appeared to impede β1-integrin internalization. Further support for the hypothesis of a coupled endocytosis of the two receptors is the clathrin dependence of LRP1 and β1-integrin in the process of internalization in this experimental setup.

5.4 Impact of disturbed β1-integrin endocytosis on cell adhesion

The heterodimeric integrin receptor connects the ECM with the cellular cytoskeleton by forming focal adhesion complexes at the sites of integrin binding. Initially, integrin receptors bind to proteins of the ECM followed by integrin clustering and the intracellular recruitment of proteins of the adhesome (Zaidel-Bar et al., 2007). Therefore, the initial binding surveyed by the assembly of focal contacts enables cells to adhere to the extracellular milieu. Dependent on the composition of the surface integrin proteome and activation state, cells adhere preferentially to certain ECM proteins. The surface retention of LRP1 in the functional knock-out model potentially reduced β1-integrin internalization to a great extent in this study and thus resulted in surface accumulation of β1-integrin. A disproportionally high surface representation of β1-integrin due to reduced internalization might have further effects on the physiology of the NPxY2 ki MEF cells such as on cell adhesion. Observations of Schwann cells harboring an LRP1 knock-out displayed increased cell adhesion to fibronectin detected

in an *in vitro* assay (Mantuano et al., 2010). Therefore, an adhesion assay was performed by using two distinct ECM proteins, fibronectin and collagen I, both ligands of β1-integrin. Cells were seeded in coated dishes and allowed to adhere for 30 or 60 min respectively. After proper washing and fixation cells were stained by crystal violet. The absorption was measured in a multi plate reader, reflecting the amount of adhered cells.

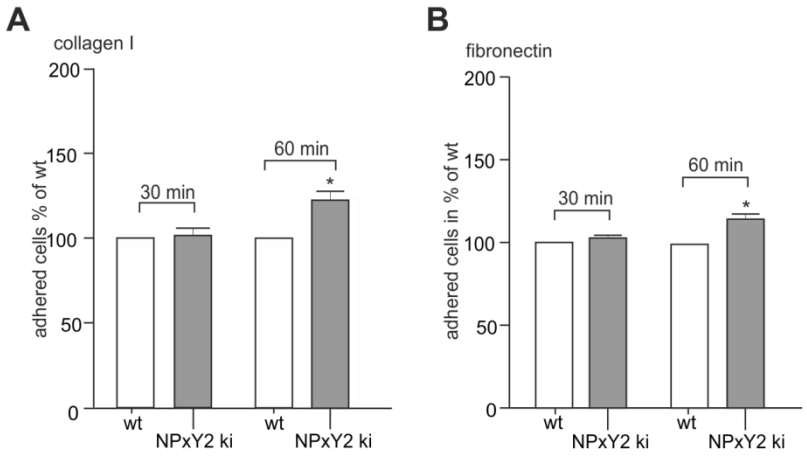

Figure 11: Surface accumulation of β1-integrin evoked increased cell adhesion: Cell adhesion of the MEF LRP1 NPxY2 ki cells and the MEF wt cells on fibronectin and collagen I was analyzed after 30 and 60 min post-seeding. Adhered cells were stained with crystal violet, after solubilizing the cells, the absorption was measured at 595nm by the use of a multi-plate reader. Results are shown in percent (%) of wt adhered cells, which were set as 100%. Densitometric results represent mean + s.e.m. of a minimum of three independent experiments. $p < 0.05$ (*t*-test) was considered statistically significant *. **A)** Cells seeded on collagen I exhibited augmented adhesion for MEF LRP1 NPxY2 ki cells in comparison to MEF wt cells after 60 min. After 30 min cell adhesion was comparable between the two cell lines. **B)** Cells seeded on fibronectin revealed similar tendencies, after 60 min, significantly more MEF LRP1 NPxY2 ki cells adhered than MEF wt cells, after 30 min cell adhesion was comparable between MEF wt and MEF LRP1 NPxY2 ki cells.

Adhesion of a cell is dependent on the composition of the ECM and the availability of active integrin surface receptors. The examination of cell adhesion in the MEF LRP1 NPxY2 ki model on the ECM protein collagen I revealed hardly any difference in adhesion after 30 min. Measurement of cell adhesion after 60 min depicted an increase in cell adhesion in the NPxY2 ki cells compared to wt MEFs (Fig. 11 A). Strikingly, the effect of the surface accumulation of β1-integrin on cell adhesion on collagen I appeared to be time dependent (Fig. 11 A). Cell adhesion on a second ligand of β1-integrin, the RGD sequence containing fibronectin was also investigated. Under these conditions MEF NPxY2 ki cells showed comparable adhesion behavior to wt controls after 30 min and only after 60 min of incubation significantly more MEF NPxY2 ki cells adhered to fibronectin than wt controls, reflecting the results of adhesion on collagen I (Fig. 11 B). The surface retention of LRP1 correlated with accumulating

surface levels of β1-integrin impairs the cell adhesion dynamics of the NPxY2 ki model, however, the effect first appears after a time-span of 60 min.

5.5 Surface retention of β1-integrin impairs cell spreading

Subsequent to adhesion, cells start to spread on the surface in a 2D model (Dubin-Thaler et al., 2004). Here, the membrane of the cell protrudes and thus enlarges the cellular area in forms of lamellipodia and filopodia. Moreover, stress fibers, which are composed of contractile actomyosin filaments, are formed in a GTPase driven manner (Tojkander et al., 2012). In order to get insight into further cellular consequences of the severely reduced endocytosis of LRP1 and the coupled reduction in β1-integrin internalization, cell spreading on two distinct ECM proteins was examined. Both MEF cell lines were seeded on ECM protein substrates under serum free conditions and spreading was analyzed 2h and 4h later by fluorescently labelling the actin cytoskeleton using phalloidin staining. The surface area of cells was evaluated by turning the acquired confocal image acquired at the laser scanning microscope LSM710 (Zeiss) into a monochrome image, and measuring the pixels of black cells on a white background of a cell with the ImageJ software.

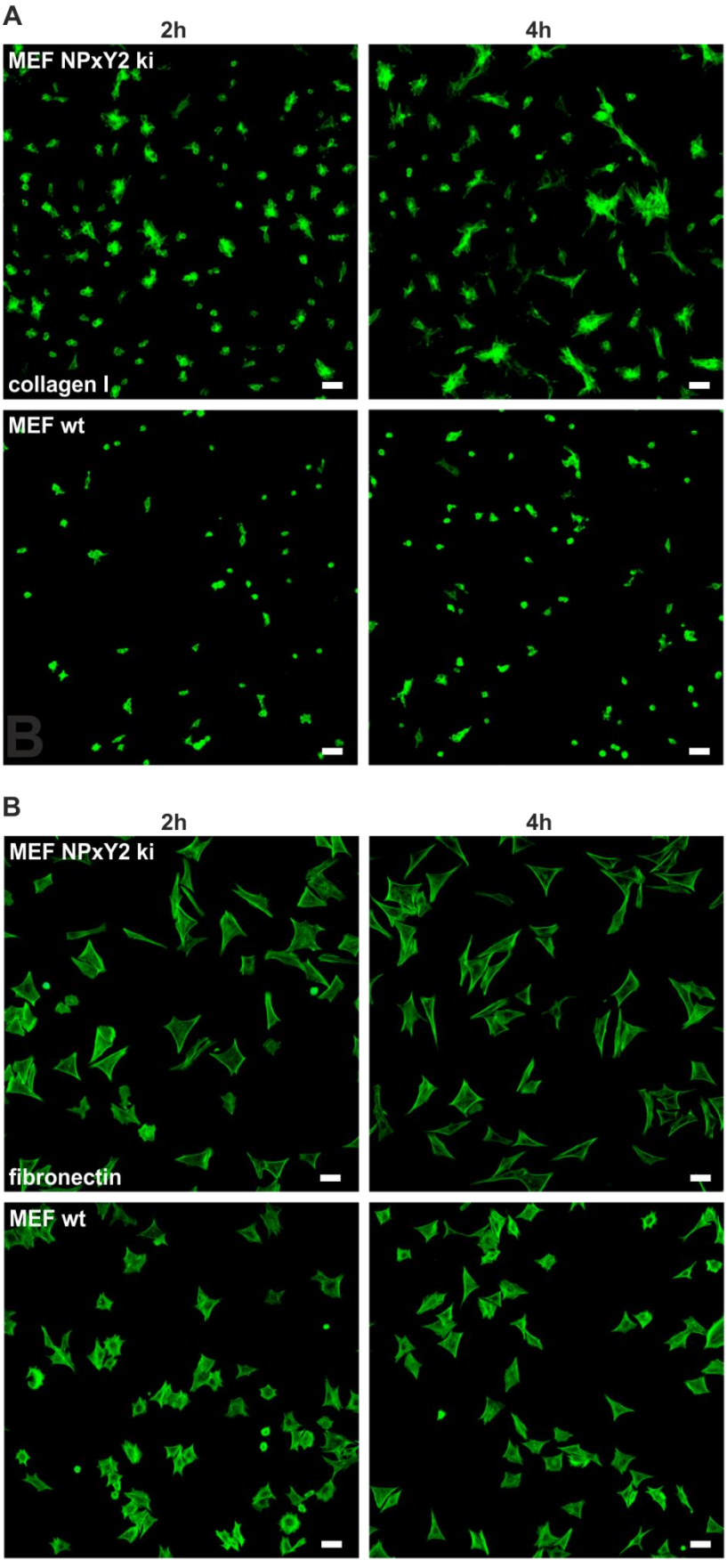
A
2h
4h
MEF NPxY2 ki
collagen I
MEF wt
B
B
2h
4h
MEF NPxY2 ki
fibronectin
MEF wt

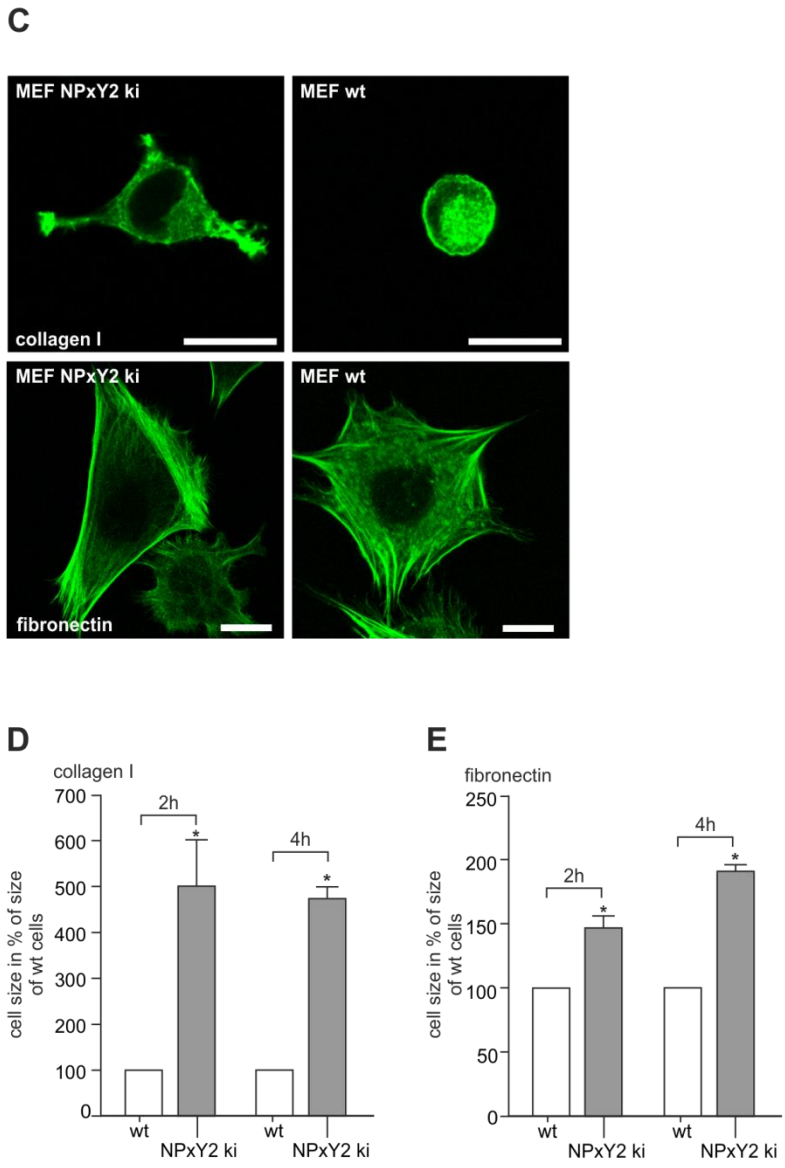

Figure 12: Enhanced cell spreading caused by the functional knock-out of LRP1: Cell spreading of MEF wt and MEF LRP1 NPxY2 ki cells was examined by seeding the cell lines either on collagen I coated substratum or on fibronectin coated dishes. The actin cytoskeleton was stained by the use of Alexa488-labelled phalloidin (green) after 2h and 4h of seeding. Images were acquired at a confocal laser scanning microscope. **A, B)** Overview images of MEF LRP1 NPxY2 ki cells (upper panel) and MEF wt cells (lower panel) are shown for the time points of 2h and 4h post-seeding on collagen I (A) and fibronectin (B). NPxY2 ki cells showed enlarged cells. Scale bar 50µm. **C)** Close up of MEF LRP1 NPxY2 ki cells (left panel) and MEF wt cells (right panel) seeded on collagen I (upper panel) or fibronectin (lower panel) confirmed the increased cell size of the NPxY2 ki cells on both ECM proteins. Scale bar 20µm **D, E)** Cell size measurement using the ImageJ software affirmed the enhanced cell spreading of MEF LRP1 NPxY2 ki cells on collagen I (D) and fibronectin (E) after 2h and 4h of incubation time. Statistical analyzes represent mean + s.e.m and a value of $p < 0.05$ was considered as statistically significant* after the *t*-test was performed.

In figure 12 A and B the actin cytoskeleton was stained by phalloidin (green) and displays an immense difference of cell spreading either on collagen I or on fibronectin of the MEF LRP1 NPxY2 ki cells in overview confocal images. The upper panel shows

the adhered NPxY2 ki cells on the ECM proteins collagen I or fibronectin, respectively. The lower panel represents the MEF wt controls. Particularly, LRP1 functional knock out MEF cells tended to cluster by intense cell-cell contacts (Fig. 12 A upper panel). A close up of one representative cell of each cell line and ECM substrate after 2h is shown in figure 12 C. Strikingly, the increase in spreading of the MEF NPxY2 ki cells seeded on collagen I compared to the wt controls is very remarkable (Fig. 12 C, upper panel). MEF cells expressing LRP1 wt are still round, whereas cells harboring the functional LRP1 knock-out spread and show prominent membrane protrusions. While cells of both models seeded on fibronectin are spread, the organization of stress fibers is distinct in the NPxY2 ki cells. Stress fibers are concentrated around the contour of the cell and ventral fibers dominate. Furthermore, filopodia structures appeared to accumulate at the upper part of the MEF NPxY2 ki cell, which might be the leading edge of the cell. Stress fibers are equally spread in MEF cells expressing LRP1 wt and both dorsal and ventral stress fibers were observed. Filopodial structures and lamellipodias were spread throughout the cell (Fig. 12 C lower panel). After quantitative analyzes of the cell size a significant difference in spreading between the NPxY2 ki cells and the MEF wt cells can be observed for both substrates after 2h and 4h. However, the increase in spreading is even greater for cells seeded on collagen I.

Apparently, the lack of β1-integrin internalization in an LRP1 dependent manner resulted in a cellular phenotype in the NPxY2 ki model. Alterations in cell adhesion on the seeding substrates of β1-integrin could be detected after 60 min (Fig. 11). In addition the subsequent process to cell adhesion, the cell spreading involving reorganization of the actin cytoskeleton is significantly altered in this model. Cell size aberrations associated with surface accumulation of β1-integrin were observed, as well as effects on the structural organization of the cytoskeleton during spreading (e.g. the stress fiber distribution throughout the cell (Fig. 12)). Treating adhered MEF cells with siRNA directed against β1-integrin yielded in a previous study to a size enlargement and cellular clustering (Huveneers et al., 2008). As a resume of the results one could hypothesize a severe impairment in β1-integrin function in the NPxY2 ki model evoked by reduced LRP1 mediated internalization of β1-integrin.

5.6 Decline in β1-integrin endocytosis causes an increase in focal adhesion complexes

After analyzing cellular phenotypes correlated with the surface accumulation of β1-integrin the investigations concentrated on the involved core unit in cell adhesion and spreading, the focal adhesions. Subsequent to integrin receptor binding to proteins of the ECM, focal points form which can mature to FAs. A characteristically component of FAs is the non-receptor phospho-tyrosine focal adhesion kinase (FAK) in its autophosphorylated form at tyrosine 397 (Brami-Cherrier et al., 2014; Hanks et al., 1992). Another protein associated with the adhesome and commonly used as marker for FAs, is the talin binding protein vinculin (Bershadsky et al., 1987; Campbell and Ginsberg, 2004a; Tachibana et al., 1995).

Since β1-integrin accumulates at the cells surface of MEF LRP1 NPxY2 ki cells, the on surface integrin dependent structure of FAs was examined. FA presence was visualized by immunocytochemical detection of vinculin and following quantitative analyzes. Additionally, protein levels of FAK and the autophosphorylated variant pFAK Y397 were examined by western blotting experiments in the MEF LRP1 NPxY2 ki model to get insight the downstream effects of reduced β1-integrin endocytosis, which is potentially mediated by LRP1.

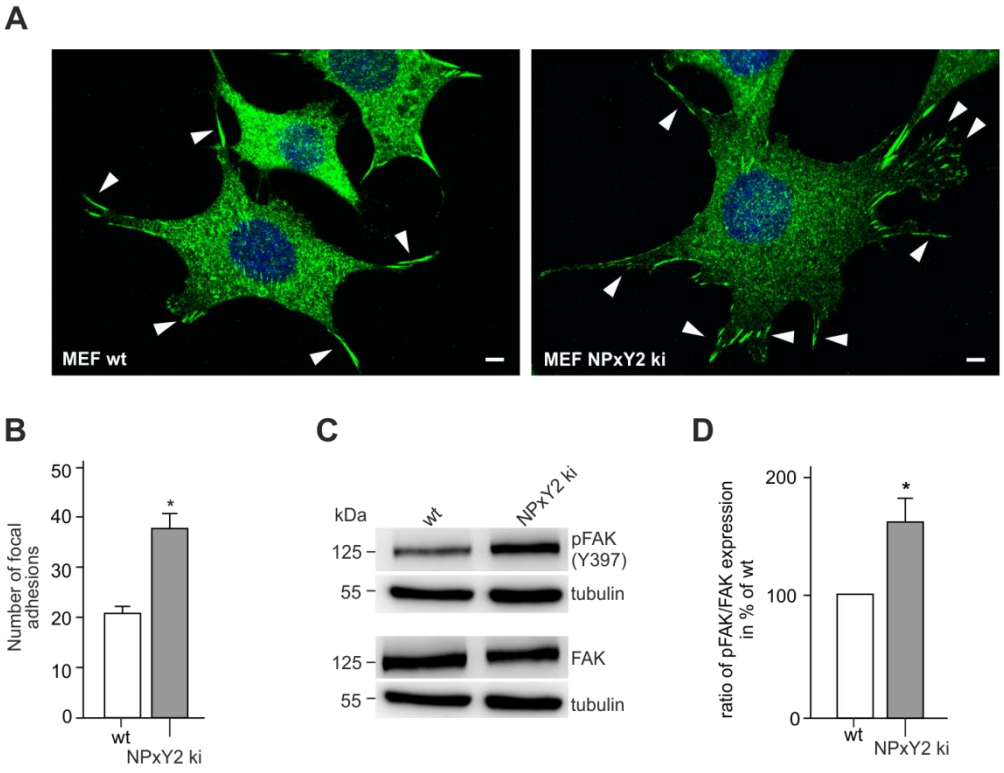

Figure 13: Reduced internalization rates of β1-integrin increased FAs: A) FAs were immunocytochemically stained for vinculin (green). Therefore, MEF NPxY2 LRP1 ki cells and MEF wt cells were seeded on fibronectin

coated dishes for 3h. Arrows indicate sites of FAs. Comparing both cell lines, remarkably more FAs were present in the LRP1 NPxY2 ki MEF cells compared to MEF wt cells. Scale bar 10µm. **B)** Quantification and subsequent statistical analyzes by the use of the *t*-test revealed a significant increase in the number of FAs for the NPxY2 ki model. Results represent mean + s.e.m. of focal adhesion numbers of a minimum 15 cells per cell type. A value of $p < 0.05$ was considered as statistically significant *. **C)** Analyzes of the FAK activity in cell lysates generated from the MEF wt and MEF LRP1 NPxY2 ki cells revealed elevated levels of activated, autophosphorylated pFAK Y397 in the NPxY2 ki cells. Total FAK expression remained comparable between the two cell lines. Subsequent to SDS.PAGE and western blotting, blots were incubated in the polyclonal FAK antibody generated against FAK or with the specifically pFAK Y397 detecting polyclonal rabbit antibody. Tubulin was used as loading control. **D)** Five independent experiments were densitometrically analyzed followed by statistical *t*-test analyzes. The ratio of activated pFAK to FAK was formed and MEF wt levels were set as 100%. The ratio of pFAK/FAK was increased by 60% to wt levels. A value of $p < 0.05$ was considered as statistically significant *.

The immunocytochemical detection of focal adhesions was performed by staining MEF wt and MEF LRP1 NPxY2 ki cells seeded on fibronectin for 2h with an antibody directed against vinculin (green). The analyzes of the acquired images revealed increased amounts of FAs in the LRP1 NPxY2 ki cells. The arrows indicate sites of FAs (Fig. 13 A). After quantitative evaluation of a minimum of 15 cells per cell line, a significant increase in FA´s of the MEF NPxY2 ki cell line was confirmed (Fig. 13 B).
Biochemical analyzes of one core member of FAs, the FAK displayed a comparable expression level of the kinase in both cell lines. Strikingly, the amount of the phosphorylated pFAK Y397 variant was increased in cells expressing the functional knock-out variant of LRP1 (Fig. 13 C). Densitometric analyzes revealed an elevated ratio of pFAK Y397 to FAK in the NPxY2 ki cells compared to wt MEFs (Fig. 13 D).
The biochemical analyzes of the FAK activation reflected the aberrations detected in cell adhesion and spreading. An increased number of surface β1-integrin might lead to an enhanced amount of FA assembly and thus causing an elevated rate of cell adhesion and spreading, all processes depending on β1-integrin. Moreover, the dynamics of FA disassembly might be impaired.

5.7 β1-integrin silencing reduced FAK activity

It has been described that a knockdown or silencing by antibody treatment of β1-integrin in carcinogenic cell lines yielded a reduction of cell migration and adhesion and thus reduced the invasiveness of these cells (Grzesiak et al., 2011). Inhibiting β1-integrin in a human head and neck cancer cell line revealed a decline in the activated pFAK Y397, whereas total FAK protein remained equally compared to cells treated control antibodies (Eke et al., 2012). In this study, a surface accumulation of β1-integrin caused an increase in pFAK Y397, raising the question if the effect could be reversed by

a β1-integrin knockdown. Therefore, MEF LRP1 NPxY2 ki cells were transfected with siRNA generated against β1-integrin following western blot analyzes of protein levels.

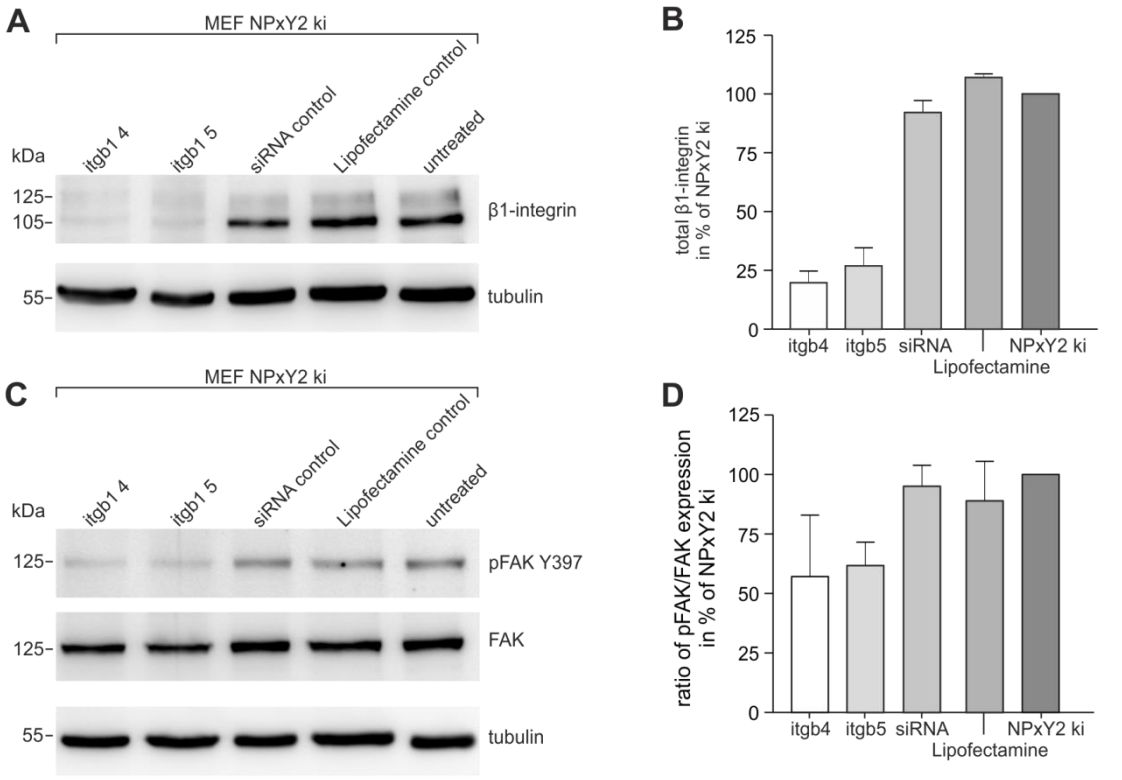

Figure 14: β1-integrin siRNA knock-down decreased FAK activation: MEF LRP1 NPxY2 ki cells were transiently transfected with two variants of siRNA, which were directed against β1-integrin. As negative control an unspecific siRNA construct and the transfection reagent only were used. **A)** SDS-PAGE and subsequent western blotting (anti-β1-integrin pAb7 antibody) revealed a severe decline in β1-integrin expression in the MEF LRP1 NPxY2 ki cells. Tubulin was used as loading control. **B)** Densitometric analyzes of two independent experiments was performed and statistically analyzed by one-way analyzes of variance. Protein levels of untreated cells were set as 100%. Results represent mean + s.e.m. β1-integrin expression was reduced to less than 30% of the untreated cells in the β1-integrin-siRNA transfected cells. **C)** Immunoblotting analyzes of the same samples for examining the levels of activated FAK depicted an immense decline in pFAK levels, however, total FAK levels were only slightly reduced (antibodies against FAK and pFAK Y397). Tubulin was used as loading control. **D)** Densitometric analyzes of two independent experiments and subsequent statistical analyzes by the one-way analyzes of variance method revealed a decline in the pFAK/FAK ratio of 40%. The ratio of untreated NPxY2 ki cells was set as 100%. Results represent mean + s.e.m.

The knockdown of β1-integrin diminished its protein levels to 25% of untreated NPxY2 ki cells in western blot analyzes (quantified by densitometric analyzes (Fig. 14 A,B)). Examination of the FAK expression and phosphorylation revealed a decrease in the activated pFAK Y397 form in β1-integrin silenced samples, total FAK levels were slightly reduced (Fig. 14 C). The ratio of pFAK to FAK declined to levels of 60% compared to untreated MEF NPxY2 ki cells. Interestingly, the effect of an increased amount of phosphorylated FAK in the LRP1 NPxY2 ki model could be reversed by integrin knockdown. In conclusion, the lack of β1-integrin endocytosis mediated by

LRP1 in the NPxY2 ki model appeared to cause a functional knock-out of β1-integrin to a certain extent.

5.8 β1-integrin surface accumulation alters the downstream Ras/Raf/MEK signaling cascade

The Ras/Raf/MEK/ERK pathway can be activated through downstream signaling of the FAs. Alternatively, the activating mechanism driven by LRP1 ligand binding and subsequent phosphorylation of the NPxY motifs can trigger the activation of this pathway.

On basis of the detection of cellular impairments like the elevated levels of FAs in the LRP1 NPxY2 ki model, the role of the related ERK signaling pathway was examined by western blot analyzes of ERK1/2 in the LRP1 functional knock-out system.

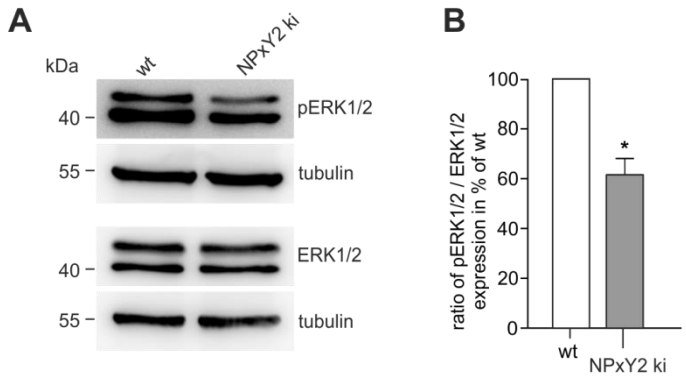

Figure 15: Impaired β1-integrin-LRP1 interaction decreased ERK1/2 phosphorylation: A) Cell lysates of MEF wt and MEF LRP1 NPxY2 ki cells were examined by SDS-PAGE and western blotting for the levels of activated pERK1/2. Tubulin was used as a loading control. pERK1/2 levels were reduced in the MEF LRP1 NPxY2 ki cells compared to wt MEF cells. **B)** After densitometric analyzes of three independent experiments combined with statistical analyzes using the *t*-test, a significant decrease in the ratio of pERK/ERK could be detected compared to the MEF wt ratio (set as 100%). Results represent mean + s.e.m. and a value of $p < 0.05$ was considered as statistically significant *.

MEF cells generated from LRP1 NPxY2 ki mice exhibited a diminished activation of the ERK pathway by reduced amounts of pERK1/2 levels in the western blot analyzes (Fig. 15 A). Densitometric quantifications validated these results to be significantly different by comparing wt MEF cells to LRP1 NPxY2 ki cells (Fig. 15 B). As both receptors mediate ERK activation by downstream signaling either via ligand binding or focal adhesion formation, the decline in ERK1/2 activation might be caused by the impairment of LRP1 endocytosis and the related surface accumulation of β1-integrin.

Alterations in downstream signaling via the FA or via the alterations in the LRP1 receptor itself might also participate in the reduction of phosphorylated ERK1/2 levels.

5.9 Reduction in β1-integrin internalization decreased cell migration

Cell motility in forms of migration is dependent on a dynamic equilibrium of focal adhesion assembly and disassembly. Therefore, different mechanisms participate in regulating the FA disassembly. In order to get further insight into the role of LRP1 mediated endocytosis of β1-integrin, the process of cell migration, being utterly dependent on β1-integrin internalization, was analyzed by a Boyden-chamber assay. MEF LRP1 NPxY2 ki cells and MEF wt as controls were seeded on filters coated with either the ECM protein collagen I or fibronectin and allowed to adhere and migrate through the chamber to a gelatine coated filter for 6.5h. Afterwards, migrated cells were counterstained following statistically analyzation. The pretreatment of MEF wt cells with the specific active β1-integrin blocking antibody (clone Ha2/5) was constituted to mimic the effects of a functional β1-integrin knock-out. This experiment was performed by Kristina Götze.

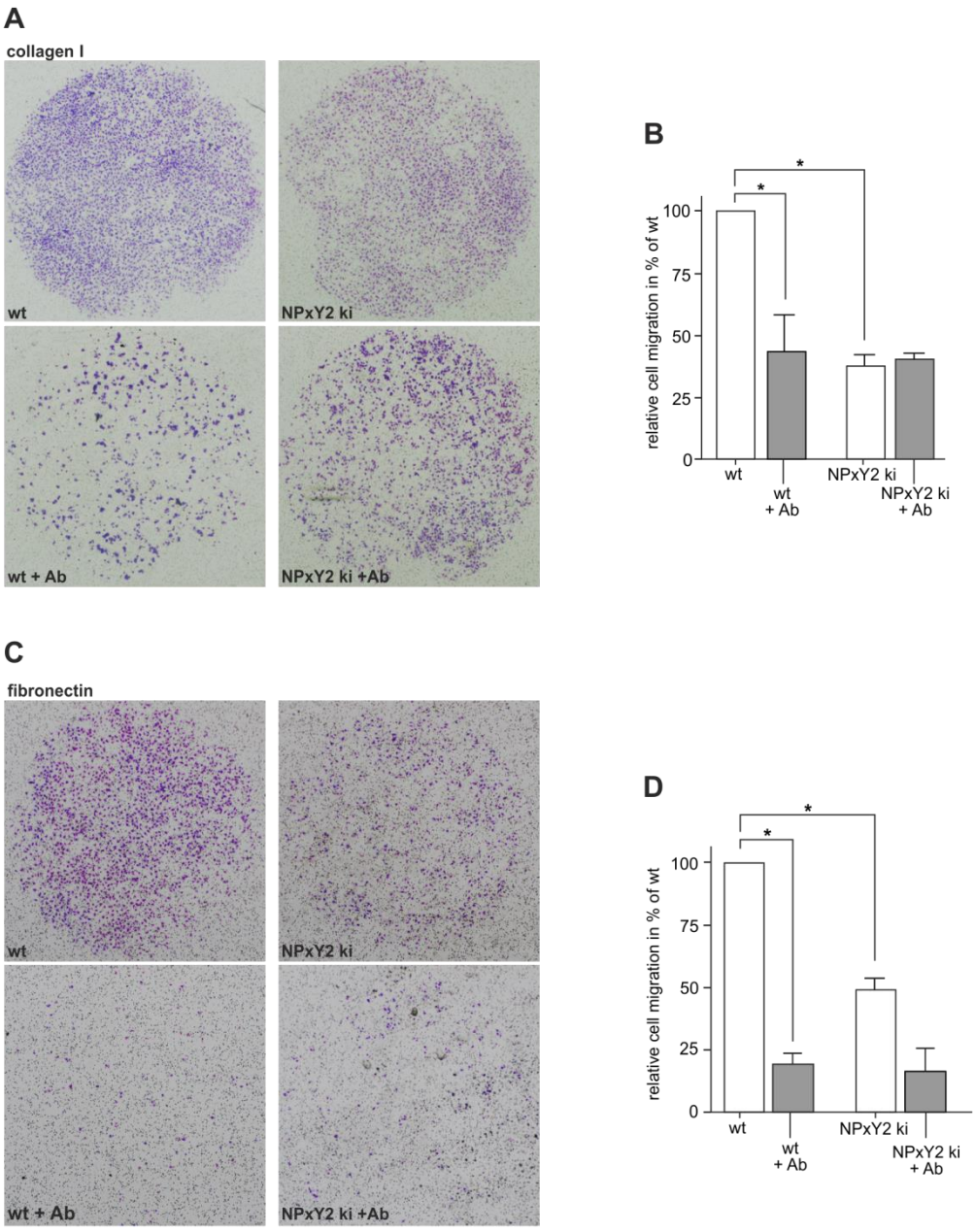

Figure 16: Reduced cell migration rates in the NPxY2 ki MEF cells: Cell migration of the MEF LRP1 NPxY2 ki cells and MEF wt cells was examined by the use of a standardized Boyden chamber assay. **A, C)** Equal amounts of cells were seeded on collagen I (A) (1.5 mg/ml) or fibronectin (C) (10 µg/ml) coated filters and allowed to migrate for 6.5h. β1-integrin dependent cell migration was inhibited, as cells were pre-incubated with a β1-integrin specific monoclonal hamster to mouse antibody (clone Ha2/5), which stabilizes the inactive conformation of β1-integrin. As shown by representative images, cell migration rates of MEF LRP1 NPxY2 ki cells was dramatically reduced compared to wt migration rates on both substrates. Antibody treatment decreased migration in MEF wt cells on collagen I (A) and fibronectin (C), however, MEF LRP1 NPxY2 ki cells treated with the antibody and seeded on fibronectin revealed a further decline in cell migration, NPxY2 ki cells seeded on collagen I and pre-treated with the antibody showed no difference in migration after treatment compared to migration rates before the antibody treatment. **B, D)** Quantification of migration on collagen I (B) and fibronectin (D) confirmed the observed decline in migration of the MEF LRP1 NPxY2 ki cells compared to MEF wt cells on both substrates. Migration of MEF wt cells treated with the Ha2/5 antibody exhibited a significant reduction in cell migration on collagen I (B) and fibronectin (D). Results are expressed in percent (%) of wt and represent mean + s.e.m. of two independent experiments, each including four to sixteen separate wells per data point and condition. $p < 0.05$ was considered as significant * by using one-way ANOVA.

Cell migration of the NPxY2 ki MEF cells examined in the Boyden chamber assay revealed a severe decline in cell migration on collagen I compared to equally treated MEF wt cells (Fig. 16 A). After statistical analyzes a reduction in migration of more than 50% could be observed (Fig. 16 B). Blocking the active form of β1-integrin by antibody treatment diminished cell migration rates of MEF wt cells to 40% of untreated cells. Remarkably, MEF NPxY2 ki cells treated with the β1-integrin blocking antibody migrated equally to untreated NPxY2 ki cells (Fig 16 A,B). The same experimental setup was also used for cells seeded on fibronectin coated filters. Compared to MEF wt migration the migration rate of the NPxY2 ki MEFs remained 20% of wt. Antibody treatment of the MEF wt cells reduced migration to an equal rate compared to NPxY2 ki cells. Strikingly, the inhibition of active surface β1-integrin by antibody treatment lead to a further drop in cell migration rates among LRP1 NPxY2 ki cells seeded on fibronectin. However, cell migration of LRP1 NPxY2 ki cells seeded on collagen I remained unaltered after blocking active β1-integrin by antibody treatment (Fig. 16 C,D).

In accordance with the former results, a further cellular process crucially depending on integrin is altered by the surface accumulation of β1-integrin in the LRP1 NPxY2 ki model. A lack in LRP coupled integrin internalization impedes proper FA disassembly and therefore potentially reduces cell migration on β1-integrin specific substrates. Blocking the active form of β1-integrin by stabilizing inactive β-integrin via antibody treatment probably alters the complete β1-integrin outside-in signaling pathway and thus reduces cell adhesion and motility on both substrates. Inhibition of active β-integrin in the NPxY2 ki system revealed no effect on cell migration on collagen I, as reduced integrin internalization rates mediated by the functionally knocked-out LRP1 derange downstream signaling and therefore potentially reduce FA disassembly. However, antibody treatment of LRP1 NPxY2 ki cells seeded on fibronectin further reduced cell migration.

5.10 LRP1 regulates MMP 2/9 activation

Matrix metalloproteases (MMP) proteolytically degrade the ECM and thus facilitate cellular motility. Up-regulation in MMP activity is frequently reported in the context of tumors, patients showing increased MMP activity often have poor prognosis (Tetu et al., 2006). Particularly, aberrations in MMP2 and MMP9 expression have been observed

along with numerous types of carcinomas (Komatsu et al., 2004; Song et al., 2009). LRP1 displays a binding receptor for MMPs, as it directly internalizes a complex of MMP2 and thrombospondin-2 and mediates the endocytosis of tissue metalloproteinase inhibitor (TIMP). LRP1 thus regulates the amount of active MMPs in the extracellular milieu in an indirect manner (Yamamoto et al., 2015). Cell migration is inevitably depending on ECM degradation. Concerning the LRP1 NPxY2 ki model, cell migration rates were shown to be decreased (Fig. 15). Moreover, MMP expression has been shown to be modulated by surface integrin receptors (Iyer et al., 2005). Therefore, the examination of MMPs in the studied model system was the next purpose of the investigations. With this in mind, the activity of MMP 2 and MMP9 were assayed by gelatine zymography. Thereto, samples were separated by SDS-PAGE with a gelatine containing gel. After renaturation, active gelatinases MMP2 and MMP9 proteolytically degraded the gelatine o.n. and lytic plaques could be detected. By the use of coomassie staining the lytic plaques could be visualized as unstained bands.

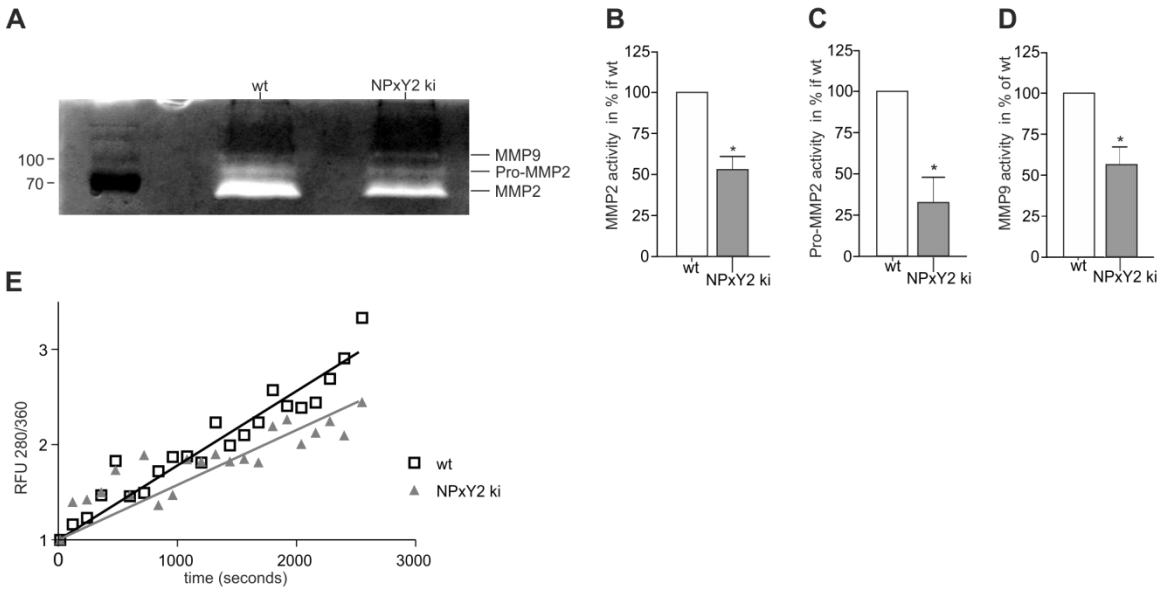

Figure 17: Decline in MMP2 and MMP9 activity in the NPxY2 ki model: A) For gelatine zymography, supernatants of MEF wt cells and MEF LRP1 NPxY2 ki cells were collected for 24h and reduced in volume by centrifugation. After electrophoresis, MMPs were allowed to proteolytically degrade the gelatine of the gel for 16h. Gels were stained with coomassie blue and images were acquired at the LAS 3000mini (Fujifilm). For better illustration, a representative image was converted into a monochrome image. In comparison to the MMP activity of MEF wt cells, decreased activity of MMP2, Pro-MMP2 and MMP9 could be detected in the MEF LRP1 NPxY2 ki cells. **B, C, D)** Three independent experiments were densitometrically analyzed and results represent mean + s.e.m. $p < 0.05$ (t-test) was considered as significant *. **E)** An *in vitro* enzyme activity assay of MMP2 and MMP9 proteolytic activity was performed by collecting phenol-red deficient supernatant of both cell lines for 24h. A fluorescently marked peptide was added to the cells and samples were purchased for fluorescence for 1h at 37°C. After MMP cleavage, the fluorophore was cleaved off the peptide, which increased fluorescence. The graph represents the mean of the measured fluorescence of triplets for each condition of MEF wt (black) or MEF NPxY2 ki

cells (grey) for 45 min. Self-fluorescence of cells was substracted. Lines represent linear regression of single values; the graph was prepared by using GraphPad Prism4.

Figure 17 A represents a black and white image of the performed gelatine zymography. The activity of MMP2 and MMP9 was analyzed by coomassie staining and measuring the size of the lytic plaques by densitometric analyzes. Strikingly, a lytic plaque at the size of the inactive pro-MMP2 form could be observed in both samples. After renaturation by removing the SDS from the gel, MMPs undergo conformational changes, also enabling the inactive pro-form of MMPs to be proteolytically active. Focusing on the comparison of the MMP activity between the functional knock-out MEF cell line and MEF cells expressing LRP1 wt a distinct difference in MMP activation was observed. Pro-MMP2 was detected on the height of 72kDa, the activated MMP2 was present at a height of 62kDa. Especially MMP2 depicted a significant decline in activation in the extracellular milieu of the LRP1 NPxY2 ki cells compared to wt controls (Fig. 17 A,B). Furthermore, the pro-variant of MMP2 revealed a decrease in proteolytic activity in the NPxY2 ki sample (Fig. 17 A,C). The lytic plaque at the height of around 100kDa resembled the activity of the 92kDa MMP9. By contrast with the wt controls, MMP9 activity in NPxY2 ki supernatant was reduced to about 60% of wt activity (Fig. 17 A,D). It should be noted, that the renaturation of MMPs after SDS-PAGE performance the enzymatic activity examined in zymography is not necessarily analogous to the activity in a physiological system. To evaluate MMP2 and MMP9 real proteolytic activity, a protease cleavage assay using a MMP2 and MMP9 specific peptide was performed. Both gelatinases cleave after the amino acid leucine; therefore, the same peptide could be used. Once cleaved, the linked fluorescent group of the peptide is released and emits measureable light. Measurements were performed by using the supernatant of MEF LRP1 NPxY2 ki and MEF wt cells and light absorption was detected for 1h at 37°C. The same trend as observed in the zymography was also evident for the peptide cleavage assay; the overall activity of both gelatinases was reduced in the MEF LRP1 NPxY2 ki samples (Fig. 17 E).

The interrupted endocytosis dynamics of LRP1 in the LRP1 NPxY2 ki model and the correlated reduction in β1-integrin declined MMP activity. The obtained results correlate perfectly with the lowered migration rate of the MEF LRP1 NPxY2 ki cells, utterly depending on MMP activity.

5.11 Coupled endocytosis of LRP1 and β1-integrin affected focal adhesions in neurons

LRP1 and β1-integrin are expressed in the neuronal system and are involved in the neuronal actin-cytoskeleton organization. As MEF cells of the LRP1 NPxY2 ki model revealed aberrations in cellular processes involving the actin-cytoskeleton dynamics, the effect of the disturbed interaction between LRP1 and β1-integrin in the CNS was examined next. β1-integrin is known to be involved in neuronal cell migration, neurite outgrowth and branching, synapse formation and plasticity, all processes, requiring a crosstalk of the interior and exterior of neurons and resulting in a rearrangement of the cytoskeleton (Belvindrah et al., 2007; Ribeiro et al., 2013; Tan et al., 2011; Warren et al., 2012). Besides β1-integrin, LRP1 is widely expressed in neurons and was shown to be involved in neurite outgrowth (Qiu et al., 2004; Wolf et al., 1992; Yoon et al., 2013). Based on the knowledge of the correlation between LRP1 and β1-integrin endocytosis, the investigations were extended and primary cortical neurons generated from either C57BL6 control mice or from C57Bl6 LRP1 NPxY2 ki animals were analyzed. At first, it had to be assured, that both proteins are closely located in the cell in order to allow receptor interaction. Therefore, outgrowing cortical neurons of the LRP1 NPxY2 ki mouse model were immunocytochemically stained for LRP1 and β1-integrin.

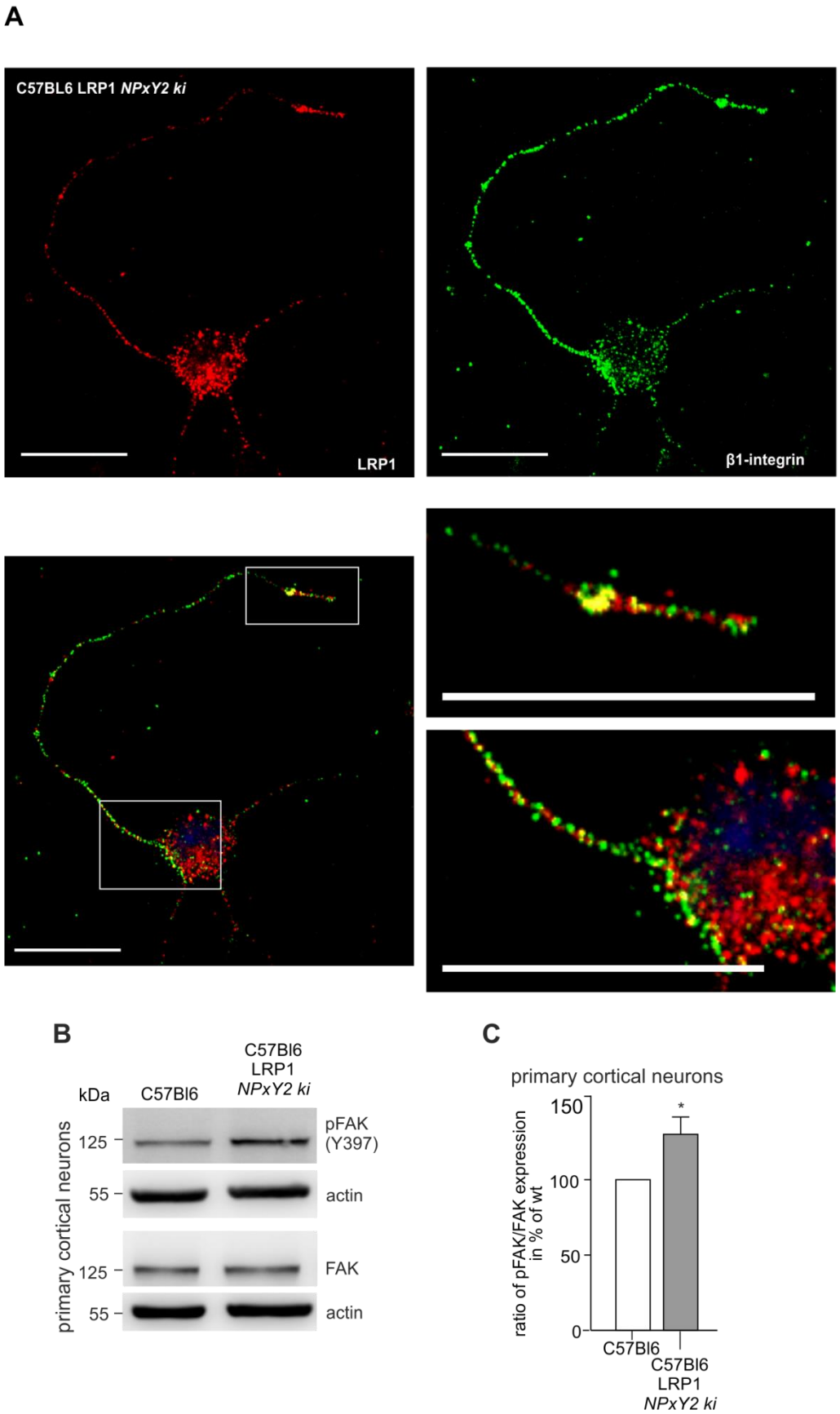

Figure 18: The interplay of LRP1 and β1-integrin impaired focal contacts in neurons: A) Immunocytochemical surface staining of primary cortical neurons generated from C57Bl6 NPxY2 ki animals for LRP1 (red, antibody B411E2) and β1-integrin (green, antibody pAb7) depicted co-localization of both receptors. Images in the upper panel represent the single channel surface staining of LRP1 and β1-integrin, the lower panel shows the overlay of the

channels for the imaged neuron (DIV 5). A close up of the sites of co-localization underlines the close location of both receptors. Scale bar 20µm. **B)** Lysates of C57Bl6 and C57Bl6 LRP1 NPxY2 ki neurons (DIV 15) analyzed for levels of activated FAK revealed an increase in pFAK Y397 in the NPxY2 ki neurons compared to wt controls. Total FAK expression was comparable to levels of wt neurons. Actin was used as loading control. **C)** Densitometric and subsequent statistical analyzes of a confirmed a significant increase in the pFAK/FAK ratio for C57Bl6 NPxY2 ki neurons. Protein levels were normalized to actin. Results represent + s.e.m. and $p < 0.05$ of three independent experiments was considered as statistically significant *.

The immunocytochemical verification of the cellular localization of LRP1 and β1-integrin in cortical neurons of the LRP1 NPxY2 ki mouse model in DIV 5 revealed several sites of co-localization in a surface staining (Fig. 18 A). The most dominant co-localization could be detected at the edge of the outgrowing axon. Further co-localizations were observed around the cell body and throughout the axon. The staining affirmed close localizations of both proteins. The single channels of the LRP1 (red) and β1-integrin (green) surface stainings are depicted in the upper panel of figure 18 A. Both receptors are equally distributed across the cell body and the outgrowing axon.

Focal point contacts of neurons are equally composed as focal adhesions of other cells types. The previous results showed an alteration in the FAK activation caused by lack of LRP1 mediated internalization of β1-integrin and an accumulation of focal adhesions (Fig. 13). Western blot analyzes of primary cortical neurons displayed equal interruption in the FAK activation. Levels of active pFAK Y397 were significantly elevated in samples generated from LRP1 NPxY2 ki mice in comparison to wt mice (Fig. 18 B,C).

Bringing all results together, an important role of LRP1 in β1-integrin endocytosis can be shown for two different cellular models.

5.12 Alterations in β1-integrin endocytosis interrupted neuronal cell migration

Cell migration is a major feature in embryonic brain development. After the invagination of the neuronal tube its development starts from the anterior end and the emergence of several progenitor cells starts. Brain development of vertebrates can be roughly subdivided into 5 major steps: the generation and proliferation of progenitor cells, the classification into neurons and glia cells, directional migration to their final location in the brain, guided outgrowth of axons and dendrites and finally the interconnection into a neuronal network by synapses formation (Cooper, 2013).

The subventricular zone (SVZ) is a part of the brain situated around the lateral ventricle, generating neuronal progenitor cells throughout a lifetime. The progenitor cells migrate

to the *bulbus olfactorius,* the center for olfactory perception and learning. Especially rodents are constantly confronted with unknown odors which they learn to categorize. This process requires the generation of new neurons and their integration into the relay of the *bulbus olfactorius*. Post-generation, the neuronal progenitor cells move rostral along the rostral migratory stream (RMS) to their destination, the olfactory bulb, where they differentiate into neurons. The migrating cells organize themselves into polarized chains and migrate along the RMS until they reach the olfactory bulb where they migrate radially into the different layers (Lois et al., 1996). Organized in chains, the neuronal progenitors are in direct contact with each other and other surrounding cell types such as endothelial cells of the vascular system (Bovetti et al., 2007). Moreover, the connection with the ECM via integrin receptors has emerged to determine proper chain formation. Deletion of β1-integrin in the CNS of mice implicated a disruption in chain formation of migrating neuroblasts along the RMS (Belvindrah et al., 2007).

In this study an impact of LRP1 mediated endocytosis of β1-integrin on cell migration of MEF cells has been observed (Fig. 16), therefore the examination of migration in a neuronal system would further underline the physiological importance of the crosstalk between the two receptors. The morphology of the RMS was therefore analyzed by the use of two distinct methods, the Nissl staining of sagittal brain sections and the *in vivo* marking of proliferating cells via BrdU following immunohistochemical staining of brain sections. C57Bl6 and C57Bl6 LRP1 NPxY2 ki mice were transcardially perfused and tissue was immediately fixed with PFA followed by the staining methods.

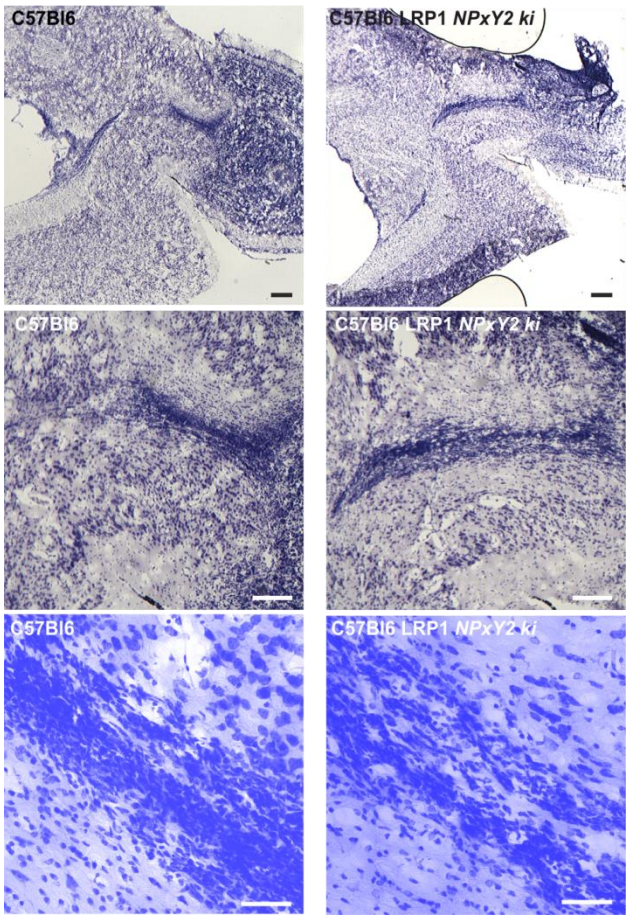

Figure 19 Nissl staining revealed an altered morphology of the RMS in LRP1 NPxY2 ki animals: Sagittal brain sections of C57Bl6 NPxY2 ki (right panel) and C57Bl6 (left panel) animals were stained with the Nissl method. The upper panel shows an overview image of the RMS acquired with a transmitted light microscope. A close-up of the RMS in the second panel depicted a loose organization of cell chains, migrating along the RMS in the NPxY2 ki mouse model. This observation was validated by a further close-up image of the RMS, which is shown in the lower panel. These images acquired at the confocal laser scanning microscope LSM710 illustrated a deranged chain formation of the RMS. Scale bar 50µm.

The comparison of the RMS organization between C57Bl6 sections and the C57Bl6 LRP1 NPxY2 ki samples pointed to a dramatic difference in RMS organization between the two mouse models (Fig. 19). The overview images of the first panel show the dense organization of the neuroblasts migrating along the RMS stained by kresyl violet, which visualizes nuclei and ribosomes, both located in the soma of neuronal cells. A close up of the RMS in the middle panel of figure 19 illustrated a less dense organization of the progenitor cells in the NPxY2 ki mouse model compared to wt controls. Analyzing the structure of the RMS by confocal laser scanning microscopy, it appeared as if the chain organization in the NPxY2 ki mice was diturbed, whereas neuroblasts of C57Bl6 mice were organized in tight cains (Fig. 19).

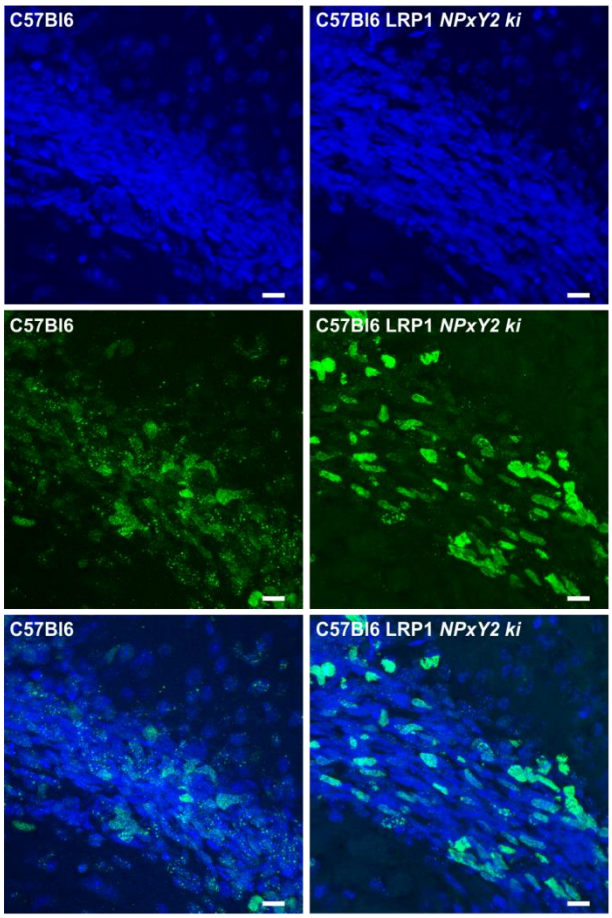

Figure 20: Chain formation of the RMS is destructed in C57Bl6 LRP1 NPxY2 ki animals: Proliferating neuronal progenitor cells migrating along the RMS were marked by *in vivo* injection of BrdU (green, middle panel) of four C57Bl6 NPxY2 ki mice and corresponding C57Bl6 controls. Nuclei were counterstained by DRAQ5 (blue, upper panel). Representative images illustrate, that migrating neuroblasts of C57Bl6 mice were organized in linear chains (left panel), whereas cells of the RMS of the C57Bl6 LRP1 NPxY2 ki mice lost the compact chain organization (right panel). Representative pictures of four animals of each genotype. Scale bar 10µm.

To exclude a destruction of the tissue during sample preparation and thus a biased effect on the RMS organization, proliferating cells were marked *in vivo* by intraperitoneal injection of BrdU into three months old LRP1 NPxY2 ki mice and wt controls. BrdU incorporates into the DNA of proliferating cells and thus marks neuronal progenitor cells generated in the SVZ and migrating along the RMS. Immunohistochemical stainings of the sagital sections against BrdU (green) and marking cell bodies with DRAQ5 (blue) revealed the same difference in RMS organization as observed in the Nissl staining. The chain formation of the neuroblasts in the NPxY2 ki animals was altered, since the dense chain formation was lost. Analyzing the RMS of C57Bl6

animals depicted a tight chain organization of the progenitor cells migrating along the RMS (Fig. 20).

The observed phenotype of deranged cell migration along the RMS in the NPxY2 ki animals reflects the observations of the morphology of the RMS of β1-integrin CNS knock-out animals. Due to these parallels the hypothesis of a functional knock-out of β1-integrin in a model showing dramatically reduced LRP1 internalization arises. The linked internalization of both receptors appeared to impair several linked downstream events influencing cellular behavior, which could be shown in a neuronal system as well as in fibroblasts.

5.13 Modifications of dendritic spines in the LRP1 NPxY2 ki model

Spines are membrane protrusions first described by Cajal in 1891 as protrusion of neurons consisting of a thin neck and a head (Ramón y Cajal, 1891). One neuron can have many spines, mostly forming excitatory synapses with axons of other neurons. Here, representing the post-synaptic site, spines were shown to be dynamically changing in number and morphology. Spines show morphological divergence and can be subdivided in three major types: the thin spines, stubby spines and mushroom spines, characterized by their head and neck diameter (Peters and Kaiserman-Abramof, 1970). The actin filaments permeate the neck and the head up to the postsynaptic density of spines, where actin binding proteins are present (Landis and Reese, 1983; Wyszynski et al., 1997). By locally stimulating spines, a morphological change has been demonstrated in the context of spine diameter and formation (Engert and Bonhoeffer, 1999; Matsuzaki et al., 2004). Long-term potentiation (LTP) has been shown to drive actin polymerization and thus enhancing the diameter of spines (Fukazawa et al., 2003). LTP is a process associated with learning and memory formation. In order to be able to generate new neuronal pathways after learning, new synapses have to be formed. Therefore new spines emerge by membrane protrusions, based on actin polymerization (Holscher, 1999). Actin cytoskeleton dynamics such as polymerization and depolymerization is the basis for spine plasticity. In different cell models integrins as ECM receptors are involved in the regulation of cytoskeleton dynamics and in transforming LTP in spine plasticity (Chan et al., 2003; Kramar et al., 2002).

Besides the crucial role of β1-integrin, LRP1 is also reported to be involved in LTP and synapse formation. Conditional forebrain knock-out of LRP1 led to a decline in PSD95 and synaptophysin, both synaptic marker proteins (Liu et al., 2010). Moreover, LRP1

mediates signal transduction after its ligand binding of tPA to the NMDA receptor and is involved in the endocytosis of NMDA subunits, whereby LRP1 influences LTP generation (Maier et al., 2013; Martin et al., 2008). The NPxY2 ki mice exhibited behavioral phenotypes like hyperactivity and an altered spatial memory. Therefore, a correlation between β1-integrin internalization mediated by LRP1 and a possible change in spine morphology or plasticity was hypothesized. To analyze spines of primary cortical neurons of the LRP1 NPxY2 ki mouse strain and of C57Bl6 controls, neurons were transiently transfected with a pEGFP plasmid for visualizing the morphology of the neurons. Subsequently, cells were fixed and images were acquired at a laser scanning microscope. Dendrites of second degree in branching were used for studying the spine morphology by using the NeuronStudio software.

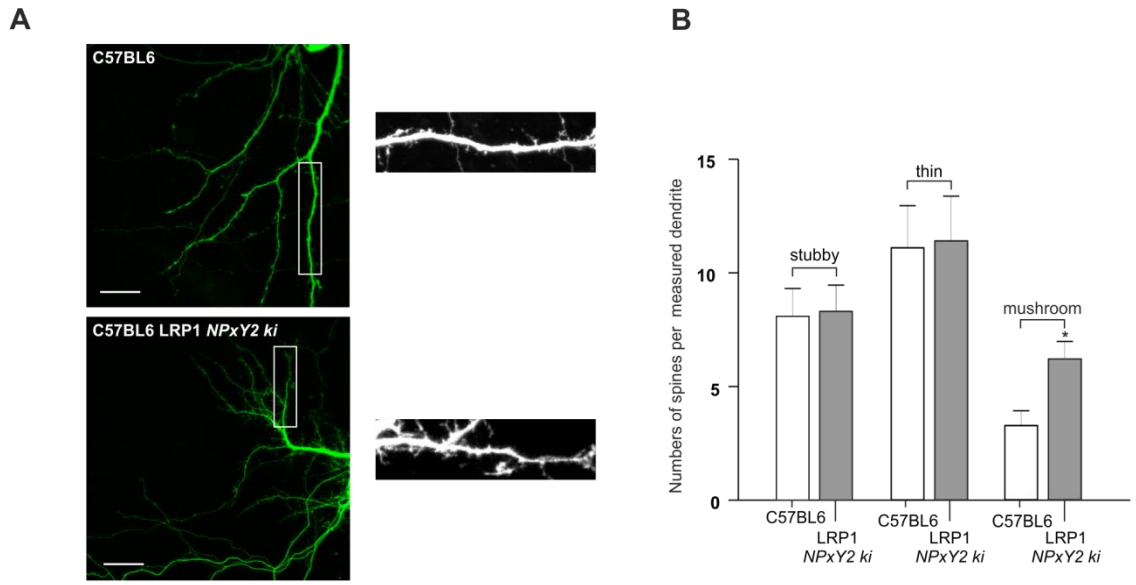

Figure 21: Spine plasticity is altered in C57Bl6 NPxY2 ki mice: A) Representative images (Z-Stack overlay images) of GFP transfected primary cortical neurons (DIV 15) of C57Bl6 (upper panel) and C57Bl6 LRP1 NPxY2 ki mice (lower panel). For spine analyzes dendrites of second degree of branching (white boxes) were chosen, two representative dendrites are marked by a white box. In the second panel two close-ups of the marked dendrite are illustrated as black and white images to improve the visualization of spines. **B)** Analyzes of the number of the three spine types stubby, thin and mushroom were performed with the use of the NeuronStudio software. Spines of a minimum of 5 dendrites of distinct neurons generated from two independent preparations per genotype were analyzed. For statistical analyzes (*t*-test) the amounts of the same spine type were compared between the C57Bl6 neurons and the C57Bl6 LRP1 NPxY2 ki neurons. Results represent the + s.e.m. and $p < 0.05$ was considered to be statistically significant *. Amounts of stubby and thin spines were comparable between the two genotypes. The number of mushroom spines was significantly increased in the C57Bl6 LRP1 NPxY2 ki neurons.

A representative GFP transfected cortical neuron of each mouse strain and a close up of the selected part of the neurons, converted into a black and white picture to improve visualization of spines are depicted in figure 21 A. In order to distinguish between the three major types of spines, thin, stubby and mushroom, dendrites of the second degree of branching were selected for spine analyzes. Depending on the type, different criteria have to be met in order to categorize the spines. In general, there was no distinct difference in total spine numbers between the analyzed neurons of the two mouse strains (not shown). However, comparing each spine subtype, stubby, thin and mushroom with each other a significant elevation of mushroom spines in the LRP1 NPxY2 ki animals could be observed (Fig. 21 B).

The gained results implicate a role of LRP1 mediated β1-integrin internalization on spine morphology, heavily depending on cytoskeleton reorganization. As shown for MEF cells generated from the LRP1 NPxY2 ki animals the interplay between the two receptors influences actin cytoskeleton organization, making the hypothesis of altered spine morphology and thus potentially explaining the deficits in spatial learning of the NPxY2 ki animals more likely.

6. Discussion

6.1 Is β1-integrin endocytosed in a LRP1 dependent manner?

LRP1 and β1-integrin are both cell surface receptors, transducing signaling across the plasma membrane. Heterodimeric integrin receptors link cells to the ECM and transduce downstream signaling subsequent to binding ECM proteins. In contrast, LRP1 is a major endocytic receptor, internalizing numerous extracellular ligands and thus regulating the composition of the extracellular surrounding. Although they subserve distinct cellular roles, there are studies linking the two receptors (Salicioni et al., 2004). Both proteins were found to be localized at the leading edge of migrating cells, bringing them in close proximity, facilitating potential interaction.

LRP1 in its function as the main endocytic receptor binds and internalizes a great variety of ligands and thus is involved in signal transduction, endocytosis and cell migration (Cao et al., 2006; Herz and Strickland, 2001). The presence of LRP1 at the plasma membrane appeared to be crucial for the transport of β1-integrin to the cell surface, since LRP1 ko cells (CHO 13-5-1) and CHO 14-2-1 cells, expressing endoplasmatic reticulum (ER) and Golgi complex remaining LRP1 showed decreased surface levels of β1-integrin in a former publication (Salicioni et al., 2004). Interestingly, intracellular phosphorylation of LRP1 has been linked to the recruitment of β1-integrin to the surface (Czekay et al., 2003; Hu et al., 2007). In this study the previous findings were expanded by stepwise narrowing down the potential interaction site of β1-integrin and LRP1. Interaction of LRP1 β1-integrin revealed to be independent oh the LRP1 extracellular domains, however, the intracellular part of LRP1 was shown to be essential for the receptor interaction, since co-immunoprecipitation failed by using a LRP1 domain IV mini-receptor, lacking the complete intracellular domain (Fig. 9). Further experiments using constructs harboring single amino acid exchanges in the NPxY motifs of LRP1 from tyrosine to phenylalanine placed the focus for further investigations on the NPxY2 motif of LRP1 as potential interaction site (Fig. 9). The NPxY motifs of LRP1 play a pivotal role in intracellular binding of proteins, which is accompanied by tyrosine phosphorylation of the NPxY motifs (Li et al., 2000). In the context of cancer, the role of LRP1 is still controversial; however in a rescue trial the expression of a LRP1 mini-receptor in LRP1 deficient cells, which were subsequently xenografted in nude mice, demonstrated to be tumor protective. However,

in the same setup LRP1 deficient cells expressing a construct with a single amino acid exchange in the NPxY2 motif failed to be tumor protective. This amino acid exchange prohibited tyrosine phosphorylation in the NPxY2 motif of LRP1 and mimicked the tumor promoting properties of LRP1 deficiency (Zhang et al., 2008). The NPxY motif of LRP1 appeared to be a determining factor upon the impact of LRP1 on cell migration, therefore, the LRP1 NPxY2 ki model was chosen for investigating in the interaction of LRP1 and β1-integrin. Here, the tyrosine of the NPxY2 motif of LRP1 was replaced with a multiple alanine cassette resulting in a functional knock-out for LRP1, depicted by severely reduced endocytosis of surface LRP1 (Reekmans et al., 2010; Roebroek et al., 2006). However, surface protein level analyzes of MEF cells generated from the NPxY2 ki model revealed a surface accumulation of LRP1 accompanied by a five-fold increase in surface β1-integrin levels (Fig. 8, D,E).

Additionally, a shift from mature to an elevated rate of immature β1-integrin could be detected in the LRP1 NPxY2 ki cell model (Fig. 8 D). Maturation of β1-integrin was previously described to be LRP1 dependent, where a pulse chase experiment revealed decelerated maturation of β1-integrin in LRP1 ko cells (Salicioni et al., 2004). The role of LRP1 in β1-integrin maturation was here verified by analyzing the LRP1 NPxY2 ki model, since the functional knock-out of LRP1 revealed increased amounts of immature β1-integrin levels (Fig. 8). In addition, total protein levels of β1-integrin were elevated in the LRP1 NPxY2 ki MEF cells. However, by reversing the situation by knocking out β1-integrin in LRP1 wt expressing MEF cells, the LRP1 β-chain protein levels were only slightly altered (Fig. 10 C). The β-chain emerges after furin cleavage of full length LRP1, and assembles non-covalently with the α-chain to the functional LRP1 receptor, which seemed to be β1-integrin independent. A possible explanation for the increased total β1-integrin protein levels in the LRP1 NPxY2 ki MEF cells might be a compensatory reaction to the surface accumulation of β1-integrin. Due to the possibly impaired downstream signaling function of β1-integrin in the functional knock-out model of LRP1, β1-integrin levels might be elevated to maintain the cellular function of β1-integrin. Reduced amounts of endocytosed β1-integrin might result in a decline of the intracellular-pool of β1-integrin, reducing the available integrin receptors for newly formed contacts to the ECM and might result in a compensatory overexpression of β1-integrin in the LRP1 NPxY2 ki model. There are several examples for similar compensatory mechanisms: e.g. FAK knock-out endothelial cells which up-regulate proline-rich tyrosine kinase 2 (Pyk2) to compensate for some functions of FAK (Weis et

al., 2008). Furthermore, alterations in β1-integrin levels of NPxY2 ki cells might also be caused by a lack of degradation in the lysosomal system. β1-integrin remains at the cell surface and the lysosomal degradation pathway is impeded by its reduced endocytosis mediated by LRP1 (Bottcher et al., 2012; Chao and Kunz, 2009; Lobert et al., 2010).

The reduction in endocytosis of β1-integrin in the NPxY2 ki model was validated by performing a biotin based internalization assay. Blocking clathrin mediated endocytosis of LRP1 wt expressing cells with CPZ revealed a reduction in internalization equal to the LRP1 NPxY2 ki cells, indicating the combined endocytosis of LRP1 and β1-integrin in a clathrin dependent manner (Fig. 10 C). The internalization of the endocytic LRP1 receptor has been shown to be mainly driven by clathrin coated pits (Harasaki et al., 2005). Concerning integrins, the internalization pathway heavily depends on the receptor type and the cell type. Clathrin mediated integrin internalization from the cell surface was described as a crucial event for myosin driven FA disassembly (Chao and Kunz, 2009). The process of cell migration depends on a dynamic equilibrium of focal adhesion assembly and disassembly enabling the cells to move on the attached surface (Broussard et al., 2008; Webb et al., 2002). Strikingly, the migration rate of the NPxY2 ki cells as well as β1-integrin antibody blocked MEF cells expressing LRP1 wt showed severely reduced migration rates both, on fibronectin and collagen I (Fig. 16). The fibronectin receptor α5β1-integrin for instance has been demonstrated to be internalized in a clathrin dependent manner (Caswell et al., 2009). Clathrin was observed to accumulate around disassembling FA and departed from these sites in combination with integrins (Ezratty et al., 2009). Furthermore, clathrin depletion studies supported the hypothesis of clathrin dependence of β1-integrin internalization, since depletion lead to integrin surface accumulation and a reduction in cell migration (Ezratty et al., 2009). Clathrin internalization can only be initiated by the recruitment of adapter proteins to the target of internalization such as the adaptor protein 2 (AP2) or the disabled homologue 2 (Dab2). Dab2 is an NPxY sequence specific protein, which is known to be involved in LDL receptor endocytosis in general, amongst them LRP1 (Maurer and Cooper, 2006). Moreover, FA disassembly in human fibrosarcoma cells and NIH3T3 fibroblasts has been demonstrated to be clathrin and Dab2 dependent by mediating β1-integrin internalization. The disruption in the NPxY2 motif of β1-integrin by the exchange of tyrosine to phenylalanine caused a severe decline in clathrin mediated endocytosis of β1-integrin in fibroblasts (Pellinen et al., 2008). When tyrosine is replaced by alanine in the NPxY2 motif of LRP1 a reduced binding affinity of LRP1 to

Dab-2 could be observed (Zhang et al., 2008). Dab2 may therefore link β1-integrin to LRP1 in an NPxY2 motif dependent manner and mediate the coupled endocytosis of the two receptors. Unfortunately, binding of Dab2 is probably inhibited in the LRP1 NPxY2 ki model due to the replacement of the NPxY2 motif by a multiple alanine cassette leading to reduced clathrin dependent internalization of LRP1 and thus β1-integrin and resulting in an altered cell migration.

There seems to be similarities between the observed LRP1 influence on β1-integrin maturation and internalization and the published interaction between LRP1 and the amyloid precursor protein (APP) (Pietrzik et al., 2004; Yoon et al., 2007). APP and LRP1 undergo joint endocytosis from the plasma membrane in a clathrin dependent manner and are linked by the cytosolic adaptor protein Fe65 (Pietrzik et al., 2004). Similar to β1-integrin, surface amounts of mature APP are reduced in CHO 14-2-1 cells (Salicioni et al., 2004; Waldron et al., 2008). Expression of an LRP1 construct lacking the NPxY2 motif has been shown to result in surface accumulation of APP, which correlates with the findings of surface accumulation of β1-integrin in LRP1 ki cells (Fig. 8) (Pietrzik et al., 2002). APP, LRP1 and β1-integrin were demonstrated to be endocytosed jointly by forming a complex with the scaffolding protein Ran-binding protein 9 (RanBP9) (Woo et al., 2012b). The interaction of RanBP9 and LRP1 takes place at the last 37 amino acids of the LRP1 C-terminus, which implies the NPxY2 motif (Lakshmana et al., 2009). A knockdown of RanBP9 resulted in surface accumulation of LRP1 and β1-integrin. One could hypothesize that the interaction of LRP1 and RanBP9 is disturbed in the NPxY2 ki system due to the modified NPxY2 motif and therefore results in increased surface presence of both proteins. The joint endocytosis of the APP, LRP1, β1-integrin and RanBP9 complex has been shown to play an important role in the pathology of Alzheimer's disease (AD), since the beta-site APP cleaving enzyme 1 (BACE1) is responsible for the generation of amyloid beta peptide (Aβ) after internalization of APP from the cell surface. Elevated levels of RanBP9 in brains of AD patients correlated with reduced amounts of β1-integrin at the cell surface. This might lead to impairment in processes depending on the presence of surface β1-integrin such as neuronal arborization, and was demonstrated for a mouse model overexpressing RanBP9 (Lakshmana et al., 2010; Woo et al., 2012a; Woo et al., 2012b). Furthermore, an increased scatter of FAs caused by RanBP9 overexpression and related elevated endocytosis of β1-integrin was observed. Overexpression of

RanBP9 leads to pathological disruptions of the neuronal cytoskeleton resulting in loss of synaptic plasticity and therefore impairs memory (Woo et al., 2015).

Combining former results and the results of the present study, there are clear indications for joint endocytosis of LRP1 and β1-integrin, potentially including an adaptor protein such as Dab2 or RanBP9 linking both receptors to each other. Moreover, LRP1 is involved in the process of β1-integrin maturation.

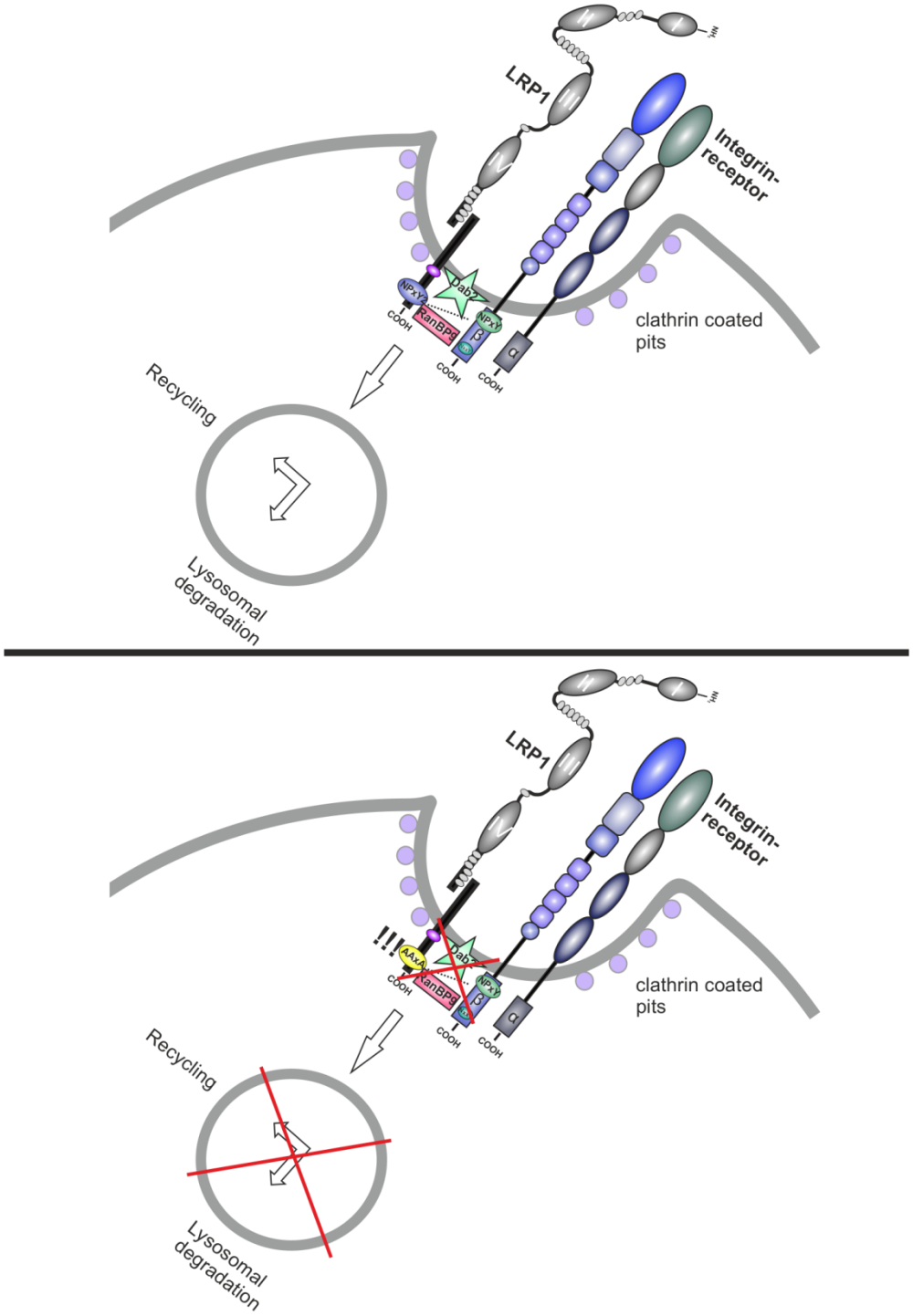

Figure 22: Sketch of the possible interaction between LRP1 and β1-integrin: The upper panel illustrates the potential interaction of LRP1 and β1-integrin via the NPxY2 motif of LRP1, mediated by Dab2 as scaffolding protein by binding to the NPxY motifs. The triple complex might be endocytosed in a clathrin-dependent manner. The second potential candidate for crosslinking LRP1 and β1-integrin and thus enabling coupled endocytosis is the scaffolding protein RanBP9. RanBP9 might also interact with the NPxY2 motif of LRP1 and thus link it to the c-terminal part of β1-integrin. The lower panel illustrates the situation in the LRP1 NPxY2 ki model. The derangement of the LRP1 NPxY2 motif prohibits the binding of the adapter proteins to LRP1; hence, the coupled, clathrin-dependent endocytosis of LRP1 and β1-integrin is inhibited.

6.2 Joint endocytosis of LRP1 and β1-integrin regulates cellular behavior

The obtained results of the present investigations support the hypothesis of interplay between LRP1 and β1-integrin resulting in combined endocytosis, and being a crucial way of regulating surface presence of β1-integrin. Interruption of the endocytic pathway resulted in morphological alterations and changes in cellular behavior of the LRP1 NPxY2 ki MEF cells. Tissues are associations of one or several cell types, all connected to each other and their extracellular surrounding. Integrin surface receptors take over the task of anchoring cells to the ECM by binding ECM proteins. Subsequently to the initial binding focal contacts are formed. Then, proteins of the adhesome such as the tyrosine kinase FAK are recruited to sites of integrin binding and intracellular downstream signaling is initiated. Adhesion of cells is a process dependent on the surface expression of integrin receptors (Cavalcanti-Adam et al., 2007; Hynes, 2002). After the initial association of focal contacts they maturate to nascent focal adhesions and cells start to spread. This process was shown to depend on the distance between the ECM contact points (Cavalcanti-Adam et al., 2007). β1-integrin knock down has been demonstrated to reduce cell adherence and spreading of human fetal islet pancreatic cells (Saleem et al., 2009). Stable shRNA knockdown of β1-integrin in human breast carcinoma cells led to increased cell spreading and elevated numbers of FA resulting in reduction of cell migration (Costa et al., 2013). Moreover, silencing β1-integrin via siRNA transfection in adhered fibroblasts resulted in augmented spreading and prominent clustering of cells (Huveneers et al., 2008). Comparing these results to the present study revealed that the reduction of surface β1-integrin internalization in the LRP1 NPxY2 ki model was similar to the results observed in the β1-integrin knockdown experiments. Cell adhesion behavior was significantly increased in the NPxY2 ki model after 60 min, after 30 min only slight differences in adhesion could be detected (Fig. 11). In the first step of adhering to ECM substrate, the only difference between the examined NPxY2 ki model and wt cells is in the surface levels of β1-integrin. Hereafter, cells either mature their contact sites to focal adhesions in a force and actin polymerizing dependent manner, or contact point turn over can be observed (Wolfenson et al., 2014). But as turn-over of contact points requires endocytosis of β1-integrin, this is extremely reduced in the LRP1 NPxY2 ki model (Fig. 10) (Ezratty et al., 2009). In fibroblasts the cycle of adhesion formation, maturation and disassembly takes place in a time range of 60 seconds to less than one hour, depending on the size and maturation degree of the FAs (Berginski et al., 2011). Conceivably, formed FAs in the LRP1 NPxY2 ki MEF cells can mature;

however, turnover is inhibited by the lack of β1-integrin internalization, whereby FAs of MEF cells expressing LRP1 wt pursue the dynamic cycle of FA assembly and disassembly within 60 min. Hence, different adhesion rates could only be detected after 60 min (Fig. 11).

Alongside anchoring cells to their extracellular surrounding, focal contacts, nascent and mature FAs play a pivotal role in cytoskeletal organization and in turn structures of the cytoskeleton regulate FA assembly and disassembly. Talin as an example binds to the intracellular part of β-integrins and is bound to filamentous actin and thus connects the cytoskeleton directly to the exterior (Campbell and Ginsberg, 2004b). The intracellular recruitment of numerous proteins forming FAs results in downstream activation of GTPases, which in turn regulate cytoskeleton reorganization to enable cell spreading and subsequently cell motility. Membrane protrusions, the initial structures in spreading and migration, emerge due to the signaling cascade of the Rho-GTPase Rac1. Rac1 controls lamellipodia formation by actin polymerization through activating the WAVE-Arp2/3 complex and thus causing actin flow (Cory and Ridley, 2002; Nobes and Hall, 1995). Typical morphological hallmark appearing during spreading of fibroblasts are stress fibers, which are composed of bundled actin filaments containing myosin II (Tojkander et al., 2012). Depending on the type of stress fiber they can be directly linked to focal adhesion complexes or forming a stabilizing arch. These contractile structures associate downstream of RhoA activation and subsequently of the Rho associated coiled-coil forming kinase (ROCK), which reinforces myosin contractility by downstream phosphorylating the myosin light chain (Amano et al., 1996; Matsui et al., 1996). The mammalian homolog of Drosophila diaphanous (mDia1) is activated by RhoA signaling and stimulates actin filament elongation and polymerization (Watanabe et al., 1997). Investigations concerning cell spreading of the LRP1 NPxY2 ki MEF cells revealed increased cellular spreading if LRP1 and β1-integrin endocytosis is reduced (Fig. 12). Because of the lack of β1-integrin endocytosis, the disassembly of FA is most likely restricted in the functional LRP1 knock-out system, potentially leading to mis-activation of Rac1 and RhoA. Further experiments focusing on the activation state of Rac1 and RhoA should be performed with the NPxY2 ki model. Interestingly, LRP1 knock-out in Schwann cells resulted in increased cell adhesion, reduced cell migration and hyper activation of RhoA, indicating an important role of LRP1 in the regulation of the cytoskeletal organization (Mantuano et al., 2010). A further hint for an alteration in activation of the Rho GTPases besides increased spreading is the augmented formation

of filopodia of the MEF NPxY2 ki cells seeded on fibronectin and the overrepresentation of ventral stress fibers at the leading edge (Fig. 12 C).

Supplementary to the internalization of ligand bound integrins as a necessary event for cell motility, further components enable cell motility. During FA formation, the FAK is recruited to sites of integrin clustering and initiates the focal adhesion association (Hamadi et al., 2005). Subsequently, FAK is autophosphorylated at tyrosine 397, which seems to be crucial event for related downstream signaling, since mice lacking tyrosine 397 are embryonically lethal (Corsi et al., 2009; Schaller et al., 1994). Notably, autophosphorylation of FAK can also be triggered by receptor binding of growth factors such as EGF (Sieg et al., 2000). Hereafter, Src-kinases are recruited to the assembling FA and bind via their SH2 and SH3 motif, resulting in their activation (Calalb et al., 1995). Activated Src-kinase in turn trigger further phosphorylation of FAK at tyrosine 576, 577 and 925, here two signaling pathways branch (Calalb et al., 1995). On one hand paxillin is phosphorylated followed by GTPase activation of Rho and Rac1, leading to reorganization of the cytoskeleton (Schaller and Parsons, 1995). On the other hand the Ras/Raf/MEK/ERK pathway is activated by increasing Grb2 binding affinity to FAK via phosphorylation at tyrosine Y925 (Schlaepfer and Hunter, 1996). Moreover, phosphorylation of FAK at 925 has been shown to facilitate FAK detachment of FA and thus enhancing FA disassembly (Kadare et al., 2015). In the case of the LRP1 NPxY2 ki model, hyper-phosphorylation of FAK at tyrosine 397 was observed in combination with augmented numbers of vinculin containing FAs (Fig. 13). Caused by the increased surface amounts of β1-integrin and the lack of LRP1 mediated β1-integrin endocytosis more focal adhesions were formed and remained stable, since β1-integrin endocytosis was diminished. Therefore, the autophosphorylated form of FAK accumulated in these cells compared to wt controls. In order to validate the observed results, β1-integrin was silenced and the opposite result emerged. FAK Y397 phosphorylation was reduced along with equal amounts of total FAK (Fig. 14), indicating a crucial role of LRP1 mediated β1-integrin internalization in FA disassembly. Interestingly, LRP1 has been reported to be a docking site for FA assembly and in turn regulating FA disassembly in an ERK1/2 dependent manner (Langlois et al., 2010). Therefore, focusing on downstream signaling of FAs, the target ERK1/2 was revealed to be less activated in the LRP1 NPxY2 ki model (Fig. 15). These results indicate that an impairment of FA turnover caused by LRP1 and β1-integrin surface continuance inhibits cell migration rates and thus affects downstream signaling cascades. Moreover, former studies indicate

an involvement of LRP1 in cell migration dynamics not merely by localizing to sites of FAs, but actively participating in the cell migration processes. An LRP1 knock-out severely decreased migration of Schwann cells (Mantuano et al., 2010), and in fact, treating MEF LRP1 knock-out cells with the plasminogen activator inhibitor-1 (PAI 1), a ligand of LRP1 enhancing cell migration in MEF wt cells, resulted in reduced cell migration rates (Degryse et al., 2004; Kozlova et al., 2015). Initiation of focal adhesion disassembly has been reported to be altered by treatment of bovine aortic endothelial cells with the receptor associated protein (RAP). RAP binds to lipoprotein receptors such as LRP1 and blocks their ligand endocytosis, thus focal adhesion disassembly is most likely lipoprotein dependent (Herz et al., 1991). Further support for participation of LRP1 in focal adhesion disassembly comes from experiments silencing LRP1 in FTC133 human follicular thyroid carcinoma cells, which resulted in dramatic reduction of malignant cell invasion. Effective focal adhesion disassembly was reduced in these cells (Dedieu et al., 2008). Therefore, disruption of the LRP1 coupled endocytosis of β1-integrin and the observed reduction in cell migration in LRP1 NPxY2 ki cells further underlines the important role of LRP1 in cell behavior regulation (Fig. 16). Additionally, stabilizing the inactive form of β1-integrin via antibody treatment resulted in a severe decrease in MEF wt cell migration to the levels of LRP1 NPxY2 ki cells, giving further proof for the functional knock-out of β1-integrin due to lacking endocytosis in the NPxY2 ki system. Strikingly, a further decrease in cell migration of the NPxY2 ki cells after antibody treatment seeded on fibronectin could also be detected, indicating an additional LRP1 independent effect of the antibody treatment on cell migration. One possible explanation for this might be that there are two distinct β-integrin receptors, β1 and β3, which bind to fibronectin. The alterations in β1-integrin trafficking caused by the functional knock-out of LRP1 might be compensated to a certain extent by the second fibronectin receptor $\alpha_V\beta3$-integrin in LRP1 NPxY2 ki MEF cells seeded on fibronectin. If β1-integrin activity is inhibited by pre-treatment of cells with an antibody specifically stabilizing the inactive form of β1-integrin, less integrin receptors might be able to bind to the coated surface of the Boyden chamber resulting in reduced numbers of adhered cells. Respectively, fewer cells can migrate through the Boyden chamber, an affect which is LRP1 independent. Furthermore, blocking β1-integrin activity might influence the joint endocytosis of the $\alpha_5\beta1$ receptor and fibronectin (Lobert et al., 2010). As a consequence, less fibronectin can be degraded and the modification of the ECM, which facilitates cell migration, is reduced. The observed

reduction of cell migration in LRP1 NPxY2 ki cells after antibody treatment on fibronectin might therefore be an LRP1 independent effect.

6.3 LRP1 β1-integrin interplay in the context of malignancy

LRP1 and β1-integrin are both known to contribute to the pathology of cancer, especially concerning tumor invasiveness. LRP1 knock-out was reported to be tumor enhancing, which was shown to be rescued by the expression of LRP1 mini-constructs (Zhang et al., 2008). In malignant cells, low levels of LRP1 have often been detected, however one should keep in mind, that LRP1 can be shedded at the cell surface by various metalloproteinases such as MT1-MMP (Rozanov et al., 2004). LRP1 in its function as a major endocytic receptor controls the internalization of MMP´s either directly or indirectly as a complex, shown for several MMPs such as MMP2 and MMP9 (Hahn-Dantona et al., 2001; Yang et al., 2001). Furthermore, the MMP inhibitors, TIMPs are also endocytosed via LRP1, thus regulating the activity of the extracellular MMPs (Scilabra et al., 2013). Even though the shedded soluble part of LRP1 re-associated with the remaining intracellular tail and is still capable of binding its ligands, alterations in ligand endocytosis are the consequence of LRP1 shedding (Quinn et al., 1999). Indeed, increased LRP1 shedding disturbed MMP2 and MMP9 internalization and thus potentially its degradation in cultures of human endometrial explants (Selvais et al., 2009). Upregulation of MMPs is coupled with enhanced invasiveness and metastasis of tumor cells due to enhanced degradation of ECM proteins and modification of the ECM, which facilitates cell migration and thus metastasis (Vihinen et al., 2005). Therefore, the lack of LRP1 in many cancer types might lead to a fatal reduction in MMP endocytosis and thus enhances cell motility by increased ECM degradation of MMPs.

However, in the LRP1 NPxY2 ki system ERK1/2 activity, which is involved in LRP1 dependent regulation of MMP activity, was reduced and consequently MMP2 and MMP9 activity revealed to be decreased (Fig. 15, 17). As a result, ECM degradation by MMPs was reduced, leading to significantly declined cell migration of MEF cells generated from LRP1 NPxY2 ki animals (Fig. 16). Cell migration has also been shown to be declined in the LRP1 silenced human glioblastoma cell line U87. In this pervious study MMP9 expression was observed to be regulated by LRP1 through post-ligand binding signaling mediated by ERK1/2 (Song et al., 2009). The functional knock-out of LRP1 might directly influence MMP2 and MMP9 activity and expression levels, since

LRP1 silencing has been predicted to decrease their expression (Hahn-Dantona et al., 2001; Song et al., 2009; Yang et al., 2001). In addition to the effects of the LRP1 functional knock-out on MMP activity, β1-integrin has also been observed to impact MMPs. In a former study, β1-integrin silencing in human ovarian cancer cells reduced cell migration combined with decreased MMP levels (Zhang and Zou, 2015). Therefore, reduction in β1-integrin internalization and thus probably a functional knock-out of β1-integrin led to an immense decline in cell migration and diminished MMP2 and MMP9 activity in the LRP1 NPxY2 ki system (Fig. 16, 17).

In immortalized keratinocytes and human breast cancer cells ligand binding of integrins triggered MMP expression probably mediated by the downstream signaling of the adhesome (Iyer et al., 2005; Morozevich et al., 2009). Silencing the fibronectin receptor α5β1 integrin by siRNA decreased MMP2 expression levels and diminished the cellular invasive potential. Moreover, interaction between the integrin receptor α5β1 and MMP2 was shown by co-immunoprecipitation experiments (Morozevich et al., 2009). Integrin ligand binding recruits phosphokinases following activation of the Ras/Raf/MEK/ERK pathway. ERK itself and mediated through phosphorylation of transcription factors can regulate gene expression of MMPs via this pathway (Chang et al., 2003). Interestingly, hyper-activation of the Ras/Raf/MEK/ERK pathway is often mentioned in conjunction with the pathology of cancer, since it controls cell survival and proliferation of cells (Oh et al., 2001). As described previously, LRP1 ligand binding induces ERK1/2 phosphorylation leading to MMP9 expression (Song et al., 2009). Remarkably, LRP1 and integrins share the ERK pathway in mediating signaling from extracellular ligand binding into the cell. Reduced activated ERK1/2 levels, less MMP2 and MMP9 activity resulted in declined cell migration rates of the LRP1 NPxY2 ki MEF cells (Fig. 15, 16, 17). Pro-MMP2 has been shown to be activated by the membrane-type1-MMP in an integrin clustering dependent manner, following MMP2 dependent activation of MMP9, which in turn is dependent on the presence of TIMP2 (Ellerbroek et al., 2001). TIMP2 is endocytosed by LRP1, this reciprocal dependence of integrins and LRP1 in MMP 2 and MMP9 activation highlights the importance of the interplay between the two receptors (Toth et al., 2003). Moreover, phosphorylated ERK1/2 activates the myosin-light chain kinase, thereby inducing myosin contraction (Fincham et al., 2000; Katz et al., 2003). The mechanical traction of myosin fibers enforces FA disassembly conducted by cell detachment. Through this pathway decreased ERK1/2 activation might contribute to the reduction in FA disassembly among the LRP1 NPxY2 ki model

and leading to decreased cell migration rates. Certainly, alterations in cellular behavior and related biochemical changes were induced by the interplay between LRP1 and β1-integrin and their related downstream signaling, highlighting the importance of the receptor interaction and combined endocytosis. Thinking of the altered cellular behavior in malignancy, inhibiting LRP1 endocytosis and thus β1-integrin trafficking might be a potential way to prevent or minimize tumor invasiveness by reducing cell motility.

6.4 LRP1 and β1-integrin interplay in the neuronal system

In a neuronal setting LRP1 might play a role in β1-integrin biology by regulating the formation of neuronal focal point contacts at growth cones of growing axons and dendrites. β1-integrin is linked to neuronal cell migration (Belvindrah et al., 2007), neurite pathfinding (Robles and Gomez, 2006) and dendritic arborization (Warren et al., 2012). Recovery of rat sensory neurons was enhanced after preconditioning the cells via seeding on fibronectin. As a consequence, α5 integrin, forming the fibronectin receptor together with β1-integrin, was localized at the sites of adhesion in the outgrowing axon after injury (Gardiner et al., 2007). Equal to fibroblasts, β1-integrin activation in dorsal root ganglions triggers FAK autophosphorylation at tyrosine 397 and induces actin cytoskeleton remodeling via the Rac1 RhoA pathway resulting in neuronal polarization and neurite outgrowth (Ribeiro et al., 2013). LRP1 is widely expressed in the neuronal system and is localized to neuronal dendrites and soma. Blocking LRP1 ligand binding capacity by RAP treatment resulted in LRP1 re-localization from the dendrites to the soma, indicating a role of LRP1 in dynamic outgrowth function of neurons (Billnitzer et al., 2013). Several studies predict a role of LRP1 in neurite and dendrite outgrowth by downstream activation of the Ras/Raf/MEK/ERK pathway (Yoon et al., 2013). ERK2 was demonstrated to drive axon elongation in hippocampal neurons of mice (Wang et al., 2011b). After ligand binding, LRP1 is intracellularly phosphorylated at the membrane distant NPxY2 motif followed by recruitment of Src-kinases and finally activating ERK via phosphorylation (Shi et al., 2009). Highlighting the involvement of both surface receptors in the process of neurite outgrowth leads to the assumption of a possible linked interaction in this process. Actually, both LRP1 and β1-integrin could be co-localized at the soma and along the outgrowing axon of developing cortical neurons of the LRP1 NPxY2 ki mouse model (Fig. 18 A). Since adhesion to the ECM is in some cases mediated by integrin activation driven focal contacts, increased levels of pFAK Y397 could be observed in the NPxY2 ki neurons compared to wt controls (Fig. 18

B,C). Internalization of LRP1 in the NPxY2 ki neurons has been demonstrated to be dramatically reduced, for that reason the impairment of β1-integrin internalization was assumed in the neurons generated from the LRP1 NPxY2 ki animals (Maier et al., 2013). The elevated levels of pFAK Y397 indicate a lack of β1-integrin endocytosis and a correlating inhibition of focal contact disassembly in cortical neurons. Activated ERK1/2 levels were shown to be decreased in primary cortical neurons generated from the LRP1 NPxY2 ki animals, being a further hint for the importance of the combined endocytosis of LRP1 and β1-integrin on the linked downstream signaling (Maier, 2013). A potential linker of LRP1 and β1-integrin in cells of the central nervous system might be the scaffolding protein RanBP9. Coupled endocytosis of LRP1, β1-integrin and RanBP9 has been shown for hippocampal derived HT22 cells (Woo et al., 2012a). Moreover, overexpression of RanBP9 resulted in a loss of dendritic spines and a reduction in the dendritic arbor. Both alterations involve remodeling of the actin cytoskeleton, and potentially are an effect of disproportionally high endocytosis of both receptors (Wang et al., 2014a; Wang et al., 2014b).

Cell migration is absolutely mandatory in the process of brain development. *In vitro* analyzes have located integrins, clathrin and Dab2 at the leading tip of migrating cortical interneurons, which points to an involvement of integrins and clathrin mediated endocytosis in cell migration (Shieh et al., 2011). Over lifetime, neurons are constantly generated in the subventricular zone, from where they migrate to the b*ulbus olfactorius*. A second site of neurogenesis over lifetime is the dentate gyrus (Alvarez-Buylla and Lim, 2004; Drew et al., 2013). Neuronal progenitor cells aiming the olfactory bulb migrate along the rostral migratory stream (RMS) in organized and polarized chains (Lois et al., 1996). The tangential chain migration is regulated by many factors, such as the chemoattractant netrin-1 or the flow direction of the cerebrospinal fluid (Murase and Horwitz, 2002; Sawamoto et al., 2006). In particular the expression of surface receptors like integrins in neuroblasts have been demonstrated to be crucial for directed cell migration in adult brain (Emsley and Hagg, 2003). Analyzes of cell migration along the RMS was shown to be altered when β1-integrin was conditionally knocked out in neuroblasts. Here, the authors claimed the necessity for β1-integrin to bind laminin and thus providing cell-cell-linkage between cells of the RMS (Belvindrah et al., 2007). In this present study the functionality in β1-integrin endocytosis appeared to be crucial for proper migration along the RMS, since disturbed chain formation of migrating neuroblasts of the LRP1 NPxY2 ki mice were observed compared to wt controls in two

distinct approaches. Staining of cell nuclei by the Nissl method of histological brain slices and the *in vivo* labelling of proliferating cells by BrdU and following immunohistochemical staining elucidated disrupted chain formation of neuroblasts migrating along the RMS (Fig. 19, 20). Consequently, a regulating function of LRP1 in β1-integrin internalization and its possible influence on downstream signaling in cell migration in a neuronal setting could be shown in this study.

Besides neuronal cell migration, β1-integrins play a pivotal role in synapse formation and synaptic plasticity. Spines constitute the postsynaptic site of mostly excitatory synapses and are composed of actin filaments. Since actin cytoskeleton remodeling is a mandatory requirement for synaptic plasticity, integrins as key regulators in actin reorganization play a major role in synaptic plasticity. Inhibiting integrin function by treating neurons with a specific blocking antibody or a partial knock-out lead to diminished long-term potentiation (LTP) consolidation and therefore reduced spine dynamics (Chan et al., 2003; Kramar et al., 2002). Specifically inhibiting β1-integrin via antibody treatment resulted in the prevention of actin polymerization in spines which in turn prohibited stabilization of LTP (Kramar et al., 2006). LTP contributes to the process of learning and memory formation by an elongated stimulation of a certain neuronal pathway. The actin cytoskeleton is then reorganized and new spines arise or morphological changes of already existing spines occur (Fukazawa et al., 2003; Holscher, 1999). The distinct morphology of spines has been referred to certain characteristics of spines. Thin spines are predicted to be "learning" spines, which respond quickly to alterations in synaptic activity. Moreover, mushroom spines are dedicated to be "memory" spines, and are relatively stable (Bourne and Harris, 2007). As a part of the post synapse, the NMDA receptor contributes to the generation of LTP, however, the receptor is also influenced by LRP1. Internalization of NMDA subunits by LRP1 controls its activation state in the membrane of the synaptic gap and influences LTP generation. Remarkably, the LRP1 NPxY2 ki animals showed a hyperactive behavior phenotype and deficiencies in spatial learning (Maier et al., 2013). Synaptic marker protein levels have been tested to be equal in LRP1 NPxY2 ki mice compared to wt controls, which is validated by the results of this study. In general there was no alteration in spine amounts, but strikingly, the mushroom spine type was increased in the LRP1 NPxY2 ki animals (Fig. 21). Due to the reduced dynamics in spine formation caused by the lack of β1-integrin internalization and following alterations in the capacity of actin cytoskeleton remodeling the learning skills of these mice might be

reduced. The cytoskeleton of the postsynaptic neuron cannot react fast enough to synaptic activity and thus no new synapses can be formed. Moreover, elevated numbers of mushroom spines might be a result of enhanced excitatory stimulation due to altered NMDA receptor subunit internalization via LRP1. Continuing stimulation of the post synapse is probably involved in the hyperactive behavior phenotype.
In summary, LRP1 appeared to mediate β1-integrin endocytosis in a neuronal setting, emphasized by the alterations in phosphorylated FAK and the derangement or chain migration of neuronal progenitor cells along the RMS. Furthermore, LRP1 coupled internalization of β1-integrin impacts on actin cytoskeleton organization reflected in spine formation.

In summary, this study demonstrated a crosslink between LRP1 and β1-integrin in terms of clathrin mediated endocytosis. The NPxY2 motif of LRP1 revealed to be the potential site of interaction, but it is still elusive, if the intracellular domains of LRP1 and β1-integrin interact directly or if a scaffolding protein is involved. Possible candidates are the Dab2 protein and RanBP9. Processes and signaling related to LRP1 and β1-integrin were observed to be deranged, if the intracellular NPxY2 motif of LRP1 was exchanged by an alanine cassette. Indeed, cellular behavior in adhesion, spreading and migration were impaired in the LRP1 NPxY2 ki model. Additionally, the activation of the Ras/Raf/MEK/ERK pathway was detected to be decreased in combination with diminished MMP2 and MMP9 activity. The interaction and combined endocytosis of LRP1 and β1-integrin seemed to be necessary for proper downstream processes among MEF cells. In the neuronal system both receptors possibly interact and may direct neuronal outgrowth and branching. Cell migration along the rostral migratory stream was shown to be deranged in the LRP1 NPxY2 ki animals, indicating for the requirement of coupled endocytosis of LRP1 and β1-integrin in the neuronal system. As the actin cytoskeleton organization is regulated amongst other by β1-integrin, the spine morphology of the LRP1 functional knock-out and thus β1-integrin functional knock-out model (LRP1 NPxY2 ki) was altered in primary cortical neurons generated from this model

.

7. Summary

The low density lipoprotein receptor-related protein 1 (LRP1), a member of the LDL-receptor family, is a major cell surface endocytic receptor and is able to bind and endocytose more than 40 different intracellular and extracellular ligands. The intracellular NPxY motifs of LRP1 were shown to be the major intracellular binding motifs, whereby phosphorylation of tyrosine of the NPxY motifs revealed to play a crucial role in ligand binding and downstream signaling. LRP1 previously has been shown to interact with the extracellular matrix (ECM) binding protein β1-integrin and to regulate its surface expression. β1-integrin forms heterodimeric receptors in association with α-integrin subunits and connects the actin cytoskeleton with the exterior ECM by transducing signals over the plasma membrane in both directions. Subsequent to integrin activation and binding to the ECM, the actin cytoskeleton is reorganized, which in turn regulates cell adhesion, spreading and migration. LRP1 knock-out cells exhibit altered cytoskeleton organization and decreased cell migration, indicating a functional link between LRP1 and integrins.

In order to unravel the potential interplay between LRP1 and β1-integrin and to narrow down the possible site of interaction, the LRP1 NPxY2 ki model chosen for this study. The membrane distal NPxY2 motif of LRP1 was replaced by a knock-in of a multiple alanine cassette (AAxA), resulting in severe reduction of LRP1 endocytosis. Remarkably, β1-integrin revealed to accumulate at the plasma membrane of MEF NPxY2 ki cells, which correlated with reduced internalization rates of β1-integrin. Co-immunoprecipitation experiments validated a potential interaction of LRP1 and β1-integrin via the intracellular domain of LRP1, which could be enclosed to the NPxY2 motif. Processes requiring β1-integrin internalization or re-localization such as cell adhesion and spreading were altered in the cell model. The lack of β1-integrin internalization inhibited focal adhesion (FA) disassembly, resulting in an increase of FA numbers. The reduction in integrin dynamics and a diminished activity of the matrix metalloproteinases (MMP) 2 and MMP9 resulted in reduced cell migration of MEF LRP1 NPxY2 ki cells. Moreover, the activation of the correlated Ras/Raf/MEK/ERK signaling cascade was shown to be decreased. Similar results could be observed in a corresponding mouse model, the C57Bl6 LRP1 NPxY2 ki, where the activation of focal adhesion components was altered in primary cortical neurons. Examination of neuronal

cell migration demonstrated alterations in migration characteristics along the rostral migratory stream. Furthermore, spine morphology was affected in the NPxY2 ki model, an increased number of stable “memory” mushroom spines could be detected, indicating for a restriction in spine plasticity. In summary, our results indicate that LRP1 interacts with β1-integrin by mediating integrin internalization involving its NPxY2 motif.

Consequently, the actin cytoskeleton dependent cellular processes connected to β1-integrin revealed to depend on the coupled endocytosis of LRP1 and β1-integrin. The disturbance of this interaction resulted in a dysfunction in *in vivo* and *in vitro* actin cytoskeleton dependent cellular processes such as adhesion, migration and spine plasticity.

Zusammenfassung

Der transmembrane Endocytose-Rezeptor *low density lipoprotein receptor-related protein 1* (LRP1) gehört zur Familie der *low density lipoprotein* Rezeptoren und kann mehr als 40 verschiedene extrazelluläre und intrazelluläre Liganden binden. Die beiden C-terminalen NPxY Motive spielen eine wichtige Rolle in der intrazellulären Liganden Bindung, außerdem reguliert ihre Phosphorylierung unter anderem die Liganden-Internalisierung und die nachfolgende Signaltransduktion. Eine Interaktion zwischen LRP1 und dem extrazellulären Matrix (EZM)-bindenden Protein β1-Integrin konnte bereits in einer vorangegangenen Studie gezeigt werden, LRP1 beeinflusste hier die Oberflächen-Expression von β1-Integrin. In Assoziation mit α-Integrin-Untereinheiten bildet β1-Integrin heterodimere Oberflächen-Rezeptoren, die durch Bindung an die EZM das Zytoskelett mit der EZM verbindet und Signale in beide Richtungen über die Plasma-Membran transduziert. Nach der Rezeptor-Bindung an Proteine der EZM findet eine Reorganisation des Aktin-Zytoskeletts statt, wodurch Prozesse der Zell-Adhäsion und Spreizung initiiert werden. LRP1 knock-out Zellen zeigten Veränderungen des Zytoskeletts und ihres Migrationsverhaltens, was eine mögliche Verbindung von LRP1 und β1-Integrin vermuten lässt.

Für die Analyse der potentiellen Interaktion der beiden Rezeptoren wurde hauptsächlich das LRP1 NPxY2 ki Modell verwendet. Hier wurde das LRP1 NPxY2 Motiv durch eine Alanin-Kassette (AAxA) ersetzt, wodurch sich die Endozytose-Rate von LRP1 stark reduzierte. Die Internalisierungsrate von β1-Integrin im LRP1 NPxY2 ki Modell war im Vergleich zu wildtypischen Zellen deutlich reduziert, wodurch β1-Integrin an der Oberfläche akkumulierte, und zu Veränderungen in β1-Integrin abhängigen Prozessen wie der Zelladhäsion und Spreizung führte. Die Lokalisation der Interaktion von LRP1 und β1-Integrin konnte mittels Co-Immunopräzipitation auf den C-Terminus, insbesondere auf das NPxY2 Motiv von LRP1 eingeengt werden. Die verringerte Internalisierung von β1-Integrin im LRP1 NPxY2 ki Modell beeinflusste potentiell die Auflösung der fokalen Adhäsionen (FAs), dies resultierte in einer erhöhten Anzahl an FAs. Zusätzlich zur verringerten Internalisierung von β1-Integrin wurde eine Abnahme in der Aktivität der Matrix-Metalloproteasen MMP2 und MMP9 festgestellt. Dies führte zu einer reduzierten Migrationsrate der LRP1 NPxY2 ki Zellen. Die mit LRP1 und β1-Integrin verbundene Signalkaskade Ras/Raf/MEK/ERK zeigte reduzierte Aktivität im verwendeten Zell-Modell. Die erlangten Ergebnisse konnten bei Untersuchungen des C57Bl6 LRP1 NPxY2 ki Mausmodells bestätigt werden. Im neuronalen System wurde

eine erhöhte Aktivierung von Komponenten der FAs beobachtet. Außerdem wurden Veränderungen in der charakteristischen, neuronalen Zellmigration entlang des rostralen migratorischen Stroms festgestellt. Die Anzahl an stabilen, neuronalen *„mushroom“* Dornfortsätzen von primären, kortikalen Neuronen der LRP1 NPxY2 ki Tiere war erhöht, weshalb eine Beeinträchtigung in der neuronalen Plastizität vermutet wurde.

Die erlangten Ergebnisse deuten auf eine Interaktion in Form von gekoppelter Endozytose von LRP1 und β1-Integrin hin, wobei das LRP1 NPxY2 Motiv eine wichtige Rolle spielt. Wird die Interaktion durch eine Mutation im NPxY2 Motiv von LRP1 verhindert, ist eine Dysfunktion von Prozessen wie beispielsweise der Zellmigration oder der neuronalen Plastizität sowohl *in vitro* als auch *in vivo* festzustellen, welche von der Aktin-Zytoskelett-Dynamik abhängig sind.

8. References

Acosta, J.J., R.M. Munoz, L. Gonzalez, A. Subtil-Rodriguez, M.A. Dominguez-Caceres, J.M. Garcia-Martinez, A. Calcabrini, I. Lazaro-Trueba, and J. Martin-Perez. 2003. Src mediates prolactin-dependent proliferation of T47D and MCF7 cells via the activation of focal adhesion kinase/Erk1/2 and phosphatidylinositol 3-kinase pathways. *Mol Endocrinol*. 17:2268-2282.

Adair, B.D., J.P. Xiong, C. Maddock, S.L. Goodman, M.A. Arnaout, and M. Yeager. 2005. Three-dimensional EM structure of the ectodomain of integrin {alpha}V{beta}3 in a complex with fibronectin. *J Cell Biol*. 168:1109-1118.

Aguirre-Ghiso, J.A., D. Liu, A. Mignatti, K. Kovalski, and L. Ossowski. 2001. Urokinase receptor and fibronectin regulate the ERK(MAPK) to p38(MAPK) activity ratios that determine carcinoma cell proliferation or dormancy in vivo. *Mol Biol Cell*. 12:863-879.

Alpizar-Alpizar, W., B.S. Nielsen, R. Sierra, M. Illemann, J.A. Ramirez, A. Arias, S. Duran, A. Skarstein, K. Ovrebo, L.R. Lund, and O.D. Laerum. 2010. Urokinase plasminogen activator receptor is expressed in invasive cells in gastric carcinomas from high- and low-risk countries. *Int J Cancer*. 126:405-415.

Alvarez-Buylla, A., and D.A. Lim. 2004. For the long run: maintaining germinal niches in the adult brain. *Neuron*. 41:683-686.

Amano, M., M. Ito, K. Kimura, Y. Fukata, K. Chihara, T. Nakano, Y. Matsuura, and K. Kaibuchi. 1996. Phosphorylation and activation of myosin by Rho-associated kinase (Rho-kinase). *The Journal of biological chemistry*. 271:20246-20249.

Andersen, O.M., J. Reiche, V. Schmidt, M. Gotthardt, R. Spoelgen, J. Behlke, C.A. von Arnim, T. Breiderhoff, P. Jansen, X. Wu, K.R. Bales, R. Cappai, C.L. Masters, J. Gliemann, E.J. Mufson, B.T. Hyman, S.M. Paul, A. Nykjaer, and T.E. Willnow. 2005. Neuronal sorting protein-related receptor sorLA/LR11 regulates processing of the amyloid precursor protein. *Proceedings of the National Academy of Sciences of the United States of America*. 102:13461-13466.

Andersen, O.M., C.H. Yeung, H. Vorum, M. Wellner, T.K. Andreassen, B. Erdmann, E.C. Mueller, J. Herz, A. Otto, T.G. Cooper, and T.E. Willnow. 2003. Essential role of the apolipoprotein E receptor-2 in sperm development. *The Journal of biological chemistry*. 278:23989-23995.

Anderson, R.G., E. Vasile, R.J. Mello, M.S. Brown, and J.L. Goldstein. 1978. Immunocytochemical visualization of coated pits and vesicles in human fibroblasts: relation to low density lipoprotein receptor distribution. *Cell*. 15:919-933.

Asai, M., C. Hattori, B. Szabo, N. Sasagawa, K. Maruyama, S. Tanuma, and S. Ishiura. 2003. Putative function of ADAM9, ADAM10, and ADAM17 as APP alpha-secretase. *Biochem Biophys Res Commun*. 301:231-235.

Asati, V., D.K. Mahapatra, and S.K. Bharti. 2016. PI3K/Akt/mTOR and Ras/Raf/MEK/ERK signaling pathways inhibitors as anticancer agents: Structural and pharmacological perspectives. *Eur J Med Chem*. 109:314-341.

Baum, L., Z.Y. Dong, K.W. Choy, C.P. Pang, and H.K. Ng. 1998. Low density lipoprotein receptor related protein gene amplification and 766T polymorphism in astrocytomas. *Neurosci Lett*. 256:5-8.

Beisiegel, U., W. Weber, G. Ihrke, J. Herz, and K.K. Stanley. 1989. The LDL-receptor-related protein, LRP, is an apolipoprotein E-binding protein. *Nature*. 341:162-164.

Belvindrah, R., S. Hankel, J. Walker, B.L. Patton, and U. Muller. 2007. Beta1 integrins control the formation of cell chains in the adult rostral migratory stream. *The Journal of neuroscience : the official journal of the Society for Neuroscience*. 27:2704-2717.

Berginski, M.E., E.A. Vitriol, K.M. Hahn, and S.M. Gomez. 2011. High-resolution quantification of focal adhesion spatiotemporal dynamics in living cells. *PLoS One*. 6:e22025.

Bershadsky, A.D., I.S. Tint, and T.M. Svitkina. 1987. Association of intermediate filaments with vinculin-containing adhesion plaques of fibroblasts. *Cell motility and the cytoskeleton*. 8:274-283.

Bi, X., G. Lynch, J. Zhou, and C.M. Gall. 2001. Polarized distribution of alpha5 integrin in dendrites of hippocampal and cortical neurons. *J Comp Neurol*. 435:184-193.

Billnitzer, A.J., I. Barskaya, C. Yin, and R.G. Perez. 2013. APP independent and dependent effects on neurite outgrowth are modulated by the receptor associated protein (RAP). *J Neurochem*. 124:123-132.

Borrirukwanit, K., P. Pavasant, T. Blick, M.A. Lafleur, and E.W. Thompson. 2014. High threshold of beta1 integrin inhibition required to block collagen I-induced membrane type-1 matrix metalloproteinase (MT1-MMP) activation of matrix metalloproteinase 2 (MMP-2). *Cancer Cell Int*. 14:99.

Bos, C.R., S.L. Shank, and M.D. Snider. 1995. Role of clathrin-coated vesicles in glycoprotein transport from the cell surface to the Golgi complex. *J Biol Chem*. 270:665-671.

Bottcher, R.T., C. Stremmel, A. Meves, H. Meyer, M. Widmaier, H.Y. Tseng, and R. Fassler. 2012. Sorting nexin 17 prevents lysosomal degradation of beta1 integrins by binding to the beta1-integrin tail. *Nature cell biology*. 14:584-592.

Boucher, P., M. Gotthardt, W.P. Li, R.G. Anderson, and J. Herz. 2003. LRP: role in vascular wall integrity and protection from atherosclerosis. *Science*. 300:329-332.

Boucher, P., P. Liu, M. Gotthardt, T. Hiesberger, R.G. Anderson, and J. Herz. 2002. Platelet-derived growth factor mediates tyrosine phosphorylation of the cytoplasmic domain of the low Density lipoprotein receptor-related protein in caveolae. *The Journal of biological chemistry*. 277:15507-15513.

Bourne, J., and K.M. Harris. 2007. Do thin spines learn to be mushroom spines that remember? *Curr Opin Neurobiol*. 17:381-386.

Bovetti, S., Y.C. Hsieh, P. Bovolin, I. Perroteau, T. Kazunori, and A.C. Puche. 2007. Blood vessels form a scaffold for neuroblast migration in the adult olfactory bulb. *J Neurosci*. 27:5976-5980.

Boyles, J.K., C.D. Zoellner, L.J. Anderson, L.M. Kosik, R.E. Pitas, K.H. Weisgraber, D.Y. Hui, R.W. Mahley, P.J. Gebicke-Haerter, M.J. Ignatius, and et al. 1989. A role for apolipoprotein E, apolipoprotein A-I, and low density lipoprotein receptors in cholesterol transport during regeneration and remyelination of the rat sciatic nerve. *J Clin Invest*. 83:1015-1031.

Brakebusch, C., E. Hirsch, A. Potocnik, and R. Fassler. 1997. Genetic analysis of beta1 integrin function: confirmed, new and revised roles for a crucial family of cell adhesion molecules. *J Cell Sci*. 110 (Pt 23):2895-2904.

Brami-Cherrier, K., N. Gervasi, D. Arsenieva, K. Walkiewicz, M.C. Boutterin, A. Ortega, P.G. Leonard, B. Seantier, L. Gasmi, T. Bouceba, G. Kadare, J.A. Girault, and S.T. Arold. 2014. FAK dimerization controls its kinase-dependent functions at focal adhesions. *EMBO J*. 33:356-370.

Bretscher, M.S. 1989. Endocytosis and recycling of the fibronectin receptor in CHO cells. *EMBO J*. 8:1341-1348.

Bridgewater, R.E., J.C. Norman, and P.T. Caswell. 2012. Integrin trafficking at a glance. *J Cell Sci*. 125:3695-3701.

Broussard, J.A., D.J. Webb, and I. Kaverina. 2008. Asymmetric focal adhesion disassembly in motile cells. *Current opinion in cell biology*. 20:85-90.

Bu, G., H.J. Geuze, G.J. Strous, and A.L. Schwartz. 1995. 39 kDa receptor-associated protein is an ER resident protein and molecular chaperone for LDL receptor-related protein. *EMBO J*. 14:2269-2280.

Burden, J.J., X.M. Sun, A.B. Garcia, and A.K. Soutar. 2004. Sorting motifs in the intracellular domain of the low density lipoprotein receptor interact with a novel domain of sorting nexin-17. *J Biol Chem*. 279:16237-16245.

Burridge, K., C.E. Turner, and L.H. Romer. 1992. Tyrosine phosphorylation of paxillin and pp125FAK accompanies cell adhesion to extracellular matrix: a role in cytoskeletal assembly. *J Cell Biol*. 119:893-903.

Calalb, M.B., T.R. Polte, and S.K. Hanks. 1995. Tyrosine phosphorylation of focal adhesion kinase at sites in the catalytic domain regulates kinase activity: a role for Src family kinases. *Mol Cell Biol*. 15:954-963.

Calderwood, D.A., B. Yan, J.M. de Pereda, B.G. Alvarez, Y. Fujioka, R.C. Liddington, and M.H. Ginsberg. 2002. The phosphotyrosine binding-like domain of talin activates integrins. *The Journal of biological chemistry*. 277:21749-21758.

Campbell, I.D., and M.H. Ginsberg. 2004a. The talin-tail interaction places integrin activation on FERM ground. *Trends Biochem Sci*. 29:429-435.

Campbell, I.D., and M.H. Ginsberg. 2004b. The talin-tail interaction places integrin activation on FERM ground. *Trends Biochem Sci*. 29:429-435.

Cao, C., D.A. Lawrence, Y. Li, C.A. Von Arnim, J. Herz, E.J. Su, A. Makarova, B.T. Hyman, D.K. Strickland, and L. Zhang. 2006. Endocytic receptor LRP together with tPA and PAI-1 coordinates Mac-1-dependent macrophage migration. *The EMBO journal*. 25:1860-1870.

Carlstrom, L.P., J.H. Hines, S.J. Henle, and J.R. Henley. 2011. Bidirectional remodeling of beta1-integrin adhesions during chemotropic regulation of nerve growth. *BMC Biol*. 9:82.

Carriero, M.V., S. Del Vecchio, M. Capozzoli, P. Franco, L. Fontana, A. Zannetti, G. Botti, G. D'Aiuto, M. Salvatore, and M.P. Stoppelli. 1999. Urokinase receptor interacts with alpha(v)beta5 vitronectin receptor, promoting urokinase-dependent cell migration in breast cancer. *Cancer Res*. 59:5307-5314.

Caswell, P.T., S. Vadrevu, and J.C. Norman. 2009. Integrins: masters and slaves of endocytic transport. *Nat Rev Mol Cell Biol*. 10:843-853.

Catasus, L., V. Llorente-Cortes, M. Cuatrecasas, C. Pons, I. Espinosa, and J. Prat. 2011. Low-density lipoprotein receptor-related protein 1 (LRP-1) is associated with highgrade, advanced stage and p53 and p16 alterations in endometrial carcinomas. *Histopathology*. 59:567-571.

Cavalcanti-Adam, E.A., T. Volberg, A. Micoulet, H. Kessler, B. Geiger, and J.P. Spatz. 2007. Cell spreading and focal adhesion dynamics are regulated by spacing of integrin ligands. *Biophys J*. 92:2964-2974.

Chan, C.S., E.J. Weeber, S. Kurup, J.D. Sweatt, and R.L. Davis. 2003. Integrin requirement for hippocampal synaptic plasticity and spatial memory. *J Neurosci*. 23:7107-7116.

Chang, F., L.S. Steelman, J.T. Lee, J.G. Shelton, P.M. Navolanic, W.L. Blalock, R.A. Franklin, and J.A. McCubrey. 2003. Signal transduction mediated by the Ras/Raf/MEK/ERK pathway from cytokine receptors to transcription factors: potential targeting for therapeutic intervention. *Leukemia*. 17:1263-1293.

Chao, W.T., and J. Kunz. 2009. Focal adhesion disassembly requires clathrin-dependent endocytosis of integrins. *FEBS letters*. 583:1337-1343.

Chazaud, B., R. Ricoux, C. Christov, A. Plonquet, R.K. Gherardi, and G. Barlovatz-Meimon. 2002. Promigratory effect of plasminogen activator inhibitor-1 on invasive breast cancer cell populations. *Am J Pathol*. 160:237-246.

Cheng, S.Y., G. Sun, D.D. Schlaepfer, and C.J. Pallen. 2014. Grb2 promotes integrin-induced focal adhesion kinase (FAK) autophosphorylation and directs the phosphorylation of protein tyrosine phosphatase alpha by the Src-FAK kinase complex. *Molecular and cellular biology*. 34:348-361.

Chigaev, A., T. Buranda, D.C. Dwyer, E.R. Prossnitz, and L.A. Sklar. 2003. FRET detection of cellular alpha4-integrin conformational activation. *Biophys J*. 85:3951-3962.

Christensen, E.I., J.O. Moskaug, H. Vorum, C. Jacobsen, T.E. Gundersen, A. Nykjaer, R. Blomhoff, T.E. Willnow, and S.K. Moestrup. 1999. Evidence for an essential role of megalin in transepithelial transport of retinol. *J Am Soc Nephrol*. 10:685-695.

Conese, M., A. Nykjaer, C.M. Petersen, O. Cremona, R. Pardi, P.A. Andreasen, J. Gliemann, E.I. Christensen, and F. Blasi. 1995. alpha-2 Macroglobulin receptor/Ldl receptor-related protein(Lrp)-dependent internalization of the urokinase receptor. *J Cell Biol*. 131:1609-1622.

Cooper, J.A. 2013. Cell biology in neuroscience: mechanisms of cell migration in the nervous system. *J Cell Biol*. 202:725-734.

Corsi, J.M., C. Houbron, P. Billuart, I. Brunet, K. Bouvree, A. Eichmann, J.A. Girault, and H. Enslen. 2009. Autophosphorylation-independent and -dependent functions of focal adhesion kinase during development. *The Journal of biological chemistry*. 284:34769-34776.

Cory, G.O., and A.J. Ridley. 2002. Cell motility: braking WAVEs. *Nature*. 418:732-733.

Costa, P., T.M. Scales, J. Ivaska, and M. Parsons. 2013. Integrin-specific control of focal adhesion kinase and RhoA regulates membrane protrusion and invasion. *PLoS One*. 8:e74659.

Cruzalegui, F.H., E. Cano, and R. Treisman. 1999. ERK activation induces phosphorylation of Elk-1 at multiple S/T-P motifs to high stoichiometry. *Oncogene*. 18:7948-7957.

Czekay, R.P., K. Aertgeerts, S.A. Curriden, and D.J. Loskutoff. 2003. Plasminogen activator inhibitor-1 detaches cells from extracellular matrices by inactivating integrins. *J Cell Biol*. 160:781-791.

D'Arcangelo, G., R. Homayouni, L. Keshvara, D.S. Rice, M. Sheldon, and T. Curran. 1999. Reelin is a ligand for lipoprotein receptors. *Neuron*. 24:471-479.

De Cesare, D., S. Jacquot, A. Hanauer, and P. Sassone-Corsi. 1998. Rsk-2 activity is necessary for epidermal growth factor-induced phosphorylation of CREB protein and transcription of c-fos gene. *Proceedings of the National Academy of Sciences of the United States of America*. 95:12202-12207.

Dedieu, S., B. Langlois, J. Devy, B. Sid, P. Henriet, H. Sartelet, G. Bellon, H. Emonard, and L. Martiny. 2008. LRP-1 silencing prevents malignant cell invasion despite increased pericellular proteolytic activities. *Mol Cell Biol*. 28:2980-2995.

Degryse, B., J.G. Neels, R.P. Czekay, K. Aertgeerts, Y. Kamikubo, and D.J. Loskutoff. 2004. The low density lipoprotein receptor-related protein is a motogenic receptor for plasminogen activator inhibitor-1. *The Journal of biological chemistry*. 279:22595-22604.

den Hertog, J., S. Tracy, and T. Hunter. 1994. Phosphorylation of receptor protein-tyrosine phosphatase alpha on Tyr789, a binding site for the SH3-SH2-SH3 adaptor protein GRB-2 in vivo. *The EMBO journal*. 13:3020-3032.

DeSimone, D.W., M.A. Stepp, R.S. Patel, and R.O. Hynes. 1987. The integrin family of cell surface receptors. *Biochem Soc Trans*. 15:789-791.

di Blasio, L., S. Droetto, J. Norman, F. Bussolino, and L. Primo. 2010. Protein kinase D1 regulates VEGF-A-induced alphavbeta3 integrin trafficking and endothelial cell migration. *Traffic*. 11:1107-1118.

Dodson, S.E., M. Gearing, C.F. Lippa, T.J. Montine, A.I. Levey, and J.J. Lah. 2006. LR11/SorLA expression is reduced in sporadic Alzheimer disease but not in familial Alzheimer disease. *J Neuropathol Exp Neurol*. 65:866-872.

Drew, L.J., S. Fusi, and R. Hen. 2013. Adult neurogenesis in the mammalian hippocampus: why the dentate gyrus? *Learn Mem*. 20:710-729.

Dubin-Thaler, B.J., G. Giannone, H.G. Dobereiner, and M.P. Sheetz. 2004. Nanometer analysis of cell spreading on matrix-coated surfaces reveals two distinct cell states and STEPs. *Biophys J*. 86:1794-1806.

Eke, I., Y. Deuse, S. Hehlgans, K. Gurtner, M. Krause, M. Baumann, A. Shevchenko, V. Sandfort, and N. Cordes. 2012. beta(1)Integrin/FAK/cortactin signaling is essential for human head and neck cancer resistance to radiotherapy. *J Clin Invest*. 122:1529-1540.

Ellerbroek, S.M., Y.I. Wu, C.M. Overall, and M.S. Stack. 2001. Functional interplay between type I collagen and cell surface matrix metalloproteinase activity. *The Journal of biological chemistry*. 276:24833-24842.

Emonard, H., G. Bellon, P. de Diesbach, M. Mettlen, W. Hornebeck, and P.J. Courtoy. 2005. Regulation of matrix metalloproteinase (MMP) activity by the low-density lipoprotein receptor-related protein (LRP). A new function for an "old friend". *Biochimie*. 87:369-376.

Emsley, J.G., and T. Hagg. 2003. alpha6beta1 integrin directs migration of neuronal precursors in adult mouse forebrain. *Exp Neurol*. 183:273-285.

Engert, F., and T. Bonhoeffer. 1999. Dendritic spine changes associated with hippocampal long-term synaptic plasticity. *Nature*. 399:66-70.

Ezratty, E.J., C. Bertaux, E.E. Marcantonio, and G.G. Gundersen. 2009. Clathrin mediates integrin endocytosis for focal adhesion disassembly in migrating cells. *J Cell Biol*. 187:733-747.

Ezratty, E.J., M.A. Partridge, and G.G. Gundersen. 2005. Microtubule-induced focal adhesion disassembly is mediated by dynamin and focal adhesion kinase. *Nat Cell Biol*. 7:581-590.

Fassler, R., and M. Meyer. 1995. Consequences of lack of beta 1 integrin gene expression in mice. *Genes Dev*. 9:1896-1908.

Fincham, V.J., M. James, M.C. Frame, and S.J. Winder. 2000. Active ERK/MAP kinase is targeted to newly forming cell-matrix adhesions by integrin engagement and v-Src. *EMBO J*. 19:2911-2923.

Fisher, J.L., P.S. Mackie, M.L. Howard, H. Zhou, and P.F. Choong. 2001. The expression of the urokinase plasminogen activator system in metastatic murine osteosarcoma: an in vivo mouse model. *Clin Cancer Res*. 7:1654-1660.

Fowlkes, J.L., J.J. Enghild, K. Suzuki, and H. Nagase. 1994. Matrix metalloproteinases degrade insulin-like growth factor-binding protein-3 in dermal fibroblast cultures. *The Journal of biological chemistry*. 269:25742-25746.

Friedland, J.C., M.H. Lee, and D. Boettiger. 2009. Mechanically activated integrin switch controls alpha5beta1 function. *Science*. 323:642-644.

Frykman, P.K., M.S. Brown, T. Yamamoto, J.L. Goldstein, and J. Herz. 1995. Normal plasma lipoproteins and fertility in gene-targeted mice homozygous for a disruption in the gene encoding very low density lipoprotein receptor. *Proceedings of the National Academy of Sciences of the United States of America*. 92:8453-8457.

Fukazawa, Y., Y. Saitoh, F. Ozawa, Y. Ohta, K. Mizuno, and K. Inokuchi. 2003. Hippocampal LTP is accompanied by enhanced F-actin content within the dendritic spine that is essential for late LTP maintenance in vivo. *Neuron*. 38:447-460.

Gardiner, N.J., S. Moffatt, P. Fernyhough, M.J. Humphries, C.H. Streuli, and D.R. Tomlinson. 2007. Preconditioning injury-induced neurite outgrowth of adult rat sensory neurons on fibronectin is mediated by mobilisation of axonal alpha 5 integrin. *Molecular and Cellular Neuroscience*. 35:249-260.

Goh, E.L., J.K. Young, K. Kuwako, M. Tessier-Lavigne, Z. He, J.W. Griffin, and G.L. Ming. 2008. beta1-integrin mediates myelin-associated glycoprotein signaling in neuronal growth cones. *Mol Brain*. 1:10.

Goldstein, J.L., R.G. Anderson, and M.S. Brown. 1979. Coated pits, coated vesicles, and receptor-mediated endocytosis. *Nature*. 279:679-685.

Goldstein, J.L., and M.S. Brown. 1976. The LDL pathway in human fibroblasts: a receptor-mediated mechanism for the regulation of cholesterol metabolism. *Curr Top Cell Regul*. 11:147-181.

Goldstein, J.L., and M.S. Brown. 1985. The LDL receptor and the regulation of cellular cholesterol metabolism. *J Cell Sci Suppl*. 3:131-137.

Gomez, T.M., F.K. Roche, and P.C. Letourneau. 1996. Chick sensory neuronal growth cones distinguish fibronectin from laminin by making substratum contacts that resemble focal contacts. *J Neurobiol*. 29:18-34.

Gotthardt, M., M. Trommsdorff, M.F. Nevitt, J. Shelton, J.A. Richardson, W. Stockinger, J. Nimpf, and J. Herz. 2000. Interactions of the low density lipoprotein receptor gene family with cytosolic adaptor and scaffold proteins suggest diverse biological functions in cellular communication and signal transduction. *J Biol Chem*. 275:25616-25624.

Graham, F.L., and A.J. van der Eb. 1973. A new technique for the assay of infectivity of human adenovirus 5 DNA. *Virology*. 52:456-467.

Gross, J., and C.M. Lapiere. 1962. Collagenolytic activity in amphibian tissues: a tissue culture assay. *Proceedings of the National Academy of Sciences of the United States of America*. 48:1014-1022.

Grzesiak, J.J., H.S. Tran Cao, D.W. Burton, S. Kaushal, F. Vargas, P. Clopton, C.S. Snyder, L.J. Deftos, R.M. Hoffman, and M. Bouvet. 2011. Knockdown of the beta(1) integrin subunit reduces primary tumor growth and inhibits pancreatic cancer metastasis. *Int J Cancer*. 129:2905-2915.

Guan, J.L., J.E. Trevithick, and R.O. Hynes. 1991. Fibronectin/integrin interaction induces tyrosine phosphorylation of a 120-kDa protein. *Cell Regul*. 2:951-964.

Hahn-Dantona, E., J.F. Ruiz, P. Bornstein, and D.K. Strickland. 2001. The low density lipoprotein receptor-related protein modulates levels of matrix metalloproteinase 9 (MMP-9) by mediating its cellular catabolism. *Journal of Biological Chemistry*. 276:15498-15503.

Hamadi, A., M. Bouali, M. Dontenwill, H. Stoeckel, K. Takeda, and P. Ronde. 2005. Regulation of focal adhesion dynamics and disassembly by phosphorylation of FAK at tyrosine 397. *J Cell Sci*. 118:4415-4425.

Han, K.Y., J. Dugas-Ford, H. Lee, J.H. Chang, and D.T. Azar. 2015. MMP14 Cleavage of VEGFR1 in the Cornea Leads to a VEGF-Trap Antiangiogenic Effect. *Invest Ophthalmol Vis Sci*. 56:5450-5456.

Hanks, S.K., M.B. Calalb, M.C. Harper, and S.K. Patel. 1992. Focal adhesion protein-tyrosine kinase phosphorylated in response to cell attachment to fibronectin. *Proceedings of the National Academy of Sciences of the United States of America*. 89:8487-8491.

Harasaki, K., N.B. Lubben, M. Harbour, M.J. Taylor, and M.S. Robinson. 2005. Sorting of major cargo glycoproteins into clathrin-coated vesicles. *Traffic*. 6:1014-1026.

Hauck, C.R., D.A. Hsia, and D.D. Schlaepfer. 2000. Focal adhesion kinase facilitates platelet-derived growth factor-BB-stimulated ERK2 activation required for chemotaxis migration of vascular smooth muscle cells. *The Journal of biological chemistry*. 275:41092-41099.

Hergott, G.J., H. Nagai, and V.I. Kalnins. 1993. Inhibition of retinal pigment epithelial cell migration and proliferation with monoclonal antibodies against the beta 1 integrin subunit during wound healing in organ culture. *Invest Ophthalmol Vis Sci*. 34:2761-2768.

Herz, J., D.E. Clouthier, and R.E. Hammer. 1992. LDL receptor-related protein internalizes and degrades uPA-PAI-1 complexes and is essential for embryo implantation. *Cell*. 71:411-421.

Herz, J., J.L. Goldstein, D.K. Strickland, Y.K. Ho, and M.S. Brown. 1991. 39-kDa protein modulates binding of ligands to low density lipoprotein receptor-related protein/alpha 2-macroglobulin receptor. *The Journal of biological chemistry*. 266:21232-21238.

Herz, J., U. Hamann, S. Rogne, O. Myklebost, H. Gausepohl, and K.K. Stanley. 1988. Surface location and high affinity for calcium of a 500-kd liver membrane protein closely related to the LDL-receptor suggest a physiological role as lipoprotein receptor. *The EMBO journal*. 7:4119-4127.

Herz, J., and D.K. Strickland. 2001. LRP: a multifunctional scavenger and signaling receptor. *The Journal of clinical investigation*. 108:779-784.

Hiesberger, T., M. Trommsdorff, B.W. Howell, A. Goffinet, M.C. Mumby, J.A. Cooper, and J. Herz. 1999. Direct binding of Reelin to VLDL receptor and ApoE receptor 2 induces tyrosine phosphorylation of disabled-1 and modulates tau phosphorylation. *Neuron*. 24:481-489.

Holscher, C. 1999. Synaptic plasticity and learning and memory: LTP and beyond. *J Neurosci Res*. 58:62-75.

Hotchin, N.A., and A. Hall. 1995. The assembly of integrin adhesion complexes requires both extracellular matrix and intracellular rho/rac GTPases. *J Cell Biol*. 131:1857-1865.

Hu, K., C. Wu, W.M. Mars, and Y. Liu. 2007. Tissue-type plasminogen activator promotes murine myofibroblast activation through LDL receptor-related protein 1-mediated integrin signaling. *J Clin Invest*. 117:3821-3832.

Hu, K., J. Yang, S. Tanaka, S.L. Gonias, W.M. Mars, and Y. Liu. 2006. Tissue-type plasminogen activator acts as a cytokine that triggers intracellular signal transduction and induces matrix metalloproteinase-9 gene expression. *The Journal of biological chemistry*. 281:2120-2127.

Huang, X.Y., G.M. Shi, R.P. Devbhandari, A.W. Ke, Y. Wang, X.Y. Wang, Z. Wang, Y.H. Shi, Y.S. Xiao, Z.B. Ding, Z. Dai, Y. Xu, W.P. Jia, Z.Y. Tang, J. Fan, and J. Zhou. 2012. Low level of low-density lipoprotein receptor-related protein 1 predicts an unfavorable prognosis of hepatocellular carcinoma after curative resection. *PLoS One*. 7:e32775.

Huang, Z., K. Shimazu, N.H. Woo, K. Zang, U. Muller, B. Lu, and L.F. Reichardt. 2006. Distinct roles of the beta 1-class integrins at the developing and the mature hippocampal excitatory synapse. *J Neurosci*. 26:11208-11219.

Huveneers, S., H. Truong, R. Fassler, A. Sonnenberg, and E.H. Danen. 2008. Binding of soluble fibronectin to integrin alpha5 beta1 - link to focal adhesion redistribution and contractile shape. *J Cell Sci*. 121:2452-2462.

Hynes, R.O. 2002. Integrins: bidirectional, allosteric signaling machines. *Cell*. 110:673-687.

Isbert, S., K. Wagner, S. Eggert, A. Schweitzer, G. Multhaup, S. Weggen, S. Kins, and C.U. Pietrzik. 2012. APP dimer formation is initiated in the endoplasmic reticulum and differs between APP isoforms. *Cell Mol Life Sci*. 69:1353-1375.

Iyer, V., K. Pumiglia, and C.M. DiPersio. 2005. Alpha3beta1 integrin regulates MMP-9 mRNA stability in immortalized keratinocytes: a novel mechanism of integrin-mediated MMP gene expression. *J Cell Sci*. 118:1185-1195.

Jacobsen, L., P. Madsen, S.K. Moestrup, A.H. Lund, N. Tommerup, A. Nykjaer, L. Sottrup-Jensen, J. Gliemann, and C.M. Petersen. 1996. Molecular characterization of a novel human hybrid-type receptor that binds the alpha2-macroglobulin receptor-associated protein. *J Biol Chem*. 271:31379-31383.

Jensen, P.H., P. Ebbesen, and J. Gliemann. 1989. Low alpha 2-macroglobulin-proteinase complex binding: a common but not exclusive characteristic of malignant cells. *In Vivo*. 3:7-9.

Johnson, M.S., N. Lu, K. Denessiouk, J. Heino, and D. Gullberg. 2009. Integrins during evolution: evolutionary trees and model organisms. *Biochim Biophys Acta*. 1788:779-789.

Kadare, G., N. Gervasi, K. Brami-Cherrier, H. Blockus, S. El Messari, S.T. Arold, and J.A. Girault. 2015. Conformational dynamics of the focal adhesion targeting domain control specific functions of focal adhesion kinase in cells. *The Journal of biological chemistry*. 290:478-491.

Kamikura, D.M., and J.A. Cooper. 2003. Lipoprotein receptors and a disabled family cytoplasmic adaptor protein regulate EGL-17/FGF export in C. elegans. *Genes Dev*. 17:2798-2811.

Kanai, Y., D. Wang, and N. Hirokawa. 2014. KIF13B enhances the endocytosis of LRP1 by recruiting LRP1 to caveolae. *J Cell Biol*. 204:395-408.

Katz, B.Z., L. Romer, S. Miyamoto, T. Volberg, K. Matsumoto, E. Cukierman, B. Geiger, and K.M. Yamada. 2003. Targeting membrane-localized focal adhesion kinase to focal adhesions: roles of tyrosine phosphorylation and SRC family kinases. *The Journal of biological chemistry*. 278:29115-29120.

Kerjaschki, D., and M.G. Farquhar. 1982. The pathogenic antigen of Heymann nephritis is a membrane glycoprotein of the renal proximal tubule brush border. *Proceedings of the National Academy of Sciences of the United States of America*. 79:5557-5561.

Kerkela, E., and U. Saarialho-Kere. 2003. Matrix metalloproteinases in tumor progression: focus on basal and squamous cell skin cancer. *Exp Dermatol*. 12:109-125.

Kim, C., F. Ye, X. Hu, and M.H. Ginsberg. 2012. Talin activates integrins by altering the topology of the beta transmembrane domain. *J Cell Biol*. 197:605-611.

Kim, D.H., H. Iijima, K. Goto, J. Sakai, H. Ishii, H.J. Kim, H. Suzuki, H. Kondo, S. Saeki, and T. Yamamoto. 1996. Human apolipoprotein E receptor 2. A novel lipoprotein receptor of the low density lipoprotein receptor family predominantly expressed in brain. *The Journal of biological chemistry*. 271:8373-8380.

Kim, J.Y., Y.S. Lee, J. Park, and J.S. Chun. 1997. Integrin-mediated activation of mitogen-activated protein kinase is independent of the activation of protein kinase C epsilon during the spreading of HeLa cells on a gelatin substratum. *Mol Cells*. 7:594-598.

King, W.G., M.D. Mattaliano, T.O. Chan, P.N. Tsichlis, and J.S. Brugge. 1997. Phosphatidylinositol 3-kinase is required for integrin-stimulated AKT and Raf-1/mitogen-activated protein kinase pathway activation. *Molecular and cellular biology*. 17:4406-4418.

Klug, W., A. Dietl, B. Simon, I. Sinning, and K. Wild. 2011. Phosphorylation of LRP1 regulates the interaction with Fe65. *FEBS Lett*. 585:3229-3235.

Kolega, J. 1986. Effects of mechanical tension on protrusive activity and microfilament and intermediate filament organization in an epidermal epithelium moving in culture. *J Cell Biol*. 102:1400-1411.

Komatsu, K., Y. Nakanishi, N. Nemoto, T. Hori, T. Sawada, and M. Kobayashi. 2004. Expression and quantitative analysis of matrix metalloproteinase-2 and -9 in human gliomas. *Brain Tumor Pathol*. 21:105-112.

Koo, E.H., and S.L. Squazzo. 1994. Evidence that production and release of amyloid beta-protein involves the endocytic pathway. *The Journal of biological chemistry*. 269:17386-17389.

Kozlova, N., J.K. Jensen, T.F. Chi, A. Samoylenko, and T. Kietzmann. 2015. PAI-1 modulates cell migration in a LRP1-dependent manner via beta-catenin and ERK1/2. *Thrombosis and haemostasis*. 113:988-998.

Kramar, E.A., J.A. Bernard, C.M. Gall, and G. Lynch. 2002. Alpha3 integrin receptors contribute to the consolidation of long-term potentiation. *Neuroscience*. 110:29-39.

Kramar, E.A., B. Lin, C.S. Rex, C.M. Gall, and G. Lynch. 2006. Integrin-driven actin polymerization consolidates long-term potentiation. *Proceedings of the National Academy of Sciences of the United States of America*. 103:5579-5584.

Lakshmana, M.K., J.Y. Chung, S. Wickramarachchi, E. Tak, E. Bianchi, E.H. Koo, and D.E. Kang. 2010. A fragment of the scaffolding protein RanBP9 is increased in Alzheimer's disease brains and strongly potentiates amyloid-beta peptide generation. *FASEB journal : official publication of the Federation of American Societies for Experimental Biology*. 24:119-127.

Lakshmana, M.K., I.S. Yoon, E. Chen, E. Bianchi, E.H. Koo, and D.E. Kang. 2009. Novel role of RanBP9 in BACE1 processing of amyloid precursor protein and amyloid beta peptide generation. *J Biol Chem*. 284:11863-11872.

Landis, D.M., and T.S. Reese. 1983. Cytoplasmic organization in cerebellar dendritic spines. *J Cell Biol*. 97:1169-1178.

Langlois, B., G. Perrot, C. Schneider, P. Henriet, H. Emonard, L. Martiny, and S. Dedieu. 2010. LRP-1 promotes cancer cell invasion by supporting ERK and inhibiting JNK signaling pathways. *PLoS One*. 5:e11584.

Legate, K.R., S.A. Wickstrom, and R. Fassler. 2009. Genetic and cell biological analysis of integrin outside-in signaling. *Genes Dev*. 23:397-418.

Li, Y., M.P. Marzolo, P. van Kerkhof, G.J. Strous, and G. Bu. 2000. The YXXL motif, but not the two NPXY motifs, serves as the dominant endocytosis signal for low density lipoprotein receptor-related protein. *The Journal of biological chemistry*. 275:17187-17194.

Liu, C.X., S. Musco, N.M. Lisitsina, E. Forgacs, J.D. Minna, and N.A. Lisitsyn. 2000. LRP-DIT, a putative endocytic receptor gene, is frequently inactivated in non-small cell lung cancer cell lines. *Cancer research*. 60:1961-1967.

Liu, D., J. Aguirre Ghiso, Y. Estrada, and L. Ossowski. 2002. EGFR is a transducer of the urokinase receptor initiated signal that is required for in vivo growth of a human carcinoma. *Cancer Cell*. 1:445-457.

Liu, Q., J. Trotter, J. Zhang, M.M. Peters, H. Cheng, J. Bao, X. Han, E.J. Weeber, and G. Bu. 2010. Neuronal LRP1 knockout in adult mice leads to impaired brain lipid metabolism and progressive, age-dependent synapse loss and neurodegeneration. *J Neurosci*. 30:17068-17078.

Lobert, V.H., A. Brech, N.M. Pedersen, J. Wesche, A. Oppelt, L. Malerod, and H. Stenmark. 2010. Ubiquitination of alpha 5 beta 1 integrin controls fibroblast migration through lysosomal degradation of fibronectin-integrin complexes. *Dev Cell*. 19:148-159.

Lois, C., J.M. Garcia-Verdugo, and A. Alvarez-Buylla. 1996. Chain migration of neuronal precursors. *Science*. 271:978-981.

Loukinova, E., S. Ranganathan, S. Kuznetsov, N. Gorlatova, M.M. Migliorini, D. Loukinov, P.G. Ulery, I. Mikhailenko, D.A. Lawrence, and D.K. Strickland. 2002. Platelet-derived growth factor (PDGF)-induced tyrosine phosphorylation of the low density lipoprotein receptor-related protein (LRP). Evidence for integrated co-receptor function betwenn LRP and the PDGF. *The Journal of biological chemistry*. 277:15499-15506.

Ma, Y.Q., J. Qin, C. Wu, and E.F. Plow. 2008. Kindlin-2 (Mig-2): a co-activator of beta3 integrins. *J Cell Biol*. 181:439-446.

Maier, W. 2013. Die Rolle von LRP1 in der Funktion des NMDA-Rezeptors. *In* Biology. Vol. doctoral degree. Johannes Gutenberg University, Mainz. 83.

Maier, W., M. Bednorz, S. Meister, A. Roebroek, S. Weggen, U. Schmitt, and C.U. Pietrzik. 2013. LRP1 is critical for the surface distribution and internalization of the NR2B NMDA receptor subtype. *Mol Neurodegener*. 8.

Mantuano, E., M. Jo, S.L. Gonias, and W.M. Campana. 2010. Low density lipoprotein receptor-related protein (LRP1) regulates Rac1 and RhoA reciprocally to control Schwann cell adhesion and migration. *The Journal of biological chemistry*. 285:14259-14266.

Marchisio, P.C., L. Bergui, G.C. Corbascio, O. Cremona, N. D'Urso, M. Schena, L. Tesio, and F. Caligaris-Cappio. 1988. Vinculin, talin, and integrins are localized at specific adhesion sites of malignant B lymphocytes. *Blood*. 72:830-833.

Martin, A.M., C. Kuhlmann, S. Trossbach, S. Jaeger, E. Waldron, A. Roebroek, H.J. Luhmann, A. Laatsch, S. Weggen, V. Lessmann, and C.U. Pietrzik. 2008. The functional role of the second NPXY motif of the LRP1 beta-chain in tissue-type plasminogen activator-mediated activation of N-methyl-D-aspartate receptors. *The Journal of biological chemistry*. 283:12004-12013.

Matsui, T., M. Amano, T. Yamamoto, K. Chihara, M. Nakafuku, M. Ito, T. Nakano, K. Okawa, A. Iwamatsu, and K. Kaibuchi. 1996. Rho-associated kinase, a novel serine/threonine kinase, as a putative target for small GTP binding protein Rho. *EMBO J*. 15:2208-2216.

Matsuzaki, M., N. Honkura, G.C. Ellis-Davies, and H. Kasai. 2004. Structural basis of long-term potentiation in single dendritic spines. *Nature*. 429:761-766.

Maurer, M.E., and J.A. Cooper. 2006. The adaptor protein Dab2 sorts LDL receptors into coated pits independently of AP-2 and ARH. *Journal of Cell Science*. 119:4235-4246.

May, P., A. Rohlmann, H.H. Bock, K. Zurhove, J.D. Marth, E.D. Schomburg, J.L. Noebels, U. Beffert, J.D. Sweatt, E.J. Weeber, and J. Herz. 2004. Neuronal LRP1 functionally associates with postsynaptic proteins and is required for normal motor function in mice. *Mol Cell Biol*. 24:8872-8883.

Missan, D.S., K. Mitchell, S. Subbaram, and C.M. DiPersio. 2015. Integrin alpha3beta1 signaling through MEK/ERK determines alternative polyadenylation of the MMP-9 mRNA transcript in immortalized mouse keratinocytes. *PLoS One*. 10:e0119539.

Moestrup, S.K., H. Birn, P.B. Fischer, C.M. Petersen, P.J. Verroust, R.B. Sim, E.I. Christensen, and E. Nexo. 1996. Megalin-mediated endocytosis of transcobalamin-vitamin-B12 complexes suggests a role of the receptor in vitamin-B12 homeostasis. *Proceedings of the National Academy of Sciences of the United States of America*. 93:8612-8617.

Moestrup, S.K., T.L. Holtet, M. Etzerodt, H.C. Thogersen, A. Nykjaer, P.A. Andreasen, H.H. Rasmussen, L. Sottrup-Jensen, and J. Gliemann. 1993. Alpha 2-macroglobulin-proteinase complexes, plasminogen activator inhibitor type-1-plasminogen activator complexes, and receptor-associated protein bind to a region of the alpha 2-macroglobulin receptor containing a cluster of eight complement-type repeats. *The Journal of biological chemistry*. 268:13691-13696.

Mokuno, H., S. Brady, L. Kotite, J. Herz, and R.J. Havel. 1994. Effect of the 39-kDa receptor-associated protein on the hepatic uptake and endocytosis of chylomicron remnants and low density lipoproteins in the rat. *J Biol Chem*. 269:13238-13243.

Morozevich, G., N. Kozlova, I. Cheglakov, N. Ushakova, and A. Berman. 2009. Integrin alpha5beta1 controls invasion of human breast carcinoma cells by direct and indirect modulation of MMP-2 collagenase activity. *Cell Cycle*. 8:2219-2225.

Morwald, S., H. Yamazaki, H. Bujo, J. Kusunoki, T. Kanaki, K. Seimiya, N. Morisaki, J. Nimpf, W.J. Schneider, and Y. Saito. 1997. A novel mosaic protein containing LDL receptor elements is highly conserved in humans and chickens. *Arterioscler Thromb Vasc Biol*. 17:996-1002.

Moser, M., B. Nieswandt, S. Ussar, M. Pozgajova, and R. Fassler. 2008. Kindlin-3 is essential for integrin activation and platelet aggregation. *Nat Med*. 14:325-330.

Mullis, K.B., and F.A. Faloona. 1987. Specific synthesis of DNA in vitro via a polymerase-catalyzed chain reaction. *Methods Enzymol*. 155:335-350.

Murase, S., and A.F. Horwitz. 2002. Deleted in colorectal carcinoma and differentially expressed integrins mediate the directional migration of neural precursors in the rostral migratory stream. *J Neurosci*. 22:3568-3579.

Muratoglu, S.C., I. Mikhailenko, C. Newton, M. Migliorini, and D.K. Strickland. 2010. Low density lipoprotein receptor-related protein 1 (LRP1) forms a signaling complex with platelet-derived growth factor receptor-beta in endosomes and regulates activation of the MAPK pathway. *The Journal of biological chemistry*. 285:14308-14317.

Nagase, H. 1997. Activation mechanisms of matrix metalloproteinases. *Biol Chem*. 378:151-160.

Nagase, H., A.J. Barrett, and J.F. Woessner, Jr. 1992. Nomenclature and glossary of the matrix metalloproteinases. *Matrix Suppl*. 1:421-424.

Nakayama, M., D. Nakajima, T. Nagase, N. Nomura, N. Seki, and O. Ohara. 1998. Identification of high-molecular-weight proteins with multiple EGF-like motifs by motif-trap screening. *Genomics*. 51:27-34.

Nassar, T., S. Akkawi, A. Shina, A. Haj-Yehia, K. Bdeir, M. Tarshis, S.N. Heyman, and A.A. Higazi. 2004. In vitro and in vivo effects of tPA and PAI-1 on blood vessel tone. *Blood*. 103:897-902.

Neels, J.G., B.M. van Den Berg, A. Lookene, G. Olivecrona, H. Pannekoek, and A.J. van Zonneveld. 1999. The second and fourth cluster of class A cysteine-rich repeats of the low density lipoprotein receptor-related protein share ligand-binding properties. *The Journal of biological chemistry*. 274:31305-31311.

Newby, A.C. 2005. Dual role of matrix metalloproteinases (matrixins) in intimal thickening and atherosclerotic plaque rupture. *Physiol Rev*. 85:1-31.

Newton, C.S., E. Loukinova, I. Mikhailenko, S. Ranganathan, Y. Gao, C. Haudenschild, and D.K. Strickland. 2005. Platelet-derived growth factor receptor-beta (PDGFR-beta) activation promotes its association with the low density lipoprotein receptor-related protein (LRP). Evidence for co-receptor function. *The Journal of biological chemistry*. 280:27872-27878.

Nielsen, B.S., F. Rank, M. Illemann, L.R. Lund, and K. Dano. 2007. Stromal cells associated with early invasive foci in human mammary ductal carcinoma in situ coexpress urokinase and urokinase receptor. *Int J Cancer*. 120:2086-2095.

Nieswandt, B., M. Moser, I. Pleines, D. Varga-Szabo, S. Monkley, D. Critchley, and R. Fassler. 2007. Loss of talin1 in platelets abrogates integrin activation, platelet aggregation, and thrombus formation in vitro and in vivo. *J Exp Med*. 204:3113-3118.

Nobes, C.D., and A. Hall. 1995. Rho, rac, and cdc42 GTPases regulate the assembly of multimolecular focal complexes associated with actin stress fibers, lamellipodia, and filopodia. *Cell*. 81:53-62.

Nykjaer, A., D. Dragun, D. Walther, H. Vorum, C. Jacobsen, J. Herz, F. Melsen, E.I. Christensen, and T.E. Willnow. 1999. An endocytic pathway essential for renal uptake and activation of the steroid 25-(OH) vitamin D3. *Cell*. 96:507-515.

Obermeyer, K., S. Krueger, B. Peters, B. Falkenberg, A. Roessner, and C. Rocken. 2007. The expression of low density lipoprotein receptor-related protein in colorectal carcinoma. *Oncol Rep*. 17:361-367.

Oh, A.S., L.A. Lorant, J.N. Holloway, D.L. Miller, F.G. Kern, and D. El-Ashry. 2001. Hyperactivation of MAPK induces loss of ERalpha expression in breast cancer cells. *Mol Endocrinol*. 15:1344-1359.

Ohazama, A., T. Porntaveetus, M.S. Ota, J. Herz, and P.T. Sharpe. 2010. Lrp4: A novel modulator of extracellular signaling in craniofacial organogenesis. *Am J Med Genet A*. 152A:2974-2983.

Okada, A., C. Tomasetto, Y. Lutz, J.P. Bellocq, M.C. Rio, and P. Basset. 1997. Expression of matrix metalloproteinases during rat skin wound healing: evidence that membrane type-1 matrix metalloproteinase is a stromal activator of pro-gelatinase A. *J Cell Biol*. 137:67-77.

Osenkowski, P., M. Toth, and R. Fridman. 2004. Processing, shedding, and endocytosis of membrane type 1-matrix metalloproteinase (MT1-MMP). *J Cell Physiol*. 200:2-10.

Pei, D., and S.J. Weiss. 1995. Furin-dependent intracellular activation of the human stromelysin-3 zymogen. *Nature*. 375:244-247.

Pellinen, T., A. Arjonen, K. Vuoriluoto, K. Kallio, J.A. Fransen, and J. Ivaska. 2006. Small GTPase Rab21 regulates cell adhesion and controls endosomal traffic of beta1-integrins. *J Cell Biol*. 173:767-780.

Pellinen, T., S. Tuomi, A. Arjonen, M. Wolf, H. Edgren, H. Meyer, R. Grosse, T. Kitzing, J.K. Rantala, O. Kallioniemi, R. Fassler, M. Kallio, and J. Ivaska. 2008. Integrin trafficking regulated by Rab21 is necessary for cytokinesis. *Developmental Cell*. 15:371-385.

Peters, A., and I.R. Kaiserman-Abramof. 1970. The small pyramidal neuron of the rat cerebral cortex. The perikaryon, dendrites and spines. *Am J Anat*. 127:321-355.

Pflanzner, T., M.C. Janko, B. Andre-Dohmen, S. Reuss, S. Weggen, A.J. Roebroek, C.R. Kuhlmann, and C.U. Pietrzik. 2011. LRP1 mediates bidirectional transcytosis of amyloid-beta across the blood-brain barrier. *Neurobiology of aging*. 32:2323 e2321-2311.

Pietrzik, C.U., T. Busse, D.E. Merriam, S. Weggen, and E.H. Koo. 2002. The cytoplasmic domain of the LDL receptor-related protein regulates multiple steps in APP processing. *The EMBO journal*. 21:5691-5700.

Pietrzik, C.U., I.S. Yoon, S. Jaeger, T. Busse, S. Weggen, and E.H. Koo. 2004. FE65 constitutes the functional link between the low-density lipoprotein receptor-related protein and the amyloid precursor protein. *J Neurosci*. 24:4259-4265.

Pinson, K.I., J. Brennan, S. Monkley, B.J. Avery, and W.C. Skarnes. 2000. An LDL-receptor-related protein mediates Wnt signalling in mice. *Nature*. 407:535-538.

Qiu, Z., B.T. Hyman, and G.W. Rebeck. 2004. Apolipoprotein E receptors mediate neurite outgrowth through activation of p44/42 mitogen-activated protein kinase in primary neurons. *The Journal of biological chemistry*. 279:34948-34956.

Quinn, K.A., V.J. Pye, Y.P. Dai, C.N. Chesterman, and D.A. Owensby. 1999. Characterization of the soluble form of the low density lipoprotein receptor-related protein (LRP). *Experimental Cell Research*. 251:433-441.

Rabiej, V.K., T. Pflanzner, T. Wagner, K. Goetze, S.E. Storck, J.A. Eble, S. Weggen, W. Mueller-Klieser, and C.U. Pietrzik. 2016. Low density lipoprotein receptor-related protein 1 mediated endocytosis of beta1-integrin influences cell adhesion and cell migration. *Exp Cell Res*. 340:102-115.

Rainero, E., and J.C. Norman. 2015. Endosomal integrin signals for survival. *Nat Cell Biol*. 17:1373-1375.

Ramón y Cajal, S. 1891. Sur la structure de l`´ecorce cérébrale de quelque mamifères. *La Cellule*. 7:124-176.

Reekmans, S.M., T. Pflanzner, P.L. Gordts, S. Isbert, P. Zimmermann, W. Annaert, S. Weggen, A.J. Roebroek, and C.U. Pietrzik. 2010. Inactivation of the proximal NPXY motif impairs early steps in LRP1 biosynthesis. *Cell Mol Life Sci*. 67:135-145.

Reinartz, J., B. Schafer, R. Batrla, C.E. Klein, and M.D. Kramer. 1995. Plasmin abrogates alpha v beta 5-mediated adhesion of a human keratinocyte cell line (HaCaT) to vitronectin. *Exp Cell Res*. 220:274-282.

Renart, J., J. Reiser, and G.R. Stark. 1979. Transfer of proteins from gels to diazobenzyloxymethyl-paper and detection with antisera: a method for studying antibody specificity and antigen structure. *Proceedings of the National Academy of Sciences of the United States of America*. 76:3116-3120.

Renaudin, A., M. Lehmann, J. Girault, and L. McKerracher. 1999. Organization of point contacts in neuronal growth cones. *J Neurosci Res*. 55:458-471.

Ribeiro, A., S. Balasubramanian, D. Hughes, S. Vargo, E.M. Powell, and J.B. Leach. 2013. beta1-Integrin cytoskeletal signaling regulates sensory neuron response to matrix dimensionality. *Neuroscience*. 248:67-78.

Roberts, P.J., and C.J. Der. 2007. Targeting the Raf-MEK-ERK mitogen-activated protein kinase cascade for the treatment of cancer. *Oncogene*. 26:3291-3310.

Robles, E., and T.M. Gomez. 2006. Focal adhesion kinase signaling at sites of integrin-mediated adhesion controls axon pathfinding. *Nature neuroscience*. 9:1274-1283.

Roebroek, A.J., S. Reekmans, A. Lauwers, N. Feyaerts, L. Smeijers, and D. Hartmann. 2006. Mutant Lrp1 knock-in mice generated by recombinase-mediated cassette exchange reveal differential importance of the NPXY motifs in the intracellular domain of LRP1 for normal fetal development. *Mol Cell Biol*. 26:605-616.

Rogaeva, E., Y. Meng, J.H. Lee, Y. Gu, T. Kawarai, F. Zou, T. Katayama, C.T. Baldwin, R. Cheng, H. Hasegawa, F. Chen, N. Shibata, K.L. Lunetta, R. Pardossi-Piquard, C. Bohm, Y. Wakutani, L.A. Cupples, K.T. Cuenco, R.C. Green, L. Pinessi, I. Rainero, S. Sorbi, A. Bruni, R. Duara, R.P. Friedland, R. Inzelberg, W. Hampe, H. Bujo, Y.Q. Song, O.M. Andersen, T.E. Willnow, N. Graff-Radford, R.C. Petersen, D. Dickson, S.D. Der, P.E. Fraser, G. Schmitt-Ulms, S. Younkin, R. Mayeux, L.A. Farrer, and P. St George-Hyslop. 2007. The neuronal sortilin-related receptor SORL1 is genetically associated with Alzheimer disease. *Nat Genet*. 39:168-177.

Royce, L.S., and B.J. Baum. 1991. Physiologic levels of salivary epidermal growth factor stimulate migration of an oral epithelial cell line. *Biochim Biophys Acta*. 1092:401-403.

Rozanov, D.V., E. Hahn-Dantona, D.K. Strickland, and A.Y. Strongin. 2004. The low density lipoprotein receptor-related protein LRP is regulated by membrane type-1 matrix metalloproteinase (MT1-MMP) proteolysis in malignant cells. *Journal of Biological Chemistry*. 279:4260-4268.

Saito, A., S. Pietromonaco, A.K. Loo, and M.G. Farquhar. 1994. Complete cloning and sequencing of rat gp330/"megalin," a distinctive member of the low density lipoprotein receptor gene family. *Proceedings of the National Academy of Sciences of the United States of America*. 91:9725-9729.

Saleem, S., J. Li, S.P. Yee, G.F. Fellows, C.G. Goodyer, and R. Wang. 2009. beta1 integrin/FAK/ERK signalling pathway is essential for human fetal islet cell differentiation and survival. *J Pathol*. 219:182-192.

Salicioni, A.M., A. Gaultier, C. Brownlee, M.K. Cheezum, and S.L. Gonias. 2004. Low density lipoprotein receptor-related protein-1 promotes beta1 integrin maturation and transport to the cell surface. *The Journal of biological chemistry*. 279:10005-10012.

Sanders, M.A., and M.D. Basson. 2000. Collagen IV-dependent ERK activation in human Caco-2 intestinal epithelial cells requires focal adhesion kinase. *The Journal of biological chemistry*. 275:38040-38047.

Sato, M., K. Kawana, K. Adachi, A. Fujimoto, M. Yoshida, H. Nakamura, H. Nishida, T. Inoue, A. Taguchi, J. Takahashi, S. Kojima, A. Yamashita, K. Tomio, T. Nagamatsu, O. Wada-Hiraike, K. Oda, Y. Osuga, and T. Fujii. 2016. Decreased expression of the plasminogen activator inhibitor type 1 is involved in degradation of extracellular matrix surrounding cervical cancer stem cells. *Int J Oncol*. 48:829-835.

Sawamoto, K., H. Wichterle, O. Gonzalez-Perez, J.A. Cholfin, M. Yamada, N. Spassky, N.S. Murcia, J.M. Garcia-Verdugo, O. Marin, J.L. Rubenstein, M. Tessier-Lavigne, H. Okano, and A. Alvarez-Buylla. 2006. New neurons follow the flow of cerebrospinal fluid in the adult brain. *Science*. 311:629-632.

Schaller, M.D., C.A. Borgman, B.S. Cobb, R.R. Vines, A.B. Reynolds, and J.T. Parsons. 1992. pp125FAK a structurally distinctive protein-tyrosine kinase associated with focal adhesions. *Proceedings of the National Academy of Sciences of the United States of America*. 89:5192-5196.

Schaller, M.D., J.D. Hildebrand, J.D. Shannon, J.W. Fox, R.R. Vines, and J.T. Parsons. 1994. Autophosphorylation of the focal adhesion kinase, pp125FAK, directs SH2-dependent binding of pp60src. *Mol Cell Biol*. 14:1680-1688.

Schaller, M.D., and J.T. Parsons. 1995. pp125FAK-dependent tyrosine phosphorylation of paxillin creates a high-affinity binding site for Crk. *Mol Cell Biol*. 15:2635-2645.

Schiller, H.B., A. Szekeres, B.R. Binder, H. Stockinger, and V. Leksa. 2009. Mannose 6-phosphate/insulin-like growth factor 2 receptor limits cell invasion by controlling alphaVbeta3 integrin expression and proteolytic processing of urokinase-type plasminogen activator receptor. *Mol Biol Cell*. 20:745-756.

Schlaepfer, D.D., and T. Hunter. 1996. Evidence for in vivo phosphorylation of the Grb2 SH2-domain binding site on focal adhesion kinase by Src-family protein-tyrosine kinases. *Mol Cell Biol*. 16:5623-5633.

Schmidt, V., A. Sporbert, M. Rohe, T. Reimer, A. Rehm, O.M. Andersen, and T.E. Willnow. 2007. SorLA/LR11 regulates processing of amyloid precursor protein via interaction with adaptors GGA and PACS-1. *J Biol Chem*. 282:32956-32964.

Scilabra, S.D., L. Troeberg, K. Yamamoto, H. Emonard, I. Thogersen, J.J. Enghild, D.K. Strickland, and H. Nagase. 2013. Differential Regulation of Extracellular Tissue Inhibitor of Metalloproteinases-3 Levels by Cell Membrane-bound and Shed Low Density Lipoprotein Receptor-related Protein 1. *Journal of Biological Chemistry*. 288:332-342.

Selvais, C., H.P.G. Chevronnay, P. Lemoine, S. Dedieu, P. Henriet, P.J. Courtoy, E. Marbaix, and H. Emonard. 2009. Metalloproteinase-Dependent Shedding of Low-Density Lipoprotein Receptor-Related Protein-1 Ectodomain Decreases Endocytic Clearance of Endometrial Matrix Metalloproteinase-2 and-9 at Menstruation. *Endocrinology*. 150:3792-3799.

Senior, R.M., G.L. Griffin, J.S. Huang, D.A. Walz, and T.F. Deuel. 1983. Chemotactic activity of platelet alpha granule proteins for fibroblasts. *J Cell Biol*. 96:382-385.

Shen, C., W.C. Xiong, and L. Mei. 2015. LRP4 in neuromuscular junction and bone development and diseases. *Bone*. 80:101-108.

Shi, F., and J. Sottile. 2008. Caveolin-1-dependent beta1 integrin endocytosis is a critical regulator of fibronectin turnover. *J Cell Sci*. 121:2360-2371.

Shi, Y., E. Mantuano, G. Inoue, W.M. Campana, and S.L. Gonias. 2009. Ligand binding to LRP1 transactivates Trk receptors by a Src family kinase-dependent pathway. *Sci Signal*. 2:ra18.

Shieh, J.C., B.T. Schaar, K. Srinivasan, F.M. Brodsky, and S.K. McConnell. 2011. Endocytosis regulates cell soma translocation and the distribution of adhesion proteins in migrating neurons. *PLoS One*. 6:e17802.

Sidenius, N., A. Andolfo, R. Fesce, and F. Blasi. 2002. Urokinase regulates vitronectin binding by controlling urokinase receptor oligomerization. *The Journal of biological chemistry*. 277:27982-27990.

Sieg, D.J., C.R. Hauck, D. Ilic, C.K. Klingbeil, E. Schaefer, C.H. Damsky, and D.D. Schlaepfer. 2000. FAK integrates growth-factor and integrin signals to promote cell migration. *Nat Cell Biol*. 2:249-256.

Smith, H.W., and C.J. Marshall. 2010. Regulation of cell signalling by uPAR. *Nat Rev Mol Cell Biol*. 11:23-36.

Smith, P.K., R.I. Krohn, G.T. Hermanson, A.K. Mallia, F.H. Gartner, M.D. Provenzano, E.K. Fujimoto, N.M. Goeke, B.J. Olson, and D.C. Klenk. 1985. Measurement of protein using bicinchoninic acid. *Anal Biochem*. 150:76-85.

Song, H., Y. Li, J. Lee, A.L. Schwartz, and G. Bu. 2009. Low-density lipoprotein receptor-related protein 1 promotes cancer cell migration and invasion by inducing the expression of matrix metalloproteinases 2 and 9. *Cancer Res*. 69:879-886.

Staquet, M.J., Y. Kobayashi, C. Dezutter-Dambuyant, and D. Schmitt. 1995. Role of specific successive contacts between extracellular matrix proteins and epidermal Langerhans cells in the control of their directed migration. *Eur J Cell Biol*. 66:342-348.

Stearns, M., and M.E. Stearns. 1996. Evidence for increased activated metalloproteinase 2 (MMP-2a) expression associated with human prostate cancer progression. *Oncol Res*. 8:69-75.

Stephens, L.E., A.E. Sutherland, I.V. Klimanskaya, A. Andrieux, J. Meneses, R.A. Pedersen, and C.H. Damsky. 1995. Deletion of beta 1 integrins in mice results in inner cell mass failure and peri-implantation lethality. *Genes Dev*. 9:1883-1895.

Storck, S.E., S. Meister, J. Nahrath, J.N. Meissner, N. Schubert, A. Di Spiezio, S. Baches, R.E. Vandenbroucke, Y. Bouter, I. Prikulis, C. Korth, S. Weggen, A. Heimann, M. Schwaninger, T.A. Bayer, and C.U. Pietrzik. 2016. Endothelial LRP1 transports amyloid-beta(1-42) across the blood-brain barrier. *J Clin Invest*. 126:123-136.

Strickland, D.K., J.D. Ashcom, S. Williams, F. Battey, E. Behre, K. McTigue, J.F. Battey, and W.S. Argraves. 1991. Primary structure of alpha 2-macroglobulin receptor-associated protein. Human homologue of a Heymann nephritis antigen. *The Journal of biological chemistry*. 266:13364-13369.

Strickland, D.K., J.D. Ashcom, S. Williams, W.H. Burgess, M. Migliorini, and W.S. Argraves. 1990. Sequence identity between the alpha 2-macroglobulin receptor and low density lipoprotein receptor-related protein suggests that this molecule is a multifunctional receptor. *J Biol Chem*. 265:17401-17404.

Tachibana, K., T. Sato, N. D'Avirro, and C. Morimoto. 1995. Direct association of pp125FAK with paxillin, the focal adhesion-targeting mechanism of pp125FAK. *The Journal of experimental medicine*. 182:1089-1099.

Taira, K., H. Bujo, S. Hirayama, H. Yamazaki, T. Kanaki, K. Takahashi, I. Ishii, T. Miida, W.J. Schneider, and Y. Saito. 2001. LR11, a mosaic LDL receptor family member, mediates the uptake of ApoE-rich lipoproteins in vitro. *Arterioscler Thromb Vasc Biol*. 21:1501-1506.

Tamkun, J.W., D.W. DeSimone, D. Fonda, R.S. Patel, C. Buck, A.F. Horwitz, and R.O. Hynes. 1986. Structure of integrin, a glycoprotein involved in the transmembrane linkage between fibronectin and actin. *Cell*. 46:271-282.

Tan, C.L., J.C. Kwok, R. Patani, C. Ffrench-Constant, S. Chandran, and J.W. Fawcett. 2011. Integrin activation promotes axon growth on inhibitory chondroitin sulfate proteoglycans by enhancing integrin signaling. *J Neurosci*. 31:6289-6295.

Taylor, D.R., and N.M. Hooper. 2007. The low-density lipoprotein receptor-related protein 1 (LRP1) mediates the endocytosis of the cellular prion protein. *Biochem J*. 402:17-23.

Tetu, B., J. Brisson, C.S. Wang, H. Lapointe, G. Beaudry, C. Blanchette, and D. Trudel. 2006. The influence of MMP-14, TIMP-2 and MMP-2 expression on breast cancer prognosis. *Breast Cancer Res*. 8:R28.

Theocharis, A.D., S.S. Skandalis, C. Gialeli, and N.K. Karamanos. 2016. Extracellular matrix structure. *Adv Drug Deliv Rev*. 97:4-27.

Tissir, F., and A.M. Goffinet. 2003. Reelin and brain development. *Nat Rev Neurosci*. 4:496-505.

Tojkander, S., G. Gateva, and P. Lappalainen. 2012. Actin stress fibers--assembly, dynamics and biological roles. *J Cell Sci*. 125:1855-1864.

Toth, M., I. Chvyrkova, M.M. Bernardo, S. Hernandez-Barrantes, and R. Fridman. 2003. Pro-MMP-9 activation by the MT1-MMP/MMP-2 axis and MMP-3: role of TIMP-2 and plasma membranes. *Biochem Biophys Res Commun*. 308:386-395.

Trommsdorff, M., M. Gotthardt, T. Hiesberger, J. Shelton, W. Stockinger, J. Nimpf, R.E. Hammer, J.A. Richardson, and J. Herz. 1999. Reeler/Disabled-like disruption of neuronal migration in knockout mice lacking the VLDL receptor and ApoE receptor 2. *Cell*. 97:689-701.

Turner, C.E., and J.T. Miller. 1994. Primary sequence of paxillin contains putative SH2 and SH3 domain binding motifs and multiple LIM domains: identification of a vinculin and pp125Fak-binding region. *J Cell Sci*. 107 (Pt 6):1583-1591.

Ulery, P.G., J. Beers, I. Mikhailenko, R.E. Tanzi, G.W. Rebeck, B.T. Hyman, and D.K. Strickland. 2000. Modulation of beta-amyloid precursor protein processing by the low density lipoprotein receptor-related protein (LRP). Evidence that LRP contributes to the pathogenesis of Alzheimer's disease. *J Biol Chem*. 275:7410-7415.

van Kerkhof, P., J. Lee, L. McCormick, E. Tetrault, W. Lu, M. Schoenfish, V. Oorschot, G.J. Strous, J. Klumperman, and G. Bu. 2005. Sorting nexin 17 facilitates LRP recycling in the early endosome. *The EMBO journal*. 24:2851-2861.

Van Leuven, F., J.J. Cassiman, and H. Van Den Berghe. 1979. Demonstration of an alpha2-macroglobulin receptor in human fibroblasts, absent in tumor-derived cell lines. *The Journal of biological chemistry*. 254:5155-5160.

Van Leuven, F., L. Stas, C. Hilliker, K. Lorent, L. Umans, L. Serneels, L. Overbergh, S. Torrekens, D. Moechars, B. De Strooper, and et al. 1994. Structure of the gene (LRP1) coding for the human alpha 2-macroglobulin receptor lipoprotein receptor-related protein. *Genomics*. 24:78-89.

Van Wart, H.E., and H. Birkedal-Hansen. 1990. The cysteine switch: a principle of regulation of metalloproteinase activity with potential applicability to the entire matrix metalloproteinase gene family. *Proceedings of the National Academy of Sciences of the United States of America*. 87:5578-5582.

Vihinen, P., R. Ala-aho, and V.M. Kahari. 2005. Matrix metalloproteinases as therapeutic targets in cancer. *Current cancer drug targets*. 5:203-220.

Waldron, E., C. Heilig, A. Schweitzer, N. Nadella, S. Jaeger, A.M. Martin, S. Weggen, K. Brix, and C.U. Pietrzik. 2008. LRP1 modulates APP trafficking along early compartments of the secretory pathway. *Neurobiology of disease*. 31:188-197.

Wang, H., M. Lewsadder, E. Dorn, S. Xu, and M.K. Lakshmana. 2014a. RanBP9 overexpression reduces dendritic arbor and spine density. *Neuroscience*. 265:253-262.

Wang, P., C. Ballestrem, and C.H. Streuli. 2011a. The C terminus of talin links integrins to cell cycle progression. *J Cell Biol*. 195:499-513.

Wang, R., J.P. Palavicini, H. Wang, P. Maiti, E. Bianchi, S. Xu, B.N. Lloyd, K. Dawson-Scully, D.E. Kang, and M.K. Lakshmana. 2014b. RanBP9 overexpression accelerates loss of dendritic spines in a mouse model of Alzheimer's disease. *Neurobiol Dis*. 69:169-179.

Wang, X., S.R. Lee, K. Arai, S.R. Lee, K. Tsuji, G.W. Rebeck, and E.H. Lo. 2003. Lipoprotein receptor-mediated induction of matrix metalloproteinase by tissue plasminogen activator. *Nat Med*. 9:1313-1317.

Wang, X., Z. Wang, Y. Yao, J. Li, X. Zhang, C. Li, Y. Cheng, G. Ding, L. Liu, and Z. Ding. 2011b. Essential role of ERK activation in neurite outgrowth induced by alpha-lipoic acid. *Biochim Biophys Acta*. 1813:827-838.

Warren, M.S., W.D. Bradley, S.L. Gourley, Y.C. Lin, M.A. Simpson, L.F. Reichardt, C.A. Greer, J.R. Taylor, and A.J. Koleske. 2012. Integrin beta1 signals through Arg to regulate postnatal dendritic arborization, synapse density, and behavior. *The Journal of neuroscience : the official journal of the Society for Neuroscience*. 32:2824-2834.

Watanabe, N., P. Madaule, T. Reid, T. Ishizaki, G. Watanabe, A. Kakizuka, Y. Saito, K. Nakao, B.M. Jockusch, and S. Narumiya. 1997. p140mDia, a mammalian homolog of Drosophila diaphanous, is a target protein for Rho small GTPase and is a ligand for profilin. *EMBO J*. 16:3044-3056.

Weaver, A.M., I.M. Hussaini, A. Mazar, J. Henkin, and S.L. Gonias. 1997. Embryonic fibroblasts that are genetically deficient in low density lipoprotein receptor-related protein demonstrate increased activity of the urokinase receptor system and accelerated migration on vitronectin. *The Journal of biological chemistry*. 272:14372-14379.

Weaver, A.M., M. McCabe, I. Kim, M.M. Allietta, and S.L. Gonias. 1996. Epidermal growth factor and platelet-derived growth factor-BB induce a stable increase in the activity of low density lipoprotein receptor-related protein in vascular smooth muscle cells by altering receptor distribution and recycling. *The Journal of biological chemistry*. 271:24894-24900.

Webb, D.J., K. Donais, L.A. Whitmore, S.M. Thomas, C.E. Turner, J.T. Parsons, and A.F. Horwitz. 2004. FAK-Src signalling through paxillin, ERK and MLCK regulates adhesion disassembly. *Nat Cell Biol*. 6:154-161.

Webb, D.J., J.T. Parsons, and A.F. Horwitz. 2002. Adhesion assembly, disassembly and turnover in migrating cells -- over and over and over again. *Nat Cell Biol*. 4:E97-100.

Wehrli, M., S.T. Dougan, K. Caldwell, L. O'Keefe, S. Schwartz, D. Vaizel-Ohayon, E. Schejter, A. Tomlinson, and S. DiNardo. 2000. arrow encodes an LDL-receptor-related protein essential for Wingless signalling. *Nature*. 407:527-530.

Wei, C., C.C. Moller, M.M. Altintas, J. Li, K. Schwarz, S. Zacchigna, L. Xie, A. Henger, H. Schmid, M.P. Rastaldi, P. Cowan, M. Kretzler, R. Parrilla, M. Bendayan, V. Gupta, B. Nikolic, R. Kalluri, P. Carmeliet, P. Mundel, and J. Reiser. 2008. Modification of kidney barrier function by the urokinase receptor. *Nat Med*. 14:55-63.

Wei, Y., R.P. Czekay, L. Robillard, M.C. Kugler, F. Zhang, K.K. Kim, J.P. Xiong, M.J. Humphries, and H.A. Chapman. 2005. Regulation of alpha5beta1 integrin conformation and function by urokinase receptor binding. *The Journal of cell biology*. 168:501-511.

Wei, Y., M. Lukashev, D.I. Simon, S.C. Bodary, S. Rosenberg, M.V. Doyle, and H.A. Chapman. 1996. Regulation of integrin function by the urokinase receptor. *Science*. 273:1551-1555.

Wei, Y., D.A. Waltz, N. Rao, R.J. Drummond, S. Rosenberg, and H.A. Chapman. 1994. Identification of the urokinase receptor as an adhesion receptor for vitronectin. *The Journal of biological chemistry*. 269:32380-32388.

Weis, S.M., S.T. Lim, K.M. Lutu-Fuga, L.A. Barnes, X.L. Chen, J.R. Gothert, T.L. Shen, J.L. Guan, D.D. Schlaepfer, and D.A. Cheresh. 2008. Compensatory role for Pyk2 during angiogenesis in adult mice lacking endothelial cell FAK. *The Journal of cell biology*. 181:43-50.

Williams, S.E., J.D. Ashcom, W.S. Argraves, and D.K. Strickland. 1992. A novel mechanism for controlling the activity of alpha 2-macroglobulin receptor/low density lipoprotein receptor-related protein. Multiple regulatory sites for 39-kDa receptor-associated protein. *The Journal of biological chemistry*. 267:9035-9040.

Willnow, T.E., J. Hilpert, S.A. Armstrong, A. Rohlmann, R.E. Hammer, D.K. Burns, and J. Herz. 1996a. Defective forebrain development in mice lacking gp330/megalin. *Proceedings of the National Academy of Sciences of the United States of America*. 93:8460-8464.

Willnow, T.E., J.M. Moehring, N.M. Inocencio, T.J. Moehring, and J. Herz. 1996b. The low-density-lipoprotein receptor-related protein (LRP) is processed by furin in vivo and in vitro. *Biochem J*. 313 (Pt 1):71-76.

Willnow, T.E., K. Orth, and J. Herz. 1994. Molecular dissection of ligand binding sites on the low density lipoprotein receptor-related protein. *The Journal of biological chemistry*. 269:15827-15832.

Wolf, B.B., M.B. Lopes, S.R. VandenBerg, and S.L. Gonias. 1992. Characterization and immunohistochemical localization of alpha 2-macroglobulin receptor (low-density lipoprotein receptor-related protein) in human brain. *Am J Pathol*. 141:37-42.

Wolfenson, H., T. Iskratsch, and M.P. Sheetz. 2014. Early events in cell spreading as a model for quantitative analysis of biomechanical events. *Biophys J*. 107:2508-2514.

Woo, J.A., T. Boggess, C. Uhlar, X. Wang, H. Khan, G. Cappos, A. Joly-Amado, E. De Narvaez, S. Majid, L.S. Minamide, J.R. Bamburg, D. Morgan, E. Weeber, and D.E. Kang. 2015. RanBP9 at the intersection between cofilin and Abeta pathologies: rescue of neurodegenerative changes by RanBP9 reduction. *Cell death & disease*. 6:1676.

Woo, J.A., A.R. Jung, M.K. Lakshmana, A. Bedrossian, Y. Lim, J.H. Bu, S.A. Park, E.H. Koo, I. Mook-Jung, and D.E. Kang. 2012a. Pivotal role of the RanBP9-cofilin pathway in Abeta-induced apoptosis and neurodegeneration. *Cell Death Differ*. 19:1413-1423.

Woo, J.A., S.E. Roh, M.K. Lakshmana, and D.E. Kang. 2012b. Pivotal role of RanBP9 in integrin-dependent focal adhesion signaling and assembly. *FASEB J*. 26:1672-1681.

Woods, A.J., D.P. White, P.T. Caswell, and J.C. Norman. 2004. PKD1/PKCmu promotes alphavbeta3 integrin recycling and delivery to nascent focal adhesions. *EMBO J*. 23:2531-2543.

Wyszynski, M., J. Lin, A. Rao, E. Nigh, A.H. Beggs, A.M. Craig, and M. Sheng. 1997. Competitive binding of alpha-actinin and calmodulin to the NMDA receptor. *Nature*. 385:439-442.

Xiao, T., J. Takagi, B.S. Coller, J.H. Wang, and T.A. Springer. 2004. Structural basis for allostery in integrins and binding to fibrinogen-mimetic therapeutics. *Nature*. 432:59-67.

Xing, Z., H.C. Chen, J.K. Nowlen, S.J. Taylor, D. Shalloway, and J.L. Guan. 1994. Direct interaction of v-Src with the focal adhesion kinase mediated by the Src SH2 domain. *Mol Biol Cell*. 5:413-421.

Xiong, J.P., T. Stehle, B. Diefenbach, R. Zhang, R. Dunker, D.L. Scott, A. Joachimiak, S.L. Goodman, and M.A. Arnaout. 2001. Crystal structure of the extracellular segment of integrin alpha Vbeta3. *Science*. 294:339-345.

Xiong, J.P., T. Stehle, R. Zhang, A. Joachimiak, M. Frech, S.L. Goodman, and M.A. Arnaout. 2002. Crystal structure of the extracellular segment of integrin alpha Vbeta3 in complex with an Arg-Gly-Asp ligand. *Science*. 296:151-155.

Xue, W., I. Mizukami, R.F. Todd, 3rd, and H.R. Petty. 1997. Urokinase-type plasminogen activator receptors associate with beta1 and beta3 integrins of fibrosarcoma cells: dependence on extracellular matrix components. *Cancer research*. 57:1682-1689.

Yamamoto, K., G. Murphy, and L. Troeberg. 2015. Extracellular regulation of metalloproteinases. *Matrix Biol*. 44-46:255-263.

Yamamoto, M., K. Ikeda, K. Ohshima, H. Tsugu, H. Kimura, and M. Tomonaga. 1997. Increased expression of low density lipoprotein receptor-related protein/alpha2-macroglobulin receptor in human malignant astrocytomas. *Cancer Res*. 57:2799-2805.

Yamazaki, H., H. Bujo, and Y. Saito. 1997. A novel member of the LDL receptor gene family with eleven binding repeats is structurally related to neural adhesion molecules and a yeast vacuolar protein sorting receptor. *J Atheroscler Thromb*. 4:20-26.

Yang, Z., D.K. Strickland, and P. Bornstein. 2001. Extracellular matrix metalloproteinase 2 levels are regulated by the low density lipoprotein-related scavenger receptor and thrombospondin 2. *The Journal of biological chemistry*. 276:8403-8408.

Yoon, C., E.A. Van Niekerk, K. Henry, T. Ishikawa, S. Orita, M.H. Tuszynski, and W.M. Campana. 2013. Low-density lipoprotein receptor-related protein 1 (LRP1)-dependent cell signaling promotes axonal regeneration. *The Journal of biological chemistry*. 288:26557-26568.

Yoon, I.S., E. Chen, T. Busse, E. Repetto, M.K. Lakshmana, E.H. Koo, and D.E. Kang. 2007. Low-density lipoprotein receptor-related protein promotes amyloid precursor protein trafficking to lipid rafts in the endocytic pathway. *FASEB J*. 21:2742-2752.

Zaidel-Bar, R., S. Itzkovitz, A. Ma'ayan, R. Iyengar, and B. Geiger. 2007. Functional atlas of the integrin adhesome. *Nat Cell Biol*. 9:858-867.

Zhang, H., J.M. Lee, Y. Wang, L. Dong, K.W. Ko, L. Pelletier, and Z. Yao. 2008. Mutational analysis of the FXNPXY motif within LDL receptor-related protein 1 (LRP1) reveals the functional importance of the tyrosine residues in cell growth regulation and signal transduction. *Biochem J*. 409:53-64.

Zhang, L., and W. Zou. 2015. Inhibition of integrin beta1 decreases the malignancy of ovarian cancer cells and potentiates anticancer therapy via the FAK/STAT1 signaling pathway. *Mol Med Rep*. 12:7869-7876.

Zhu, J., C.V. Carman, M. Kim, M. Shimaoka, T.A. Springer, and B.H. Luo. 2007. Requirement of alpha and beta subunit transmembrane helix separation for integrin outside-in signaling. *Blood*. 110:2475-2483.

Publication

Rabiej, V.K., T. Pflanzner, T. Wagner, K. Goetze, S.E. Storck, J.A. Eble, S. Weggen, W. Mueller-Klieser, and C.U. Pietrzik. 2016. Low density lipoprotein receptor-related protein 1 mediated endocytosis of beta1-integrin influences cell adhesion and cell migration. *Exp Cell Res*. 340:102-115